FREE VIBRATION ANALYSIS OF FUNCTIONALLY GRADED FOLDED PLATES UNDER THERMAL ENVIRONMENT

Thesis submitted to

FACULTY OF ENGINEERING & TECHNOLOGY
JADAVPUR UNIVERSITY

in partial fulfillment of the requirements for the degree of
MASTER OF ENGINEERING
in
Civil Engineering
&
Specialization in
STRUCTURAL ENGINEERING

Under the Guidance of
Dr. Sreyashi Das (Pal)
Associate Professor
Department of Civil Engineering

Submitted by
RAJSHEKHAR DAS
Class Roll No.: 002210402003
Examination Roll No.: M4CIV24003
Registration No.: 163456 of 2022-23

Department of Civil Engineering
Faculty of Engineering & Technology
Jadavpur University
Kolkata-700032

May 2024

FACULTY OF ENGINEERING & TECHNOLOGY
DEPARTMENT OF CIVIL ENGINEERING
JADAVPUR UNIVERSITY
KOLKATA-700032, INDIA

CERTIFICATE OF RECOMMENDATION

This is to certify that the thesis entitled "**Free Vibration Analysis of Functionally Graded Folded Plates Under Thermal Environment**" is being submitted by **Rajshekhar Das** (Class Roll No.- **002210402003**, Exam Roll No.- **M4CIV24003**, Registration No.- **163456 of 2022-23**) in partial fulfillment of the requirements for the award of the Master of Engineering in Civil Engineering with specialization in "**Structural Engineering**" from the Jadavpur University, Kolkata and it is delightfully declared that it is a record of bonafide research work carried out by him under my direct supervision in the year of 2023-2024.

This is ensured that the outcomes of the present research work have not been submitted to any other university or institution for the award of any degree or diploma.

Supervisor
Dr. Sreyashi Das (nee Pal)
Associate Professor
Department of Civil Engineering
Jadavpur University, Kolkata

Date: .....

Head of the Department
Dr. Partha Bhattacharya
Professor
Department of Civil Engineering
Jadavpur University, Kolkata

Date: .....

Dean
Prof. Dipak Laha
Faculty of Engineering & Technology
Jadavpur University, Kolkata

Date: .....

CERTIFICATE OF APPROVAL

The foregoing thesis is hereby approved as a creditable study of an engineering subject carried out and presented in a manner satisfactory to warrant its acceptance as a pre-requisite to the Degree of Master of Engineering in Civil Engineering for which it has been submitted. It is understood that by this approval the undersigned do not necessarily endorse or approve any statement made, opinion expressed or conclusion drawn therein, but approve the thesis only for the purpose for which it is submitted.

Committee of Final Examination for Evaluation of Thesis

1. _____
(Signature of Examiner)

2. _____
(Signature of Examiner)

3. _____
(Signature of Examiner)

DECLARATION

I, Rajshekhar Das, a student of Master of Engineering in Civil Engineering (Specialization in Structural Engineering), Jadavpur University, Faculty of Engineering & Technology, hereby declare that the work being presented in the thesis work entitled, "**Free Vibration Analysis of Functionally Graded Folded Plates Under Thermal Environment**", is authentic record of work that has been carried out at the Department of Civil Engineering, Jadavpur University, under the guidance of **Dr. Sreyashi Das (nee Pal)**, Associate Professor, Department of Civil Engineering, Jadavpur University.

The work contained in the thesis has not yet been submitted in part or full to any other university or institution or professional body for award of any degree or diploma or any fellowship.

…….

(RAJSHEKHAR DAS)
Class Roll No.-002210402003
Registration. No.- 163456 of 2022-23
Exam Roll No.- M4CIV24003
Department of Civil Engineering
Faculty of Engineering & Technology
Jadavpur University.

Date: .....
Place: Jadavpur University, Kolkata

ACKNOWLEDGEMENT

I wish to extend my deepest gratitude and sincere thanks to my thesis supervisor and guide **Dr. Sreyashi Das (Pal),** Associate Professor in the Department of Civil Engineering at Jadavpur University, whose astute guidance, perpetual inspiration, and unwavering encouragement have been instrumental in bringing this thesis to fruition. Dr. Das's meticulous scrutiny of the manuscript and invaluable suggestions throughout the course have significantly enriched the work. I deeply admire her patience and willingness to help whenever approached, despite her busy schedule.

I am also thankful to Dr. Partha Bhattacharya (Professor & HOD), Department of Civil Engineering and all esteemed faculty members of the Department of Civil Engineering for their direct and indirect contributions, which have been invaluable in completing this endeavor.

I thank to my parents for giving me unconditional support and encouragement to pursue my current study. I also thank to all of my friends for providing their valuable insight and help whenever they were approached as well as to the non-teaching staff of the Department for their continuous support.

I will be failing in duty if I do not acknowledge with grateful thanks to the authors of the references and other literatures referred to in this paper.

Last but clearly not the least, I am profoundly thankful to the Almighty for giving me the strength and resilience to complete my report on time.

……

Date: RAJSHEKHAR DAS

Place: Kolkata

ABSTRACT

Functionally graded materials (FGMs) are new materials whose properties change gradually in respect to their dimensions. This group of materials shows a tremendous improvement of previously used composite materials. FGM consists of two or more materials whose combination enables the achievement of specified properties in accordance with the desired application. The Ceramic-Metal FGMs can be designed to reduce thermal stresses and take advantage of the corrosion and heat resistances of ceramic and the mechanical strength, good machinability, high toughness and bonding capability of metals without severe internal thermal stresses. Use of folded plates are common nowadays for many types of structures. Judicial use of folds increases the stiffness of the structure and hence its load carrying capacity.

As the FGMs are most likely to be used in the high thermal environments, the free vibration analysis, a fundamental dynamic characteristic, of FGM flat and folded plates under thermal environment holds significant importance in understanding their mechanical behaviour and potential applications. Modal analysis of all side clamped (CCCC) FGM rectangular flat and folded plates in the thermal environment is done based on the First-order transverse shear deformation theory (FSDT). Material properties are assumed to be dependent on temperature and vary continuously in thickness direction according to power law distribution. A finite element program in MATLAB environment is developed for the present study applying folded plate transformation considering 8-noded isoparametric elements with 6 degrees of freedom per node. The effect of various parameters like crank angle β, different side to thickness ratios (b/h ratio), temperature field (uniform/linear/non-linear temperature rise) and gradient indices on the natural frequencies of FG rectangular flat and folded plates is studied. It is observed that increasing thermal load reduces the stiffness of the structure considerably. Stiffer sections can withstand more temperature than thinner sections. Presence of ridge line in folded plates make the structure stiffer compared to flat plate and hence is capable of resisting higher thermal load. The calculated results have been validated with the existing literature.

The thesis also gives an overview of the existing literature on the area of different classifications, various fabrication methods and applications of the FGMs. In recent decades, the exploration of FGMs' free vibration behavior has attracted the attention of researchers across mechanical, aerospace, civil, and biomedical engineering disciplines. The inherent complexity stemming from varying material properties within FGM plates, coupled with diverse boundary conditions and geometric configurations, necessitates advanced computational techniques for accurate analysis.

CONTENTS

Sl. No. **Chapter Name** **Page No.**

LIST OF TABLES

Table No. **Title** **Page No.**

LIST OF FIGURES

Figure No. **Title** **Page No.**

LIST OF SYMBOLS

Symbols		Description
E	:	Modulus of Elasticity/ Young's Modulus
G	:	Shear Modulus
ν	:	Poisson's Ratio
ρ	:	Mass Density
α	:	Thermal Expansion Coefficient
k	:	Thermal Conductivity
T	:	Elevated Temperature
T_0	:	Reference Temperature (=300 K)
ΔT	:	Temperature increment
Si_3N_4	:	Silicon Nitride
SUS304	:	Stainless Steel
Al	:	Aluminium
ZrO_2	:	Zirconia
a, b	:	Length and width of flat plate
a/b	:	Aspect ratio
b/h	:	Width to thickness ratio
S	:	Inclined side of folded plate
L	:	Length of folded plate
h	:	Thickness of plate
Vc	:	Volume fraction of ceramic
Vm	:	Volume fraction of metal
z	:	Distance from mid-plane
β	:	Crank angle of folded plate
N	:	Power Law Index / Gradient Index
N_i	:	Shape function at a node i
[N]	:	Shape function matrix
[B]	:	Strain displacement matrix

$[D]$	:	Stress strain matrix/ constitutive relationship matrix
A_{ij} (i,j=1,2,6)	:	Extensional stiffness
A_{ij} (i,j=4,5)	:	Shear stiffness
B_{ij}	:	Bending extensional coupling stiffness
D_{ij}	:	Bending stiffness
Ω	:	Shear correction factor
x, y, z	:	Cartesian co-ordinate system
ξ, η	:	Local natural co-ordinate system
$[J]$	:	Jacobian Matrix
$[K_e]$	:	Local element stiffness matrix
$[K'_e]$	:	Global element stiffness matrix
$[K']$	:	Global stiffness matrix after assembly
$[K_{Ge}^r]$	:	Local element geometric stiffness matrix
$[K'_{Ge}]$	:	Global element geometric stiffness matrix
$[K'_G]$	:	Global geometric stiffness matrix after assembly
$[M_e]$	:	Local element mass matrix
$[M'_e]$	:	Global element mass matrix
$[M']$	:	Global mass matrix after assembly
$\{F\}$		Internal force and moment resultants
$\{F^N\}$	:	Thermal force and moment resultants
$\{P_e^N\}$	:	Element load vector due to $\{F^N\}$
$\{P^N\}$	:	Global load vector due to $\{F^N\}$
$\{N_x, N_y, N_{xy}\}$	:	In-plane force resultants
$\{M_x, M_y, M_{xy}\}$	:	In-plane moment resultants
$\{Q_x, Q_y\}$	:	Transverse shear resultants
$\{N_x^N, N_y^N, N_{xy}^N\}$	:	Thermal force resultants
$\{M_x^N, M_y^N, M_{xy}^N\}$	:	Thermal moment resultants
u, v, w	:	Displacement in x, y and z direction
u_0, v_0, w_0	:	Mid-plane displacement in x, y and z direction
θ_x, θ_y	:	Total rotations of the plate about x and y-directions

$\emptyset_x, \emptyset_y$	:	Constant shear rotation in xz and yz planes
K_x, K_y and K_{xy}	:	Curvatures of the plate
ε_x, ε_y	:	Linear strain along x and y axis
ε_{xnl}, ε_{ynl}	:	Non-linear strain along x and y axis
[e]	:	Thermal strain vector
U	:	Potential energy of deformation
U_r	:	Potential energy of residual stresses
V_i	:	Potential energy of inertia force and moment
V_{th}	:	Potential energy of thermal force and moment resultants
$\prod$	:	Total potential energy
$\{\sigma^r\}$	:	Matrix involving residual stresses
$[S^r]$	:	Matrix involving residual stress resultants
[T]	:	Transformation matrix
ω_n	:	Natural frequency
λ	:	Non-dimensional natural frequency parameter

LIST OF ABBREVIATIONS

FGM	:	Functionally Graded Material
CPT	:	Classical Plate Theory
FSDT	:	First-order Shear Deformation Theory
TSDT	:	Third-order Shear Deformation Theory
HSDT	:	Higher-order Shear Deformation Theory
FG	:	Functionally Graded
CCCC	:	Clamped-Clamped-Clamped-Clamped
CFFF	:	Clamped-Free-Free-Free
FEM	:	Finite Element Method
FEA	:	Finite Element Analysis
IGA	:	Isogeometric Analysis
2D	:	Two Dimensional
3D	:	Three Dimensional
LC	:	Laminated Composite
NEL	:	Number of Element
DQM	:	Differential Quadrature Method
I-FSDT	:	Improved First-order Shear Deformation Theory
SCF	:	Shear Correction Factor

Chapter 1

INTRODUCTION

CHAPTER 1.
INTRODUCTION

Functionally graded materials (FGM) are composite materials which are designed to present a particular spatial variation of their properties (such as mechanical and thermal properties). This is usually achieved by forming a compound of two components whose volume fraction is changed continuously across a certain direction.

So FGMs are defined as an anisotropic material whose physical properties vary throughout the volume, either randomly or strategically, to achieve desired characteristics or functionality. FGMs differ from traditional composites in that their material properties vary continuously from one surface to another, whereas the composite changes at each laminate interface. Thereby FGMs eliminate the problem of stress concentration in laminated composites. FGMs accomplish this by gradually changing the volume fraction of the materials which make up the FGM. Thus, material properties depend on the spatial position in the structure. The properties that may be designed/controlled for desired functionality include chemical, mechanical, thermal, and electrical properties.

1.1 History of FGMs

Shen and Bever [1] first proposed the concept of gradual material composition for composite and polymer materials in 1972. However, the "first" FGM was developed in Japan in 1984-85 as the result of a spaceplane project [2]. Although the concept of FGM is recent, many materials that fit the description have existed for decades. Some FGMs also occur naturally:

- Seashells
- Bones and teeth

The human bone is an example of a FGM. It is a mix of collagen (ductile protein polymer) and hydroxyapatite (brittle calcium phosphate ceramic). The yellow marrow consists of fat which contributes to the weight and the red marrow is where the formation of red blood cells occurs. A gradual increase in the pore distribution from the interior to the surface can pass on properties such as shock resistance, thermal insulation, catalytic efficiency, and the relaxation of the thermal stress. The distribution of the porosity affects the tensile strength and the Young's modulus. The human bone has high strength at the surface as it gradually lowers toward the inside by altering the porosity. From an engineering perspective, the human bone is a remarkable material

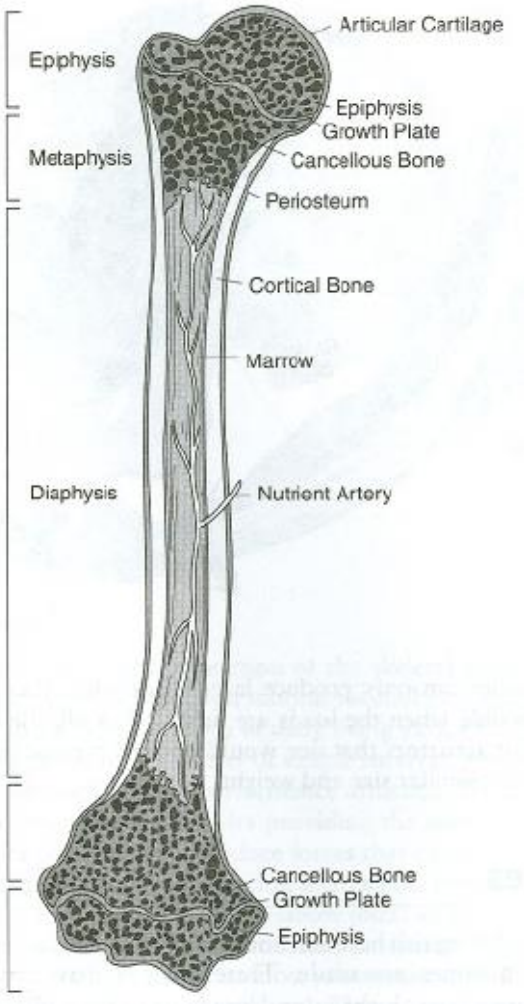

Figure 1.1.1: Human Bone

having unique material properties that has the ability to repair itself and to adapt to its mechanical environment.

1.2 Applications of FGMs

Due to its excellent thermal and mechanical properties, functionally graded materials (FGMs) are widely used in various fields and are likely to be used for other purposes. The most important applications include aerospace, energy, automobile, biomedical, defence, electrical/electronics, marine, Opto-Electronics, sport, thermoselectrics, and bioengineering. Some of the applications of functionally graded materials are highlighted below:

1. Aerospace: Functionally graded materials can withstand very high thermal gradient, this makes it suitable for use in structures and rocket engine component, space plane body etc. If only the processing technique is improved, FGMs are promising and can be used in wider areas of aerospace.

2. Medicine: Living tissues like teeth and bones are examples of functionally graded material from nature, to replace these tissues, a compatible material is needed that will serve the purpose of the original tissue. The ideal material for this application is functionally graded material. FGM has find wide range of application in dental and orthopaedic applications for teeth and bone replacement.

3. Defence: One of the most important characteristics of functionally graded material is the ability to inhibit crack propagation. This property makes it ideal material to be used in defence application, as a penetration resistant materials used for armour plates and bullet proof vests.

4. Energy: FGM are used in energy conversion devices. They can be used in making thermal barriers and are used as protective coating on turbine blades in gas turbine engine.

5. Optoelectronics: FGM also finds its application in optoelectronics as graded refractive index materials and in discs' magnetic storage media.

Other areas of application are: cutting tool insert coating, nuclear reactor components, automobile engine components, turbine blade, heat exchanger, Tribology, fire retardant doors, sensors etc. Current applications of FGMs also include:

- Structural walls that combine two or more functions including thermal and sound insulation.
- Enhanced sports equipment such as golf clubs, tennis rackets, and skis with added graded combinations of flexibility, elasticity, or rigidity.
- Enhanced body coatings for cars including graded coatings with particles such as dioxide/mica.

The list is endless and more application is springing up as the cost of production, processing technology and properties of FGMs improve.

1.3 Advantages of FGMs

FGMs are considered to be potential substitute to traditional laminated composite materials as they can mitigate some disadvantages associated with the laminates. Various advantages of FGMs are pointed out below:

- Minimization of interfacial stresses between different materials (e.g. due to temperature variation).
- Provide ability to remove stress concentrations.
- Provide multi-functionality.
- Provide ability to control deformation, dynamic response, wear, corrosion, etc. and ability to design for different complex environments.
- Provide opportunities to take the benefits (pros) of different material systems [e.g. ceramics and metals such as resistance to oxidation (rust), toughness, machinability, and bonding capability].

1.4 Challenges of FGMs

Functionally graded materials (FGMs) offer unique properties due to their tailored composition and microstructure, but they also pose some challenges:

- Mass production
- Quality control
- Design complexity
- Property prediction
- Cost

1.5 Classification of FGMs

1.5.1 Classification based on FGM structure

In general, FGM structures are classified into two general categories (Figure 1.5.1). The first category is structures that are known as discontinuous or step gradients, where the gradient factor is changing step-by-step and the second category is called continuous gradients, in which the gradient factor is continuously flowing through the volume of the material.

a) Stepwise Graded Structures

An example is a spark plug in which gradient is formed by changing its composition from a refractory ceramic to a metal.

b) Continuous Graded Structures

No clear zones or separation cut lines could be observed inside the material to distinguish the properties of each zone. In other words, not only there is no interface between one side and other side but also, there is no vestige between them. An example is the human bone in which gradient is formed by its change in porosity and composition. Change in porosity happens across the bone because of miniature blood vessels inside the bone.

Note: Desired properties gradients may be designed by controlling crystal structure and crystal orientation, particulate diameter, bonding state, etc.

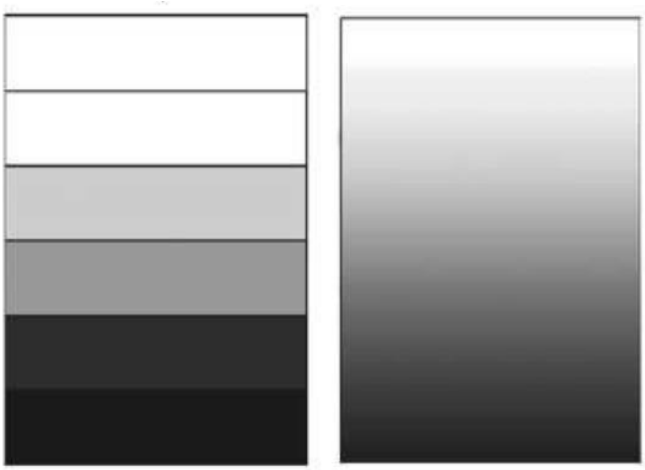

(a) (b)

Figure 1.5.1: Classification of FGM structures (a) Stepwise graded (b) Continuous graded

1.5.2 Classification based on FGM gradient type

According to gradient type FGMs can be classified into three different groups: gradient composition, gradient porosity and gradient microstructure (Figure 1.5.2) [60].

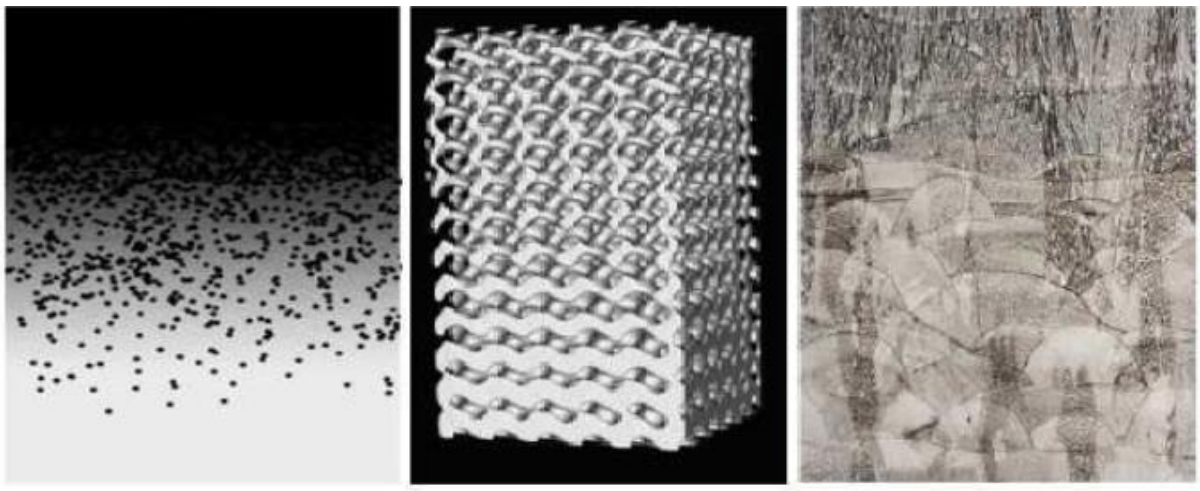

Figure 1.5.2: Classification of functionally graded materials based on type of FGM gradients: a) composition, b) porosity and c) microstructure

a) Gradient composition

In the group of gradient materials based on chemical composition, the chemical composition is gradually varied according to the spatial position. The combination of the FGM gradient depends on the composition of the material, which varies from substance to substance and leads to separate phases with diverse chemical structure.

b) Gradient porosity

In this case, the porosity varies according to the location throughout the material. In the design of FGMs with graded porosity, not only the size of the porosity is very important, but also their shape is extremely significant. From an industrial point of view, it can be seen that materials with graded porosity in the medical industry have far more applications and several studies have been published in this field.

c) Gradient microstructure

This type of FGM refers to a group whose material surface has a different microstructure than its core. Heat treatment in these materials plays a significant role as these elements are mainly produced during the cooling process. These are utilized in applications and devices where the surface must have certain capabilities such as wear-resistance and corrosion, etc. while the nucleus of the body has another property.

1.5.3 Classification based on FGM constituent materials

FGMs were initially classified by researchers under conventional composite materials depending upon the used combinations of constituents. There exist many possible material combinations that can be used to produce FGMs. Metal–metal, metal–ceramic, ceramic–ceramic or ceramic–polymer are the most common as shown in Figure 1.5.3.

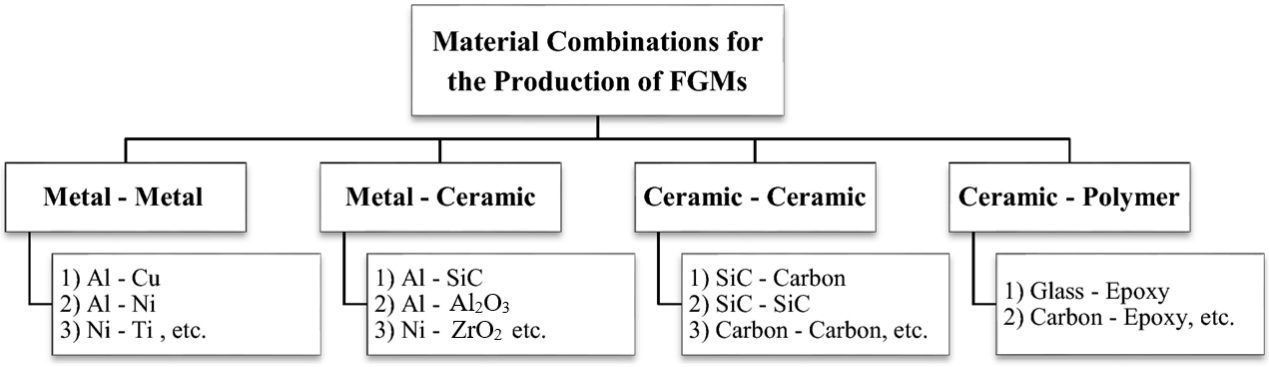

Figure 1.5.3: Examples of possible material combinations used in FGMs

1.6 Fabrication Methods of FGM

Fabrication methods being the most diverse and sophisticated field in FGM research and development, has undergone periodic evolution and progression in production technology as well as fabrication methodology. The diverse development processes that periodically came to use, range from deposition techniques to casting techniques. The suitability and feasibility of production methods were determined based on material composition, transition functionality, component geometry. Figure 1.6.1 classifies the different fabrication techniques employed for processing FGMs [61].

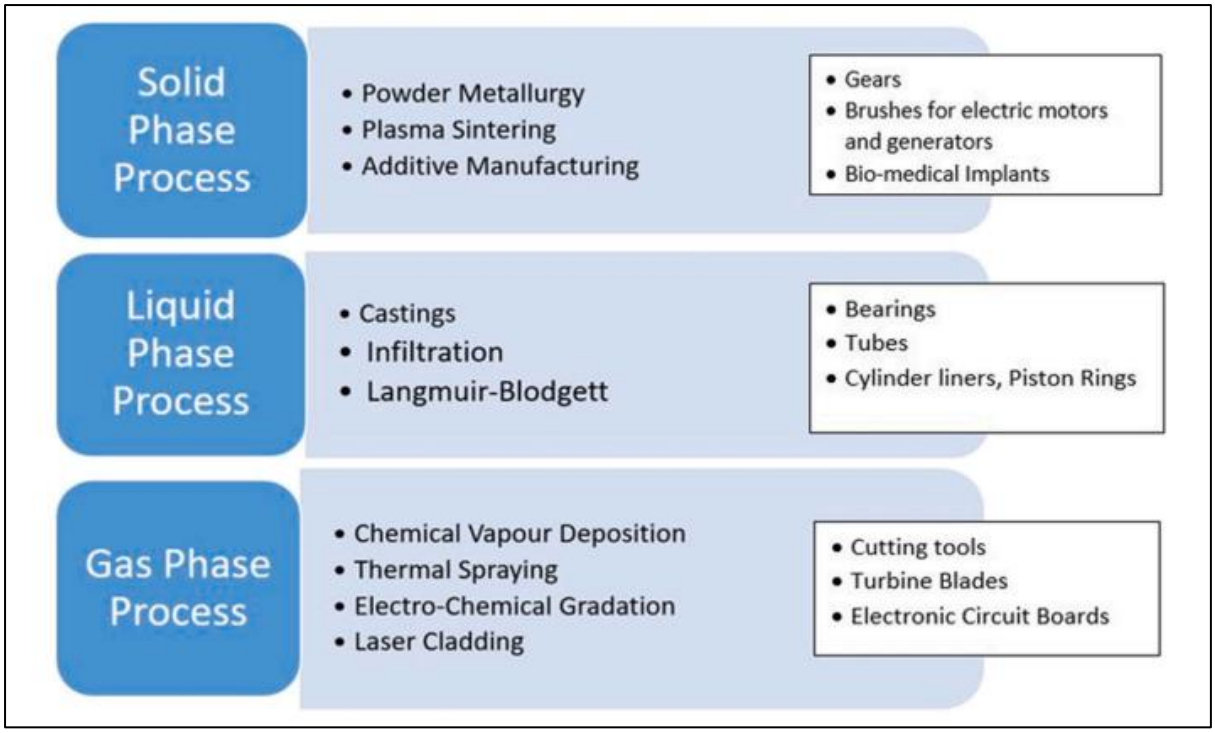

Figure 1.6.1: Various fabrication techniques for FGM.

1.7 Material properties gradation: Mathematical idealization

Functionally graded materials (FGMs) are a special kind of composite in which the material properties vary smoothly and continuously from one surface to the other. Generally, the material properties and volume content vary along the thickness direction. So, FGM is a very non-uniform material. However, it is beneficial to idealize it as a continuum so that its mechanical properties change smoothly in spatial coordinates. In order to analyse FGMs effectively, a homogenization scheme must be adopted to simplify its complex heterogeneous microstructure. The most common homogenization techniques for modelling the effective material properties are the rule of mixtures (Markworth and Saunders, 1995), the Mori–Tanaka method (Mori and Tanaka, 1973; Tanaka, 1997) and Hill's self-consistent approach (Hill, 1965). These models are available to estimate the overall properties of composites from the knowledge of the material composition and constituent properties [62]. Through this idealization, the effective properties of macroscopic homogeneous composite materials can be derived from the microscopic heterogeneous material structures. This will help us to get a mathematical model which in turn useful to include and improve numerical techniques of the FGM structures. It is vital that the conveyance of materials in the FG structure can be intended for different spatial particulars. A typical FGM represents a modern composite material with a recommended conveyance of the volume portion of the constituent stages. It is commonly expected that the material properties follow the progressive change in thickness in a nonstop way.

The material properties gradation in FGM is assumed to follow power law function, exponential function etc. which are discussed here.

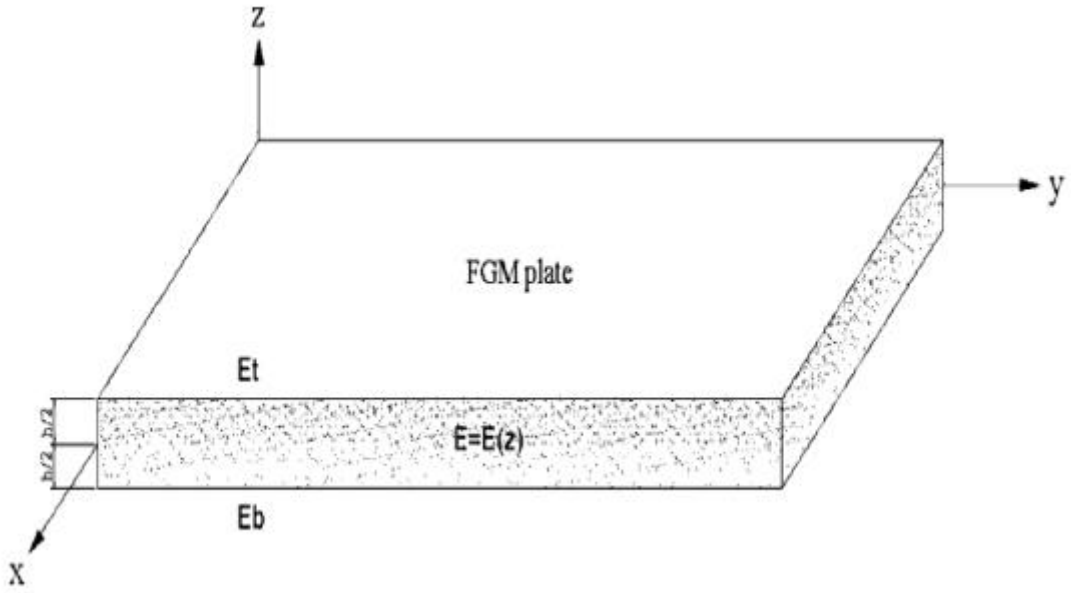

Figure 1.7.1: FGM plate geometry and it's material property variation along the depth

1.7.1 Exponential law

This law is generally adopted when we deal with the fracture mechanics problems. According to this law, the material property P(z) in a specific direction is given by,

$$P(z) = P_t e^{-0.5\left(ln\frac{P_t}{P_b}\right)\left(1-\frac{2z}{h}\right)}$$

P_t and P_b are the corresponding material characteristic values of the topmost and bottom most layer of the FG plate and 'h' is the total thickness of the plate as shown in Figure 1.7.1. It has been found many research articles that used the exponential function to express the material properties variation with the thickness of the FG plate as follows [30],

$$E(z) = E_c e^{-0.5\left(ln\frac{E_c}{E_m}\right)\left(1-\frac{2z}{h}\right)}$$

$$k(z) = k_c e^{-0.5\left(ln\frac{k_c}{k_m}\right)\left(1-\frac{2z}{h}\right)}$$

$$\alpha(z) = \alpha_c e^{-0.5\left(ln\frac{\alpha_c}{\alpha_m}\right)\left(1-\frac{2z}{h}\right)}$$

Where, $E(z)$ is the modulus of elasticity, $k(z)$ denotes the property of thermal conductivity and $\alpha(z)$ indicates the value of the coefficient of thermal expansion of the FGM plate with a thickness of h. 'c' and 'm' represents ceramic and metal respectively.

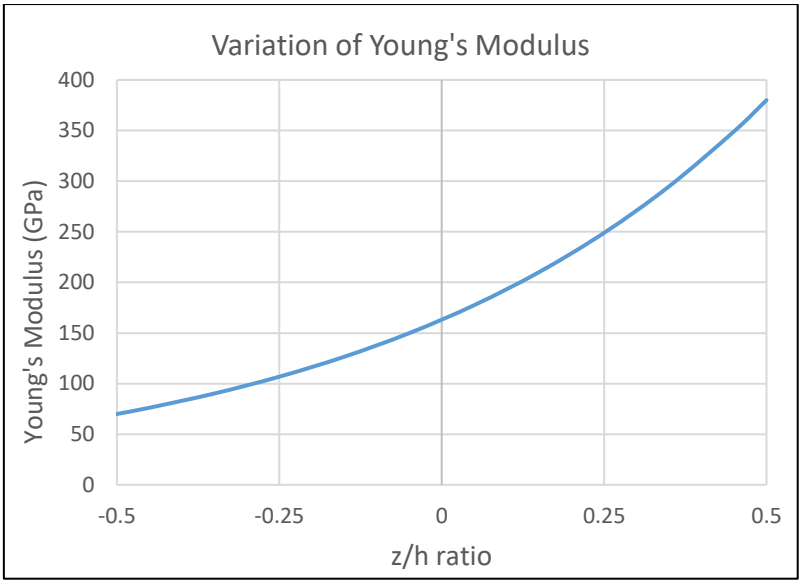

Figure 1.7.2: Variation of Young modulus (Al/Al_2O_3) with the thickness of the FG plate using exponential function [30]

Figure 1.7.2 shows the variation of modulus of elasticity in the direction of the FGM plate's thickness.

1.7.2 Power law

It is observed from the open literature that this particular power law behavior is most commonly used by many researchers. If FGM plate of uniform thickness 'h' is used for the analysis then according to this law, the material properties P(z) in a specific direction (along 'z') can be determined by,

$$P(z) = (P_t - P_b)V_f + P_b$$

P_t and P_b are the corresponding material characteristic values of the topmost and bottom most layer of the FG plate. FGM is usually designed to assume that one of the outermost layers is metal and the other layer is ceramic.

It is noted that material properties are dependent on the volume fraction 'V_f' of FGM. The constituent volume fraction of the FGM plate is supposed to change continually along the thickness direction, which follows power-law as,

$$V_f = \left(\frac{z}{h} + \frac{1}{2}\right)^N$$

where 'N' is the volume fraction exponent. The power law exponent 'N' can vary from '0' to '∞' that show the transition of material from fully ceramic to metallic phase, respectively. The variations may be seen in Figure 1.7.3, which reveals that material properties with exponential gradation usually lie between those obtained with power-law exponents, N = 0.2, 0.5, 1, 2, and 5.

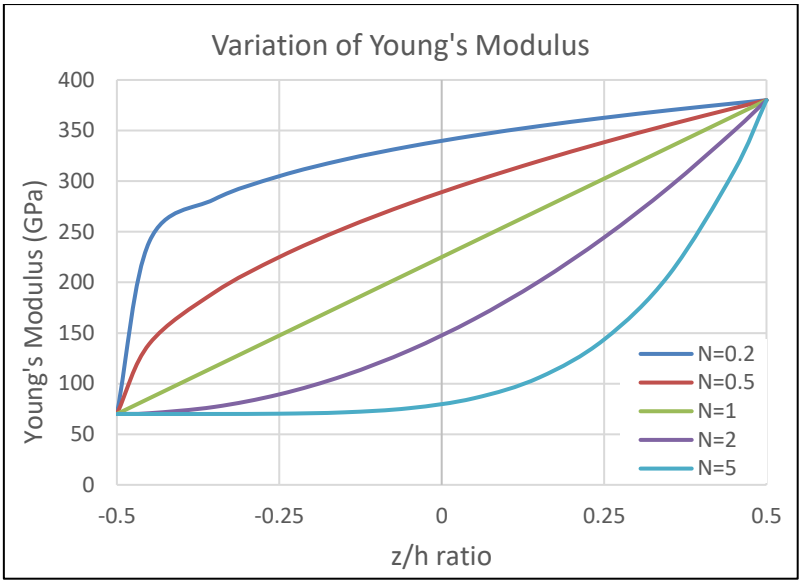

Figure 1.7.3: Variation of Young modulus (Al/Al_2O_3) with the thickness of the FG plate using the power-law [30]

1.7.3 Sigmoid law

Power-law function and exponential function are commonly used to describe the gradation of material properties of FGMs, but, in both functions, the stress concentrations appear in one of the interfaces in which the material is continuous but changing rapidly. To overcome this, Chung and Chi [65], in their work suggested the use of another law called sigmoid law which is the combination of two power-law functions. This law is not independent law; it consists of two symmetric FGM layers having power-law distribution. They also suggested that by the use of a sigmoid law the stress intensity factors of a cracked body can be reduced to a certain extend. According to this law, the two power-law functions are defined by,

$$g_t(z) = 1 - 0.5\left(1 - \frac{2z}{h}\right)^N \quad \text{for } (0 \le z \le \frac{h}{2})$$

$$g_b(z) = 0.5\left(1 + \frac{2z}{h}\right)^N \quad \text{for } (-\frac{h}{2} \le z \le 0)$$

By using the rule of mixture [i.e. $P(z) = (P_t - P_b)V_f + P_b$], Young's modulus of the Sigmoid FGM can be calculated by,

$$E(z) = g_t(z)E_t + [1 - g_t(z)]E_b \quad \text{for } (0 \le z \le \frac{h}{2})$$

$$E(z) = g_b(z)E_t + [1 - g_b(z)]E_b \quad \text{for } (-\frac{h}{2} \le z \le 0)$$

Figure 1.7.4 shows the variation of FGM volume for different values of N by employing the sigmoid function.

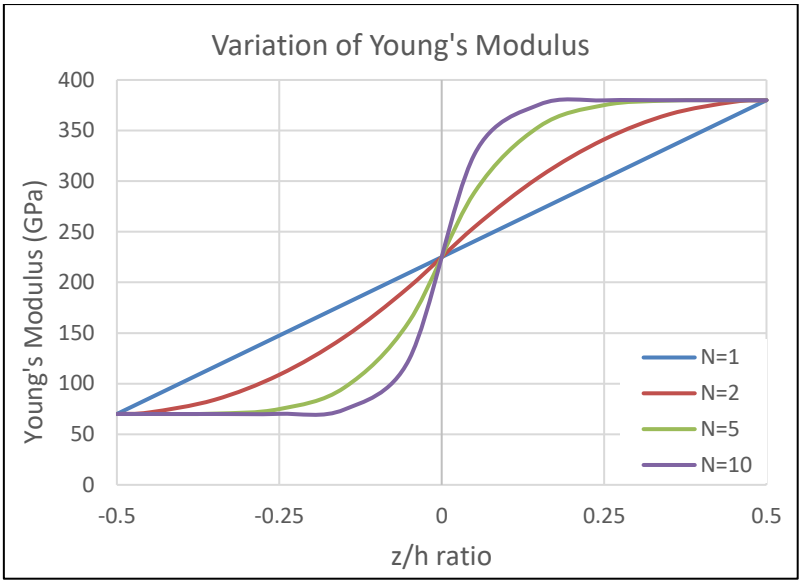

Figure 1.7.4: Variation of Young's modulus (Al/Al_2O_3) with the thickness of the FG plate using the sigmoid function [66].

1.8 Folded Plate Structures

Folded plate structures are shell structures made by assembling flat plates, bending them in different directions, and joining them along their longitudinal edges. Shells and folded plates belong to the class of stressed-skin structures which by virtue of their geometry and small flexural rigidity tend to carry applied loads primarily by direct stresses lying in their plane accompanied by little or no bending unlike slab which carries loads by flexure. Judicial use of folds increases the stiffness of the structure and hence its load carrying capacity. This makes them economical for longer spans. Folded plate structures represent an ingenious synthesis of architectural aesthetics and structural engineering principles. Characterized by their distinctive folded or corrugated configurations, these structures offer a versatile and efficient solution for a variety of architectural and engineering challenges.

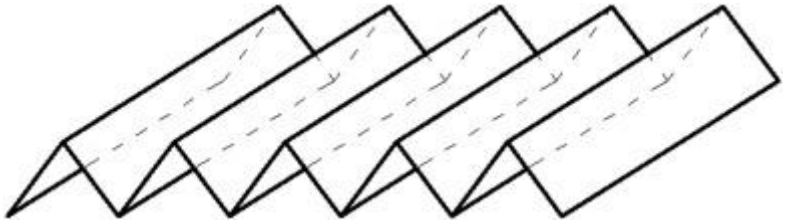

Figure 1.8.1: Folded Plate

The origins of folded plate structures can be traced back to ancient architectural traditions, where early civilizations utilized simple folded elements, such as mud bricks or stone slabs, to construct durable and stable structures. However, it wasn't until the advent of modern engineering techniques and materials that folded plate construction truly flourished as a distinct architectural typology.

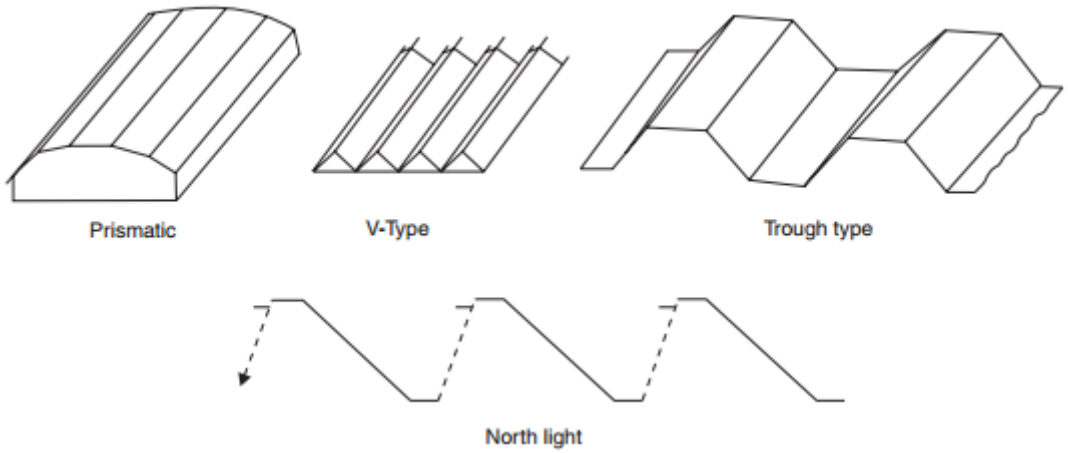

Figure 1.8.2: Various types of folded plate roofs.

1.8.1 Advantages of Folded Plate Structures

Folded plate structures differ from flat plate structures in their geometric configuration and structural behavior, leading to several advantages:

a) **Increased Structural Strength**: Folded plate structures exhibit greater stiffness and load-carrying capacity compared to flat plates. The folded configuration enhances the structural rigidity by increasing the moment of inertia, resulting in improved resistance to bending and torsional forces.

b) **Longer Spans**: Folded plate structures can span longer distances without the need for additional supports compared to flat plate structures. This makes them ideal for applications requiring large, column-free interior spaces, such as industrial buildings, stadiums, and exhibition halls.

c) **Reduced Material Usage**: Despite their increased strength and spanning capability, folded plate structures often require less material compared to flat plate structures of similar size and load-bearing capacity. This efficiency is achieved through the geometric arrangement of the folded plates, which optimizes the distribution of forces and minimizes material usage.

d) **Architectural Flexibility**: The folded configuration of plate structures allows for greater architectural freedom and creativity. Architects can explore various folding patterns, angles, and configurations to create visually striking and innovative designs that may not be achievable with flat plate structures.

e) **Aesthetic Appeal**: Folded plate structures offer unique aesthetic possibilities, with their distinctive folded or corrugated appearance adding visual interest and architectural character to buildings and structures. The interplay of light and shadow on the folded surfaces can create dynamic and engaging spatial experiences for occupants and observers.

f) **Enhanced Stability**: The folded configuration of plate structures enhances their overall stability and resistance to lateral loads, such as wind and seismic forces. This make

them well-suited for applications in regions prone to environmental hazards or where structural stability is a critical design consideration.

Overall, folded plate structures offer a compelling combination of structural efficiency, architectural flexibility, and aesthetic appeal, making them a preferred choice for a wide range of building types and applications where long spans, structural integrity, and design innovation are paramount. At its essence, a folded plate structure consists of a series of interconnected flat plates that are folded or bent along specific lines to create a continuous, three-dimensional form. This folding process not only imbues the structure with inherent strength and rigidity but also allows for the creation of large, column-free interior spaces—a hallmark feature highly sought after in modern architectural design.

1.8.2 Applications of Folded Plate Structures

The application of folded plate structures has always been relevant in different fields of engineering. Here are some common applications:

a) **Roof Structures**: Folded plate structures are frequently used in roof design, particularly for large-span buildings such as warehouses, factories, and sports arenas. The inherent rigidity of folded plates allows for the creation of expansive roof systems without the need for extensive support columns, resulting in large, open interior spaces.

b) **Bridges**: Folded plate structures can be utilized in bridge construction, especially for pedestrian bridges and small to medium-span vehicular bridges. Their structural efficiency, aesthetic appeal, and ability to span long distances make them suitable for various bridge designs.

c) **Architectural Features**: Folded plate elements can be incorporated into architectural features such as canopies, awnings, and facades to provide both structural support and visual interest. The geometric flexibility of folded plates allows architects to create innovative and unique designs that enhance the overall aesthetic of buildings.

d) **Industrial Buildings**: In industrial settings, folded plate structures are often employed in the construction of factories, warehouses, and distribution centers. Their ability to support heavy loads and provide large, uninterrupted interior spaces makes them well-suited for industrial applications where efficient use of space is critical.

e) **Stadiums and Arenas**: Folded plate structures are ideal for the construction of stadium roofs and grandstands due to their ability to span large distances and accommodate seating arrangements. Additionally, their geometric versatility allows for the creation of visually striking architectural forms that can become iconic landmarks.

f) **Exhibition Halls and Convention Centers**: Folded plate structures are commonly used in the construction of exhibition halls and convention centers where large, column-free spaces are required to accommodate trade shows, conventions, and other events. The structural efficiency of folded plates allows for the creation of vast, flexible interior spaces that can easily be adapted to suit various purposes.

g) **Residential Buildings**: While less common, folded plate structures can also be employed in residential construction, particularly for custom-designed homes and high end residential projects. Their ability to create dramatic interior spaces and support unique architectural features can add a distinctive character to residential buildings.

Overall, folded plate structures offer a versatile and efficient solution for a wide range of architectural and engineering applications, enabling the creation of innovative and visually striking designs while also providing practical benefits such as large-span capabilities and structural integrity.

1.9 Objective of Present Study

The present research aims to undertake finite element free vibration analysis of all side clamped (CCCC) functionally graded rectangular flat and folded plate structures subjected to thermal environment. Eight noded isoparametric serendipity plate bending elements considering first-order shear deformation theory (FSDT) with rotary inertia will be used. A continuous variation of material properties like Young's modulus and density per unit volume will be assumed through the plate thickness according to power law distribution. Material properties are assumed to be dependent on temperature. The effect of different crank angles (β), side to thickness ratios (b/h ratio), temperature field (uniform/linear/non-linear temperature rise) and gradient indices on the natural frequencies of FG rectangular flat and folded plates is studied.

1.10 Scope of Present Study

A computer program in MATLAB environment has been developed to study the influence of temperature on the dynamic properties of all side clamped Si_3N_4/SUS304 (Refer Table 3.1.1) FGM rectangular flat and folded plates. Eight-noded isoparametric plate bending element with six degrees of freedom at each node have been employed in the present computations using FEM. First order shear deformation plate theory (FSDT) in conjunction with rotary inertia has been used in the research due to its high efficiency, simplicity and lesser computational cost. The analysis considers material properties of the FGM at elevated temperature. Residual stresses due to thermal environment are taken into account. A three-point gauss quadrature rule is applied for evaluating the bending stiffness matrix whereas, a two-point gauss rule is applied for evaluating shear stiffness matrix to avoid shear locking. Folded plate transformation has been employed in the analysis using a 6 x 6 transformation matrix to transform the element matrices before assembly. A set of new results with various crank angles (β), side to thickness ratios (b/h ratio), temperature field (uniform/linear/non-linear temperature rise) and gradient indices are presented.

These set of results can be used to understand the behaviour of FGM plates under similar aggressive environment. Plates used in many structural systems may undergo undesirable large deflections due to attenuation of resonant frequencies caused by thermal loading during vibration. These results can be advantageously used by designers to tailor different parameters of FGM plates required to avoid resonance. A set of these parametric results can be used for assessing and monitoring the health of structures.

Chapter 2

LITERATURE REVIEW

CHAPTER 2.
LITERATURE REVIEW

Due to the broad applicability of FGM materials across diverse fields, extensive research has been conducted in this area. An in-depth analysis of previously published literature has been undertaken to enhance the understanding and knowledge of the subject. The vast historical background of published literature can be broadly classified into the following categories:

2.1 FGM Flat Plate

Shen and Bever [1] first proposed the concept of gradual material composition for composite and polymer materials in 1972. However, the "first" FGM was developed in Japan in 1984-85 as the result of a spaceplane project [2]. Although the concept of FGM is recent, many materials that fit the description have existed for decades. Some FGMs also occur naturally like seashells, bones and teeth. Praveen and Reddy [3] carried out a nonlinear thermo-elastic analysis of functionally graded ceramic–metal plates using a finite element model based on the first-order shear deformation plate theory (FSDT). Reddy [4] presented a theoretical formulation based on Navier's solutions of rectangular plates, and on third-order shear deformation theory (TSDT) to analyse the functionally graded plates. The plates are assumed to have isotropic, two-constituent material distribution through the thickness, and the modulus of elasticity of the plate is assumed to vary according to power-law distribution in terms of the volume fractions of the constituents. Vel and Batra [5] established an exact three-dimensional solution to perform free and forced vibration analysis of simply supported functionally graded plates. They assumed that the material properties are varying in the thickness direction only according to power law. The exact solutions are compared with those obtained by the classical plate theory (CPT), first order shear deformation theory (FSDT) and third order shear deformation theory (TSDT). It is seen that there are significant differences between the exact solution and results obtained from the classical plate theory whereas the results obtained from the first order and the third order shear deformation theories compare well with the exact solution specially for thin plates. Hashemi et al. [6] developed a dimensionless equation of motion to investigate the transverse vibration of thick functionally graded plates using Mindlin plate theory. Abrate [7] analysed free vibration, buckling and static deflections of FG plates based on the CPT, FSDT and TSDT. They concluded that for various type of loading the natural frequencies, in-plane buckling loads, critical temperatures or deflections of FG plates are proportional to those of the corresponding homogeneous plate. In his another study [8], he showed using CPT that, if the reference surface is chosen properly, then the FGM plate can behave like a homogeneous plate. Nguyen et al. [9] calculated the value of shear coefficient (SCF) to be used for FSDT and they found out that the value of SCF depends on the material gradation, ratio of Young's modulus of the constituent materials. Prakash et al. [10] investigated the non-linear stability behavior of skew FGM plates using FSDT based on the exact neutral surface position as the neutral surface of functionally graded plate may not coincide with its geometric mid-surface, because of the material property variation through the thickness. They found out that the neutral surface shift towards ceramic rich side and the shift increases with increase in gradient index. However, the

results obtained from the formulation based on the neutral surface position, is qualitatively similar to those of mid-surface based formulation. However, they obtained a much higher out of-plane deflection and its difference from mid-surface calculations increased with increase in gradient index and non-linearity. Hashemi et al. [11] carried out analytical solutions for free vibration analysis of moderately thick rectangular plates, which are composed of functionally graded materials (FGMs). They used first-order shear deformation theory (FSDT) to derive and solve exactly the equations of motion. The rectangular plates are considered to have two opposite edges simply supported, while all possible combinations of free, simply supported and clamped boundary conditions are applied to the other two edges. The mechanical properties of the FG plates are assumed to vary according to a power law distribution, whereas Poisson's ratio is set to be constant. Talha and Singh [12] studied the static response and free vibration analysis of FGM plates using higher order shear deformation theory (HSDT). Hashemi et al. [13] compared the analytical and numerical methods of free vibration analysis of moderately thick FG rectangular plates using Levy type solution along with Mindlin's theory of plates. Efraim [14] derived an empirical formula that gives a correlation for natural frequencies of FGM plate and isotropic ones made of containing materials, even with different Poisson ratio. The formula gives immediately accurate results for different vibrational modes and for various volume fractions of containing materials without expending much computational effort. The natural frequencies obtained are compared with results obtained with other numerical methods for thick FGM annular plates. Rasheedat et al. [15] has given an overview on FGM, describing its peculiarities, applications and processing techniques. Jha et al. [16] presented a detailed review on the research works done in various fields of FGMs. In their paper, they showed in details the amount of works done in each field and stressed the need for the development of improved 2D models that would produce much more accuracy with much less computational cost and efforts. Kennedy et al. [17] has given an equivalent isotropic plate model for the FGM plate based on CPT. This holds good only for thin FGM plates where transverse shear is negligible. Gupta and Talha [18] published a detailed review on the different processing techniques, applications, methods for material properties gradations, methods to determine effective material properties, different theories for analysis and on various research works done on FGM. Kennedy et al. [19] in his work presented an equivalent layered model for FGM plate. The idea was to replace the original FGM plate with an equivalent isotropic one, thus making the analysis much more simple. He presented a single layer isotropic model and two-layer model based on CPT by assuming Poison's ratio to be constant and varying respectively and shown that this can be extended to three-layered and four-layered composite plates if we use HSDT that would be necessary for thick FGM plate. Bernardo [20] studied the structural behavior (static and free vibration analyses) of FGM plates using FSDT and various numerical techniques and gradation laws like power law and exponential law and is compared with each other as well as with published FEM results. The layered and continuous configurations were considered and they highlight the development of a package of different methods and models that enable the selection of those that fit better the needs of the study in terms of accuracy, robustness or computational cost. Chakraborty et al. [21] carried out an overall research work on vibration problems for FG beam and plates. Hari Krishnan et al. [22] gives a very compact review on the recent developments in the modelling and analysis of FGM plates. Burlayenko et al. [23] provided 3D modelling of free vibration and static response of functionally graded

materials (FGM) sandwich plates. Marzavan et al. [24] recently presented some results regarding the free vibrations analysis of a plane, clamped circular plate. Two new, original concepts are introduced by the authors: the equivalent plate concept and the multilayer plate concept. They proposed the multilayer plate concept based on the replacement of the continuous variation (according to a given law) of the elastic properties with a step variation of them.

2.2 FGM Flat Plate under Thermal Load

A lot of work is also done in the field of free vibration analysis under thermal environment for various FGM structures. Yang and Shen [25] analysed FGM plates for thermal free and forced vibration based on HSDT. Similar analysis is done by Kim [26] to predict vibrational behavior of FG plates under thermal loadings. Sundararanjan et al. [27] developed a nonlinear formulation based on von Karman's assumptions and FSDT for free vibration analysis of functionally graded plates subjected to thermal environment. Li et al. [28] studied the thermal free vibration of FG plates using 3D elasticity theory. Subsequently, Malekzadeh et al. [29] investigated the thermal free vibration analysis of FG arbitrary straight-sided quadrilateral plates using the FSDT and the differential quadrature method (DQM). Chakraverty and Pradhan [30] analysed exponential functionally graded rectangular plates in thermal environment within the framework of Classical or Kirchhoff's plate theory (CPT). Kandasamy et al. [31] in their paper discussed about free vibration and thermal buckling analysis of moderately thick FGM structures based on FSDT. Lee et al. [32] assessed the thermal buckling responses of FGM plates based on the FSDT and the neutral surface concept. A detailed review of progressive developments in the thermal free vibration and buckling analyses of FGM plates are presented by Swaminathan and Sangeetha [33]. Zghal et al. [34] presented thermal free vibration analysis of FGM plates and panels using an improved first-order shear deformable (I-FSDT) shell model which does not require any shear correction factors. Recently, Thai et al. [35] utilized 3D elasticity theory to predict vibrational behaviour of multi-directional FGM plates under thermal conditions.

2.3 Isotropic Folded Plate

The exploration of isotropic folded plate structures traces back to Goldberg and Leve [36] who developed an exact static analysis of folded plate structures based on elasticity theory. Cheung [37] first employed the finite strip method for analyzing isotropic folded plates. Pulmano et al. [38] subsequently introduced a finite element solution for folded plates with varying thickness. Irie et al. [39] used Ritz method for free-vibration analysis of isotropic cantilever folded plates. Bar-Yoseph et. al. [40] proposed an approximate solution for the analysis of folded plates based on Vlasov's theory of thin walled beams. Golley and Grice [41], as well as Eterovic and Godoy [42], in their papers analysed folded plates using finite strip methods. Liu and Huang [43] in their study used finite element transfer matrix method to obtain the natural frequencies of cantilever folded plate structures. Spectral element method was introduced by Danial et al. [44] for dynamic analysis of isotropic folded plates, employing classical plate model. Bathe [45] and Zienkiewicz et. al. [46] presented a method for flat shell analysis, relevant to folded plate

structures. However, all these investigations primarily focused on isotropic folded plate structures.

2.4 Laminated Composite (LC) Folded Plate

Niyogi et al. [47] predicted the free and forced vibration response of laminated composite folded plate structures utilizing first order shear deformation theory (FSDT). Later Pal and Niyogi [48] extended this analysis to incorporate the free vibration of stiffened laminated composite and sandwich folded plate. Lee et al. [49] used third-order shear deformation theory (TSDT) to predict the dynamic behavior of folded composite structures. Haldar and Sheikh [50] used shear flexible sixteen noded triangular elements for the free vibration analysis of isotropic and composite folded plate. Peng et al. [51] presented bending analysis of folded plates by the FSDT and mesh free Galerkin method. Thinh et. al. [52] deals with the vibration and bending analysis of multi-folding laminated composite plate using FEM. Static and free vibration analysis of stiffened folded plates was done by Nguyen-Minh et al. [53] using a cell-based smoothed discrete shear gap method (CS-FEM-DSG3) based on FSDT. Guo et al. [54] conducted a theoretical and experimental investigation on the nonlinear vibration of Z-shaped folded plates with inner resonance using classical plate theory (CPT). Free vibration behaviour of laminated composite folded plate in hygro-thermal environment is investigated by Das and Niyogi [55] based on FSDT.

2.5 FGM Folded Plate

Published literature on the free vibration analysis of folded plates made of FGM is limited. In 2019, Mohammadi and Setoodeh [56] used an FSDT-based isogeometric analysis (IGA) approach for modal response of functionally graded skew folded (FGSF) plates. Very recently, Basu et al. [57] studied the free vibration response of functionally graded folded plates using finite element method considering first-order shear deformation theory and rotary inertia. Power-law distribution is used to vary the Young's modulus and density per unit volume continuously in the thickness direction. They have shown that the thickness and boundary conditions play a significant role in the free vibration behaviour of the FGM folded plates. Zhang and Li [58] investigated the free vibration of a functionally graded graphene platelets reinforced composite (FG-GPLRC) porous L-shaped folded plate based on Mindlin-Reissner plate theory (i.e. FSDT). Very recently, Pham et. al. [59] presented free and forced vibration analysis of unsymmetrical functionally graded porous folded sandwich plates using mixed interpolation of tensorial components technique of triangular elements (MITC3).

2.6 Critical Observation

Thermal analysis of functionally graded folded plates is an important component of the overall structural design and analysis. The performance of such structures depends on the surrounding temperature, which causes thermal stresses and variation/degradation of material properties. Folded plates are often used as industrial cladding, where thermal loads are quite common. However, research on functionally graded folded plates in thermal environments is relatively limited, as per the authors' best understanding. This knowledge gap motivates the present work.

In this study, we have analysed FGM rectangular flat and folded plate structures exposed to thermal variations. To exaggerate the effects of thermal forces, clamped boundary conditions have been applied to all edges (CCCC). To predict the free-vibration response of these structures, we have employed an eight-noded isoparametric plate bending element. First order shear deformation plate theory (FSDT) in conjunction with rotary inertia has been used in the research due to its high efficiency, simplicity and lesser computational cost. Material properties are assumed to be dependent on temperature and vary continuously in thickness direction according to power law distribution. The element matrices are transformed using a 6x6 transformation matrix, as adapted by Niyogi et al. [47], before assembly. The impact of various parameters such as crank angle, thickness, power law index and temperature field, on the natural frequencies of functionally graded plates is presented.

Chapter 3

THEORETICAL FORMULATION

CHAPTER 3.
THEORETICAL FORMULATION

3.1 Material Properties Variation Law

In this paper we have considered that the material properties of FGM (like modulus of elasticity, density, Poisson's ratio, thermal conductivity etc.) vary continuously only in the thickness direction from bottom (metal) to top (ceramic) and this variation is achieved by varying the volume fraction of constituents according to power law distribution [57]:

$$V_c = \left(\frac{z}{h} + \frac{1}{2}\right)^N \qquad \text{Eqn. (3.1.1)}$$

Similarly,

$$V_m = 1 - \left(\frac{z}{h} + \frac{1}{2}\right)^N \qquad \text{Eqn. (3.1.2)}$$

where 'N' is the power law index or gradient index, while V_c and V_m are the volume fractions of ceramic and metal respectively, at a distance 'z' from the mid-plane (Figure 3.1.1). 'h' is the overall plate thickness.

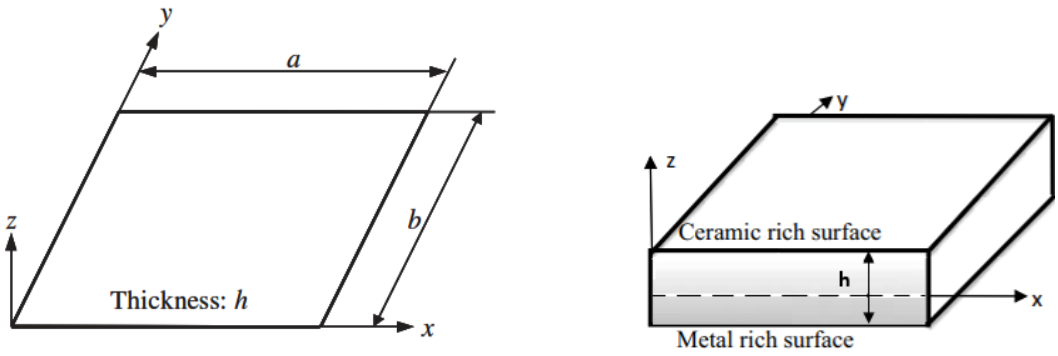

Figure 3.1.1: Geometry of FGM rectangular Flat Plate

Above FGM plate is constructed using two materials having only ceramic at the top plane (z = h/2) and only metal at the bottom plane (z = −h/2). N=0 indicates pure ceramic, and N=∞ indicates pure metal.

The material properties are considered to be dependent on temperature. A new method is proposed by Touloukian [68] to evaluate the material properties (P) of ceramics and metals depending upon the exposure temperatures (T) and is expressed as:

$$P(T) = P_0\left(\frac{P_{-1}}{T} + 1 + P_1 T + P_2 T^2 + P_3 T^3\right) \qquad \text{Eqn. (3.1.3)}$$

where T indicates the environmental temperature and P_0, P_{-1}, P_1 , P_2 , and P_3 are the constants of the specific temperature-dependent material property. Now, based on the simple rule of mixture [28], the effective material properties which are dependent on both temperature (T) and position (z) are expressed as:

$$P_{eff}\,(z,T) = P_m\,(T) + [\,P_C\,(T) - P_m\,(T)]\left(\frac{z}{h}+\frac{1}{2}\right)^N \qquad \text{Eqn. (3.1.4)}$$

where P_{eff} represents the effective material properties of FGM at the temperature T and a spatial distance z from the mid-plane. P_m and P_c are the material properties of the metal and ceramic, respectively. In our study, the effective material properties are evaluated for three types of temperature distribution namely, uniform, linear and nonlinear temperature rise, details of which are given in subsequent paragraphs.

For parametric studies, Stainless Steel (SUS304) and Silicon Nitride (Si_3N_4) are chosen to be the constituent materials of the FGM flat and folded plates. The values of temperature-dependent coefficients of these two materials are shown in Table 3.1.1. However, for validation and mesh convergence study of folded plate formulation Al/ZrO_2 FGM folded plates have been used. Temperature independent properties of Aluminium (Al) and Zirconia (ZrO_2) are listed in Table 3.1.2.

Table 3.1.1: Temperature-dependent coefficients of Young's modulus E (Pa), Poisson's ratio ν, thermal expansion coefficient α (1/K), mass density ρ (kg/m^3) and thermal conductivity k (W/mK) of Si_3N_4 and SUS304 [28].

Material (Ceramic)	Si_3N_4 (Silicon Nitride)				
	E	ν	α	ρ	k
P_{-1}	0	0	0	0	0
P_0	348.430 x 10^9	0.24	5.8723 x 10^{-6}	2370	9.19
P_1	-3.070 x 10^{-4}	0	9.095 x 10^{-4}	0	0
P_2	2.160 x 10^{-7}	0	0	0	0
P_3	–8.946 x 10^{-11}	0	0	0	0
P (at 300 K)	322.2715 x 10^9	0.24	7.4746 x 10^{-6}	2370	9.19

Material (Metal)	SUS304 (Stainless Steel)				
	E	ν	α	ρ	k
P_{-1}	0	0	0	0	0
P_0	201.04 x 10^9	0.3262	12.330 x 10^{-6}	8166	12.04
P_1	3.079 x 10^{-4}	-2.002 x 10^{-4}	8.086 x 10^{-4}	0	0
P_2	-6.534x 10^{-7}	3.797 x 10^{-7}	0	0	0
P_3	0	0	0	0	0
P (at 300 K)	207.7877 x 10^9	0.3178	1.5321 x 10^{-5}	8166	12.04

Table 3.1.2: Temperature-independent Young's modulus E (Pa), Poisson's ratio ν and mass density ρ (kg/m^3) of Aluminium (Al) and Zirconia (ZrO_2) [12].

Material	Aluminium (Al)	Zirconia (ZrO_2)
E	70 x 10^9	151 x 10^9
ν	0.3	0.3
ρ	2707	3000

3.2 Temperature Distribution

Temperature is assumed to vary only in the thickness direction and the variation is evaluated in three different ways as shown below:

3.2.1 Uniform temperature rise

The temperature field across the thickness in the case of uniform temperature rise can be expressed as [28, 33]:

$$T = T_0 + \Delta T \qquad \text{Eqn. (3.2.1)}$$

where T_0 is the temperature of free stress state (T_0 = 300 K) and ΔT is the uniform temperature rise throughout the thickness of plate.

3.2.2 Linear temperature rise

In this case the temperature variation is assumed to be a linear function of thickness coordinate (z) and it is given by [28, 33]:

$$T(z) = T_m + \Delta T\left(\frac{z}{h} + \frac{1}{2}\right) \qquad \text{Eqn. (3.2.2)}$$

where T_m and T_c are the temperatures at the metallic and ceramic face of the FGM plate (T_m = 300 K) and $\Delta T = T_c - T_m$ is the temperature gradient.

3.2.3 Non-linear temperature rise

The nonlinear variation of temperature is usually obtained from the solution of heat conduction equation. Due to the assumption of material homogeneity in the plane of the plate and its variation only in the thickness direction, the current study can be carried out using one dimensional heat conduction equation [26]:

$$-\frac{d}{dz}\left(k(z)\frac{dT}{dz}\right) = 0 \qquad \text{Eqn. (3.2.3)}$$

In our study the thermal conductivity $k(z)$ is assumed to be independent to the temperature as indicated in Table 3.1.1.

Using the boundary conditions $T = T_m$ at $z = -h/2$ and $T = T_c$ at $z = h/2$ in the above equation, the non-linear temperature distribution can be written as [26, 67]:

$$T(z) = T_m + \Delta T \frac{\int_{-h/2}^{z} \left[\frac{1}{k(z)}\right] dz}{\int_{-h/2}^{h/2} \left[\frac{1}{k(z)}\right] dz} \qquad \text{Eqn. (3.2.4)}$$

where T_m and T_c are the temperatures at the metallic and ceramic face of the FGM plate (T_m = 300 K) and $\Delta T = T_c - T_m$ is the temperature gradient.

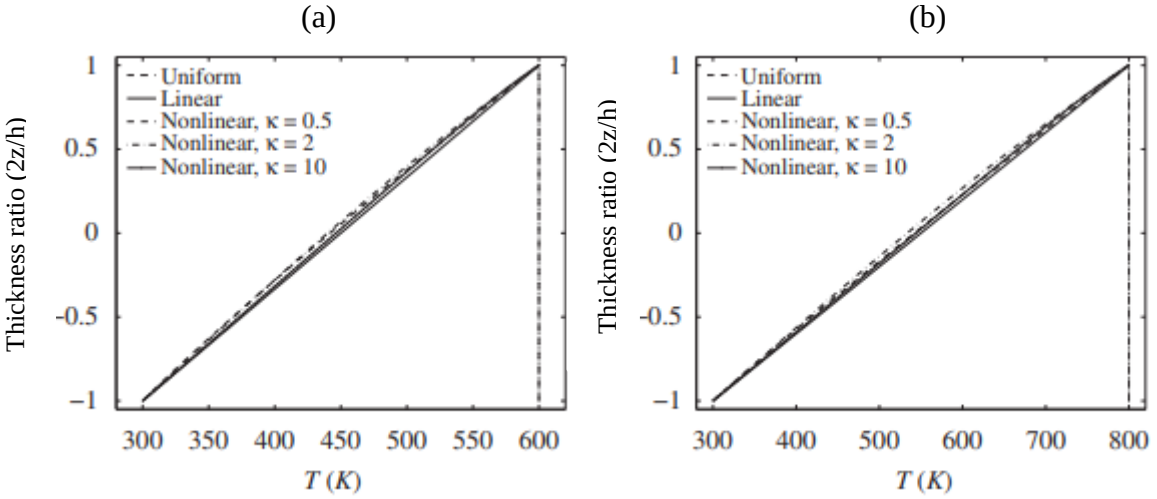

Figure 3.2.1: Variations of temperature along the thickness direction with the initial temperature T_0= 300 K: (a) ΔT= 300 K; (b) ΔT=500 K. [28]

The temperature field variations under three temperature rises along the thickness direction are depicted in Figure 3.2.1. The nonlinear temperature rise is influenced by the power law index, N. However, the impact of N is found to be insignificant. Additionally, it is evident that the curve representing linear temperature rise very closely aligns with those of nonlinear temperature rises.

3.3 Displacement Field and Strains

First-order shear deformation theory (FSDT) is considered in the present finite element analysis of the FGM folded plate structure. That means constant transverse shear strain through the plate thickness has been used.

The displacement and rotation at any point are given by [55]:

$$\begin{aligned} u(x,y,z) &= u_0(x,y) + z\theta_y \\ v(x,y,z) &= v_0(x,y) - z\theta_x \\ w &= w_0 \\ \emptyset_x &= \theta_y + w_{,x} \\ \emptyset_y &= -\theta_x + w_{,y} \end{aligned} \qquad \text{Eqn. (3.3.1)}$$

Here, $u_0(x, y)$, $v_0(x, y)$ and w_0 are corresponding mid plane displacements. θ_x and θ_y are the total rotations of the plate element about x and y-directions. $\emptyset_x$ and $\emptyset_y$ are the constant shear strains in x and y directions, respectively.

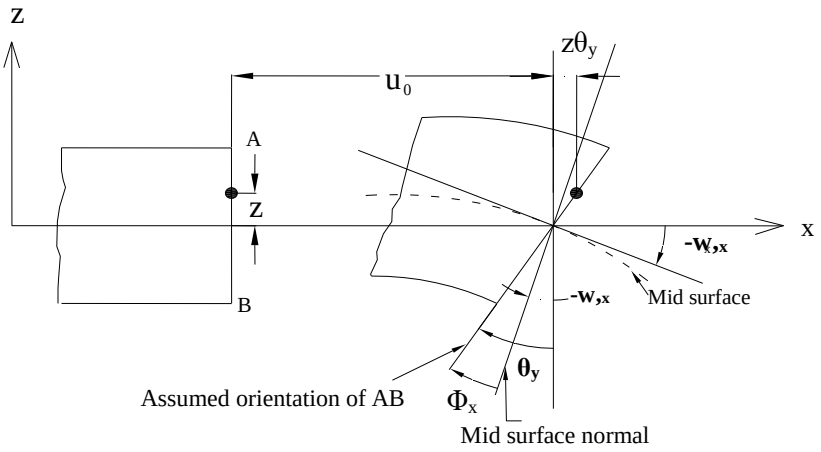

Figure 3.3.1: Detail of deformation in the Mindlin plate along x-direction.

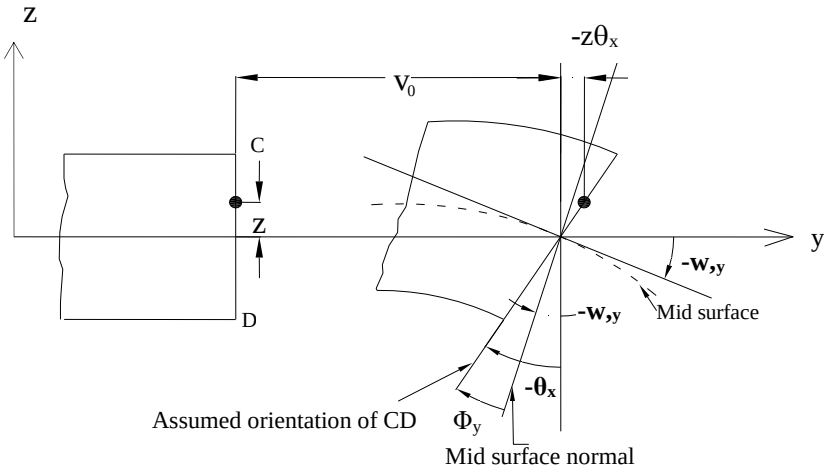

Figure 3.3.2: Detail of deformation in the Mindlin plate along y-direction.

Linear strains at any point in terms of mid-plane strains are written as:

$$\varepsilon_x = u_{,x} = u_{0_{,x}} + z\theta_{y,x} = \varepsilon_x^0 + zK_x$$
$$\varepsilon_y = v_{,y} = v_{0_{,y}} - z\theta_{x,y} = \varepsilon_y^0 + zK_y$$
$$\gamma_{xy} = u_{,y} + v_{,x} = u_{0_{,y}} + v_{0_{,x}} + z(\theta_{y,y} - \theta_{x,x}) = \gamma_{xy}^0 + zK_{xy} \qquad \text{Eqn. (3.3.2)}$$
$$\gamma_{xz} = \emptyset_x = \theta_y + w_{,x}$$
$$\gamma_{yz} = \emptyset_y = -\theta_x + w_{,y}$$
$$\varepsilon_z = 0$$

where K_x, K_y and K_{xy} are the curvatures of the plate.

The constitutive relationship matrix assuming plane-stress state is given by Kim (2005):

$$\begin{Bmatrix} \sigma_x \\ \sigma_y \\ \sigma_{xz} \\ \sigma_{yz} \\ \sigma_{xy} \end{Bmatrix} = \begin{bmatrix} c_{11} & c_{12} & 0 & 0 & 0 \\ c_{12} & c_{22} & 0 & 0 & 0 \\ 0 & 0 & c_{44} & 0 & 0 \\ 0 & 0 & 0 & c_{55} & 0 \\ 0 & 0 & 0 & 0 & c_{66} \end{bmatrix} \begin{Bmatrix} \varepsilon_x \\ \varepsilon_y \\ \gamma_{xz} \\ \gamma_{yz} \\ \gamma_{xy} \end{Bmatrix} \qquad \text{Eqn. (3.3.3)}$$

Here, the stiffness coefficients c_{ij} are obtained analytically and are functions of z and temperature T as follows:

$$c_{11} = c_{22} = \frac{E(z,T)}{[1-\nu(z,T)^2]}$$

$$c_{12} = c_{21} = \nu(z,T)c_{11}$$

$$c_{44} = c_{55} = c_{66} = G(z,T) = \frac{E(z,T)}{2[1+\nu(z,T)]}$$

Now the constitutive matrix is decomposed into two parts and the stress strain relations is rewritten in presence of thermal stress [26], as follows:

$$\begin{Bmatrix} \sigma_x \\ \sigma_y \\ \sigma_{xy} \end{Bmatrix} = \begin{bmatrix} c_{11} & c_{12} & 0 \\ c_{12} & c_{22} & 0 \\ 0 & 0 & c_{66} \end{bmatrix} \begin{Bmatrix} \varepsilon_x - \alpha(z,T)\,\Delta T(z) \\ \varepsilon_y - \alpha(z,T)\,\Delta T(z) \\ \gamma_{xy} \end{Bmatrix}$$

and Eqn. (3.3.4)

$$\begin{Bmatrix} \sigma_{xz} \\ \sigma_{yz} \end{Bmatrix} = \begin{bmatrix} c_{44} & 0 \\ 0 & c_{55} \end{bmatrix} \begin{Bmatrix} \gamma_{xz} \\ \gamma_{yz} \end{Bmatrix}$$

where, α (z,T) represents coefficient of thermal expansion at any distance z from the mid plane and at a temperature T whereas $\Delta T(z)$ is the temperature difference at a distance z.

The internal force and moment resultants are obtained by integrating the stresses over the entire plate thickness.

$$\begin{bmatrix} N_x \\ N_y \\ N_{xy} \end{bmatrix} = \int_{-h/2}^{h/2} \begin{bmatrix} \sigma_x \\ \sigma_y \\ \sigma_{xy} \end{bmatrix} dz$$

$$\begin{bmatrix} M_x \\ M_y \\ M_{xy} \end{bmatrix} = \int_{-h/2}^{h/2} \begin{bmatrix} \sigma_x \\ \sigma_y \\ \sigma_{xy} \end{bmatrix} z\, dz$$

$$\begin{bmatrix} Q_x \\ Q_y \end{bmatrix} = \int_{-h/2}^{h/2} \begin{bmatrix} \sigma_{xz} \\ \sigma_{yz} \end{bmatrix} dz$$

The constitutive equation of a plate subjected to thermal strain is given by [55]

$$\{F\} = [D]\{\varepsilon\} - \{F^N\} \qquad \text{Eqn. (3.3.5)}$$

where, $\{F\} = \{N_x \;\; N_y \;\; N_{xy} \;\; M_x \;\; M_y \;\; M_{xy} \;\; Q_x \;\; Q_y\}^T$

$\{\varepsilon\} = \{\varepsilon_x^0 \;\; \varepsilon_y^0 \;\; \gamma_{xy}^0 \;\; K_x \;\; K_y \;\; K_{xy} \;\; \varphi_x \;\; \varphi_y\}^T$

$\{F^N\} = \{N_x^N \;\; N_y^N \;\; N_{xy}^N \;\; M_x^N \;\; M_y^N \;\; M_{xy}^N \;\; 0 \;\; 0\}^T$

The constitutive matrix [D] is given by [57]:

$$[D] = \begin{bmatrix} A_{11} & A_{12} & A_{16} & B_{11} & B_{12} & B_{16} & 0 & 0 \\ A_{12} & A_{22} & A_{26} & B_{12} & B_{22} & B_{26} & 0 & 0 \\ A_{16} & A_{26} & A_{66} & B_{16} & B_{26} & B_{66} & 0 & 0 \\ B_{11} & B_{12} & B_{16} & D_{11} & D_{12} & D_{16} & 0 & 0 \\ B_{12} & B_{22} & B_{26} & D_{12} & D_{22} & D_{26} & 0 & 0 \\ B_{16} & B_{26} & B_{66} & D_{16} & D_{26} & D_{66} & 0 & 0 \\ 0 & 0 & 0 & 0 & 0 & 0 & A_{44} & A_{45} \\ 0 & 0 & 0 & 0 & 0 & 0 & A_{45} & A_{55} \end{bmatrix} \qquad \text{Eqn. (3.3.6)}$$

where,

$$A_{ij}, B_{ij}, D_{ij} = \int_{-\frac{h}{2}}^{\frac{h}{2}} c_{ij}[1, z, z^2]\, dz \quad (i, j = 1, 2 \text{ and } 6)$$

and,

$$A_{ij} = \Omega \int_{-\frac{h}{2}}^{\frac{h}{2}} c_{ij}\, dz \quad (i, j = 4 \text{ and } 5)$$

Ω = shear correction factor taken as 5/6 for FSDT [26].

The thermal force and moment resultants are,

$\{N_x^N \; N_y^N \; N_{xy}^N\}^{\mathrm{T}} = \int_{-h/2}^{h/2} c_{ij}\,[e]$ dz (i, j = 1, 2 and 6)

$\{M_x^N \; M_y^N \; M_{xy}^N\}^{\mathrm{T}} = \int_{-h/2}^{h/2} c_{ij}\,[e]\; z$ dz (i, j = 1, 2 and 6)

where $[e]$ = Thermal strain vector $= \begin{Bmatrix} \alpha(z, T)\,\Delta T(z) \\ \alpha(z, T)\,\Delta T(z) \\ 0 \end{Bmatrix}$

3.4 Non-linear Strains

Given that the deflection w does not vary with the z-direction, the non-linear portion of the overall strains in a plate can be expressed as:

$$\varepsilon_{xnl} = \frac{1}{2}(u^2{}_{,x} + v^2{}_{,x} + w^2{}_{,x})$$
$$\varepsilon_{ynl} = \frac{1}{2}(u^2{}_{,y} + v^2{}_{,y} + w^2{}_{,y})$$
$$\gamma_{xynl} = (u_{,x}\, u_{,y} + v_{,x}\, v_{,y} + w_{,x}\, w_{,y}) \qquad \text{Eqn. (3.4.1)}$$
$$\gamma_{xznl} = (u_{,x}\, u_{,z} + v_{,x}\, v_{,z})$$
$$\gamma_{yznl} = (u_{,y}\, u_{,z} + v_{,y}\, v_{,z})$$

From the Eqn. (3.3.1)

$$\varepsilon_{xnl} = \frac{1}{2}[u_0{}^2{}_{,x} + v_0{}^2{}_{,y} + w^2{}_{,x} + 2z(u_{0,x}\theta_{y,x} - v_{0,x}\theta_{x,x}) + z^2(\theta^2{}_{y,x} + \theta^2{}_{x,x})]$$
$$\varepsilon_{ynl} = \frac{1}{2}[u_0{}^2{}_{,y} + v_0{}^2{}_{,y} + w^2{}_{,y} + 2z(u_{0,y}\theta_{y,y} - v_{0,y}\theta_{x,y}) + z^2(\theta^2{}_{x,y} + \theta^2{}_{y,y})]$$
$$\gamma_{xynl} = [u_{0,x}u_{0,y} + v_{0,x}v_{0,y} + w_{,x}w_{,y} + z(u_{0,y}\theta_{y,x} + u_{0,x}\theta_{y,y}) - z(v_{0,y}\theta_{x,x} + v_{0,x}\theta_{x,y}) + z^2(\theta_{y,x}\theta_{y,y} + \theta_{x,x}\,\theta_{x,y})] \qquad \text{Eqn. (3.4.2)}$$
$$\gamma_{xznl} = [u_{0,x}\,\theta_y - v_{0,x}\,\theta_x + z(\theta_y\theta_{y,x} + \theta_x\theta_{x,x})]$$
$$\gamma_{yznl} = [u_{0,y}\,\theta_y - v_{0,y}\,\theta_x + z(\theta_y\theta_{y,y} + \theta_x\theta_{x,y})]$$

3.5 Principle of Minimum Total Potential Energy

The potential energy of deformation is given by,

$$U = \frac{1}{2}\iint_A \{\varepsilon\}^T [D]\{\varepsilon\}\, dA. \qquad \text{Eqn. (3.5.1)}$$

The potential energy of residual stresses is expressed as,

$$U_r = \iiint_v \{\varepsilon^r_{nl}\}^T \{\sigma^r\}\, dV \qquad \text{Eqn. (3.5.2)}$$

where,

$$\{\varepsilon^r_{nl}\}^T = \{\ \varepsilon_{xnl}\ \ \varepsilon_{ynl}\ \ \gamma_{xynl}\ \ \gamma_{xznl}\ \ \gamma_{yznl}\ \}$$
$$\{\sigma^r\} = \{\sigma^r{}_x\ \sigma^r{}_y\ \ \sigma^r{}_{xy}\ \ \sigma^r{}_{xz}\ \ \sigma^r{}_{yz}\ \}^T$$

in which $\sigma^r{}_x$, $\sigma^r{}_y$, $\sigma^r{}_{xy}$, $\sigma^r{}_{xz}$, $\sigma^r{}_{yz}$, are the residual stresses due to temperature.

The potential energy of inertia force and moment is expressed as,

$$V_i = -\iint_A \{u\}^T \{X\}\, dA \qquad \text{Eqn. (3.5.3)}$$

where, $\{X\} = \{Pu_0\omega^2_n, Pv_0\omega^2_n, Pw\omega^2_n, I\theta_x\omega^2_n, I\theta_y\omega^2_n,\}^T$

P and I are the elements of inertia matrix [see Eqn. (3.6.6)]

Now, the total potential energy in respect of free vibration analysis of FGM plates in thermal environment is given by [55],

$$\prod = U + U_r + V_i \qquad \text{Eqn. (3.5.4)}$$

According to the principle of minimum total potential energy by equating $\delta\prod$ to zero in Eqn. (3.5.4), the required equilibrium condition can be obtained.

3.6 Finite Element Formulation

An eight noded serendipity isoparametric element have been used as shown in Figure 3.6.1. The term 'isoparametric' suggests that both the geometry and displacement field are expressed in terms of same shape functions. The parent element in local natural co-ordinate system can be mapped to an arbitrary shape in the Cartesian co-ordinate system. The shape function N_i for 8 – noded rectangular element (also called Serendipity element) in natural coordinate system is given by:

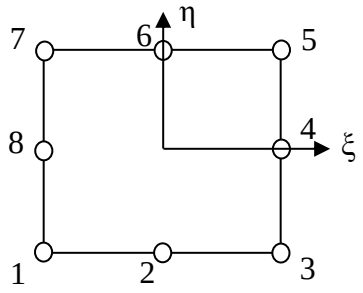

Figure 3.6.1: 8-noded rectangular element (Serendipity element).

$$N_i = \frac{(1+\xi\xi_i)(1+\eta\eta_i)(\xi\xi_i+\eta\eta_i-1)}{4} \quad \text{for } (i = 1,3,5,7)$$

$$N_i = \frac{\xi_i^2(1+\xi\xi_i)(1-\eta^2)}{2} + \frac{\eta_i^2(1+\eta\eta_i)(1-\xi^2)}{2} \quad \text{for } (i = 2,4,6,8)$$

Where, ξ and η are the local natural co-ordinates of the element and ξ_i and η_i are the value of them at node i.

The derivatives of the shape functions N_i with respect to x and y are expressed in terms of their derivatives with respect to ξ and η by the following relationship,

$$\begin{bmatrix} N_{i,x} \\ N_{i,y} \end{bmatrix} = [J]^{-1} \begin{bmatrix} N_{i,\xi} \\ N_{i,\eta} \end{bmatrix}$$

where, $[J] = \begin{bmatrix} x_{,\xi} & y_{,\xi} \\ x_{,\eta} & y_{,\eta} \end{bmatrix}$ = Jacobian matrix

The Principle of Minimum Total Potential Energy described in Sec. 3.5 is applied to derive the element wise stiffness, geometric stiffness and mass matrices.

3.6.1 Element Stiffness Matrix

The potential energy of deformation for the element, given by Eqn. (3.5.1), is

$$U = \frac{1}{2}\iint_{Ae}\{\varepsilon\}^T\,[D]\,\{\varepsilon\}dA$$

Now,

$$\{\varepsilon\} = [B]\{\delta_e\} = [[B_1]\,[B_2]\ \ldots\ldots\ldots[B_8]]\ \{\delta_e\}$$

where $\{\delta_e\} = \{u_{01}, v_{01}, w_1, \theta_{x1}, \theta_{y1}\ \ldots\ldots\ldots\ldots\ldots\ldots\ u_{08}, v_{08}, w_8, \theta_{x8}, \theta_{y8}\}^T$

$$[B_i] = \begin{bmatrix} N_{i,x} & 0 & 0 & 0 & 0 \\ 0 & N_{i,y} & 0 & 0 & 0 \\ N_{i,y} & N_{i,x} & 0 & 0 & 0 \\ 0 & 0 & 0 & 0 & N_{i,x} \\ 0 & 0 & 0 & -N_{i,y} & 0 \\ 0 & 0 & 0 & -N_{i,x} & N_{i,y} \\ 0 & 0 & N_{i,x} & 0 & N_i \\ 0 & 0 & N_{i,y} & -N_i & 0 \end{bmatrix} \quad (i = 1 \text{ to } 8) \qquad \text{Eqn. (3.6.1)}$$

Therefore,

$$U = \frac{1}{2}\int_{-a/2}^{a/2}\int_{-b/2}^{b/2}\{\delta_e\}^T\,[B]^T[D][B]\,\{\delta_e\}\,dx\,dy$$

$$= \frac{1}{2}\,\{\delta_e\}^T\,[K_e]\,\{\delta_e\}$$

in which $[K_e] = \int_{-a/2}^{a/2}\int_{-b/2}^{b/2}[B]^T[D][B]\,dx\,dy$ = element stiffness matrix.

Since $dx\,dy = |J|\,d\xi\,d\eta$, ($|J|$ is the determinant of the Jacobian matrix) the linear stiffness matrix for an element can be expressed in local natural coordinates (ξ, η) as:

$$[K_e] = \int_{-1}^{1}\int_{-1}^{1}[B]^T[D][B]|J|d\xi d\eta \qquad \text{Eqn. (3.6.2)}$$

3.6.2 Element Load Vector due to Thermal effect

The potential energy of thermal force and moment resultants for the element is

$$V_{th} = -\iint_{Ae}\{\varepsilon\}^T\ \{F^N\}\,dA$$

$$= -\int_{-a/2}^{a/2}\int_{-b/2}^{b/2}\{\delta_e\}^T\,[B]^T\{F^N\}\,dx\,dy$$

$V_{th} = -\{\delta_e\}^T\{P_e^N\}$

where, $\{P_e^N\} = \int_{-a/2}^{a/2}\int_{-b/2}^{b/2}[B]^T\{F^N\}\,dx\,dy$

is the element load vector due to thermal effects which can be expressed in natural coordinate system as:

$$\{P_e^N\} = \int_{-1}^{1}\int_{-1}^{1}[B]^T\{F^N\}\,|J|d\xi d\eta \qquad \text{Eqn. (3.6.3)}$$

3.6.3 Element Geometric Stiffness Matrix

The non-linear strain [given by Eqn. (3.4.2)] can be expressed as:

$$\{\varepsilon_{nl}^r\} = \frac{1}{2}\,[R]\{d\}$$

where,

$$\{d\} = \{\ u_{0,x}\ \ u_{0,y}\ \ v_{0,x}\ \ v_{0,y}\ \ w_x,\ \ w_y\ \ \theta_{x,x}\ \ \theta_{x,y}\ \ \theta_{y,x}\ \ \theta_{y,y}\ \ \theta_x\ \ \theta_y\ \}^T$$

Now, {d} for the element is expressed as,

$$\{d\} = [G]\{\delta_e\} = [[G_1]\,[G_2]\ldots\ldots\ldots\,[G_8]]\ \{\delta_e\}$$

where,

$$[G_i] = \begin{bmatrix} N_{i,x} & 0 & 0 & 0 & 0 \\ N_{i,y} & 0 & 0 & 0 & 0 \\ 0 & N_{i,x} & 0 & 0 & 0 \\ 0 & N_{i,y} & 0 & 0 & 0 \\ 0 & 0 & N_{i,x} & 0 & 0 \\ 0 & 0 & N_{i,y} & 0 & 0 \\ 0 & 0 & 0 & N_{i,x} & 0 \\ 0 & 0 & 0 & N_{i,y} & 0 \\ 0 & 0 & 0 & 0 & N_{i,x} \\ 0 & 0 & 0 & 0 & N_{i,y} \\ 0 & 0 & 0 & N_i & 0 \\ 0 & 0 & 0 & 0 & N_i \end{bmatrix} \qquad (i = 1 \text{ to } 8)$$

Then the potential energy of residual stresses, [using Eqn. (3.5.2)] for the element can be written as,

$$U_r = \frac{1}{2}\iiint_{ve}\{\delta_e\}^T\,[G]^T[R]^T\{\sigma^r\}\,dV$$

Since,

$$[R]^T\{\sigma^r\} = \{\sigma^r\}\,[G]\,\{\delta_e\}$$

where,

$$\{\sigma^r\} = \begin{bmatrix} \sigma_x^r & & & & & & & & & & & \\ \sigma_{xy}^r & \sigma_y^r & & & & & & & & & & \\ 0 & 0 & \sigma_x^r & & & & & & & & & \\ 0 & 0 & \sigma_{xy}^r & \sigma_y^r & & & & & & & & \\ 0 & 0 & 0 & 0 & \sigma_x^r & & & & & & & \\ 0 & 0 & 0 & 0 & \sigma_{xy}^r & \sigma_y^r & & & & & & \\ 0 & 0 & -z\sigma_x^r & -z\sigma_{xy}^r & 0 & 0 & z^2\sigma_x^r & & & & & \\ 0 & 0 & -z\sigma_{xy}^r & -z\sigma_y^r & 0 & 0 & z^2\sigma_{xy}^r & z^2\sigma_y^r & & & & \\ z\sigma_x^r & z\sigma_{xy}^r & 0 & 0 & 0 & 0 & 0 & 0 & z^2\sigma_x^r & & & \\ z\sigma_{xy}^r & z\sigma_y^r & 0 & 0 & 0 & 0 & 0 & 0 & z^2\sigma_{xy}^r & z^2\sigma_y^r & & \\ 0 & 0 & -\sigma_{xz}^r & -\sigma_{yz}^r & 0 & 0 & z\sigma_{xz}^r & z\sigma_{yz}^r & 0 & 0 & 0 & \\ \sigma_{xz}^r & \sigma_{yz}^r & 0 & 0 & 0 & 0 & 0 & 0 & z\sigma_{xz}^r & z\sigma_{yz}^r & 0 & 0 \end{bmatrix} \quad Symm$$

So, U_r can be modified as,

$$U_r = \frac{1}{2} \iiint_{ve} \{\delta_e\}^T [G]^T \{\sigma^r\} [G] \{\delta_e\} \, dV$$

$$= \frac{1}{2} \{\delta_e\}^T [K_{Ge}^r] \{\delta_e\}$$

in which $[K_{Ge}^r] = \int_{-a/2}^{a/2} \int_{-b/2}^{b/2} \int_{-h/2}^{h/2} [G]^T \{\sigma^r\} [G] \, dx \, dy \, dz$

= element geometric stiffness matrix due to residual stresses.

$[K_{Ge}^r]$ can be expressed in terms of residual stress resultants $[S^r]$ and the local natural co-ordinates of the element as,

$$[K_{Ge}^r] = \int_{-1}^{1} \int_{-1}^{1} [G]^T [S^r] [G] |J| d\xi \, d\eta \qquad \text{Eqn. (3.6.4)}$$

where,

$$[S^r] = \begin{bmatrix} N_x^r & & & & & & & & & & & \\ N_{xy}^r & N_y^r & & & & & & & & & & \\ 0 & 0 & N_x^r & & & & & & & & & \\ 0 & 0 & N_{xy}^r & N_y^r & & & & & & & & \\ 0 & 0 & 0 & 0 & N_x^r & & & & & & & \\ 0 & 0 & 0 & 0 & N_{xy}^r & N_y^r & & & & & & \\ 0 & 0 & -M_x^r & -M_{xy}^r & 0 & 0 & \frac{N_x^r t^2}{12} & & & & & \\ 0 & 0 & -M_{xy}^r & -M_y^r & 0 & 0 & \frac{N_{xy}^r t^2}{12} & \frac{N_y^r t^2}{12} & & & & \\ M_x^r & M_{xy}^r & 0 & 0 & 0 & 0 & 0 & 0 & \frac{N_x^r t^2}{12} & & & \\ M_{xy}^r & M_y^r & 0 & 0 & 0 & 0 & 0 & 0 & \frac{N_{xy}^r t^2}{12} & \frac{N_y^r t^2}{12} & & \\ 0 & 0 & -Q_{xz}^r & -Q_{yz}^r & 0 & 0 & 0 & 0 & 0 & 0 & 0 & \\ Q_{xz}^r & Q_{yz}^r & 0 & 0 & 0 & 0 & 0 & 0 & 0 & 0 & 0 & 0 \end{bmatrix} \quad Symm$$

3.6.4 Element Mass Matrix

The element mass matrix with rotary inertia is given by [55]

$$[M_e] = \iint [N]^T[\rho][N]|J|d\xi\ d\eta \qquad \text{Eqn. (3.6.5)}$$

where, inertia matrix

$$[\rho] = \begin{bmatrix} I & 0 & 0 & P & 0 \\ 0 & I & 0 & 0 & P \\ 0 & 0 & I & 0 & 0 \\ P & 0 & 0 & Q & 0 \\ 0 & P & 0 & 0 & Q \end{bmatrix} \qquad \text{Eqn. (3.6.6)}$$

where, $$I, P, Q = \int_{-\frac{h}{2}}^{\frac{h}{2}} \rho(z)[1, z, z^2]\, dz$$

$\rho(z)$ being the density varying along thickness direction. Density is assumed to be independent of temperature in our analysis as indicated by the properties tabulated in Table 3.1.1.

3.6.5 Transformation Matrix

The positive directions of the linear displacements and the rotations of the plate element are shown in Figure 3.6.2.

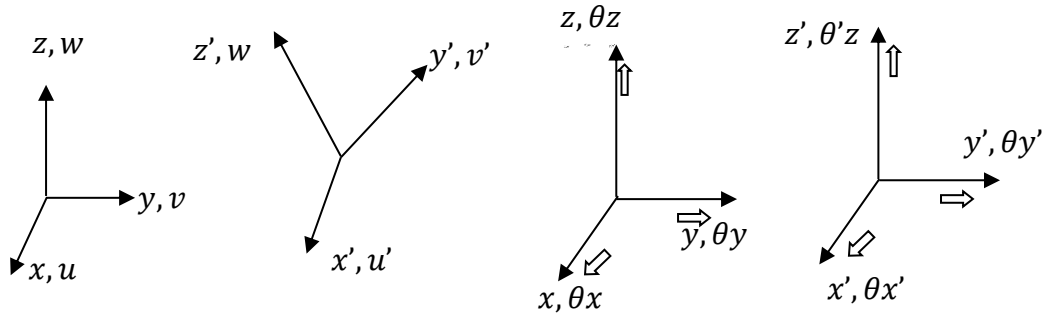

Figure 3.6.2: Transformation of translations and rotation from local x_i- to global x_i'-axes

Accordingly, to correlate the local displacements u,v,w, θ_x, θ_y, θ_z to global displacements u',v',w', θ'_x, θ'_y, θ'_z , a transformation matrix [T] is applied which is given by [55]:

$$[T] = \begin{bmatrix} cos(x',x) & cos(y',x) & cos(z',x) & 0 & 0 & 0 \\ cos(x',y) & cos(y',y) & cos(z',y) & 0 & 0 & 0 \\ cos(x',z) & cos(y',z) & cos(z',z) & 0 & 0 & 0 \\ 0 & 0 & 0 & cos(x',x) & cos(y',x) & cos(z',x) \\ 0 & 0 & 0 & cos(x',y) & cos(y',y) & cos(z',y) \\ 0 & 0 & 0 & cos(x',z) & cos(y',z) & cos(z',z) \end{bmatrix}$$

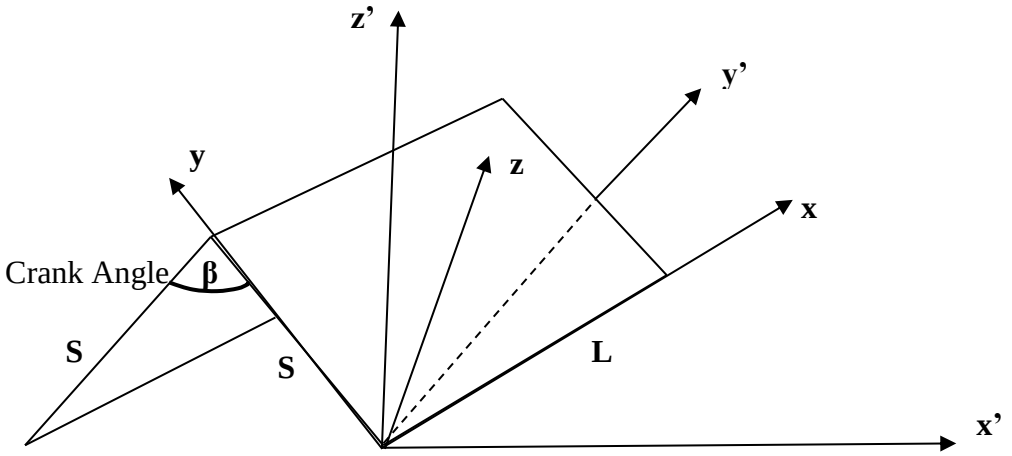

Figure 3.6.3: Local (un-primed) and global (primed) axis for FGM one-fold plate

The same transformation matrix [T] is used to convert the local element linear stiffness, geometric stiffness and mass matrices into global stiffness and mass matrices as shown below:

$[K_e'] = [T]^T[K_e][T]$,

$[K_{Ge}'] = [T]^T[K_{Ge}][T]$,

and $[M_e'] = [T]^T[M_e][T]$,

Here $[T]^T = [T]^{-1}$

since $[T]$ is orthogonal.

Before applying the transformation, the 40×40 stiffness and mass matrices are expanded to 48×48 by inserting eight θ_z drilling degree of freedom at each node of a finite element as suggested in Bathe [45].

3.6.6 Assembly and Solution

The above transformed element matrices $[K'_e]$, $[K'_{Ge}]$and $[M'_e]$ are assembled to obtained their respective global matrices $[K']$, $[K'_G]$ and $[M']$. These matrices are updated for boundary conditions before solving.

Finally, the governing equation for free vibration analysis of the FGM folded plates in thermal environment is derived from the principle of minimum total potential energy [55]:

$$([K'] + [K'_G] - \omega_n{}^2[M']) \{\delta\} = 0 \qquad \text{Eqn. (3.6.7)}$$

from which the natural frequencies are obtained.

3.6.7 MATLAB Program Flowchart

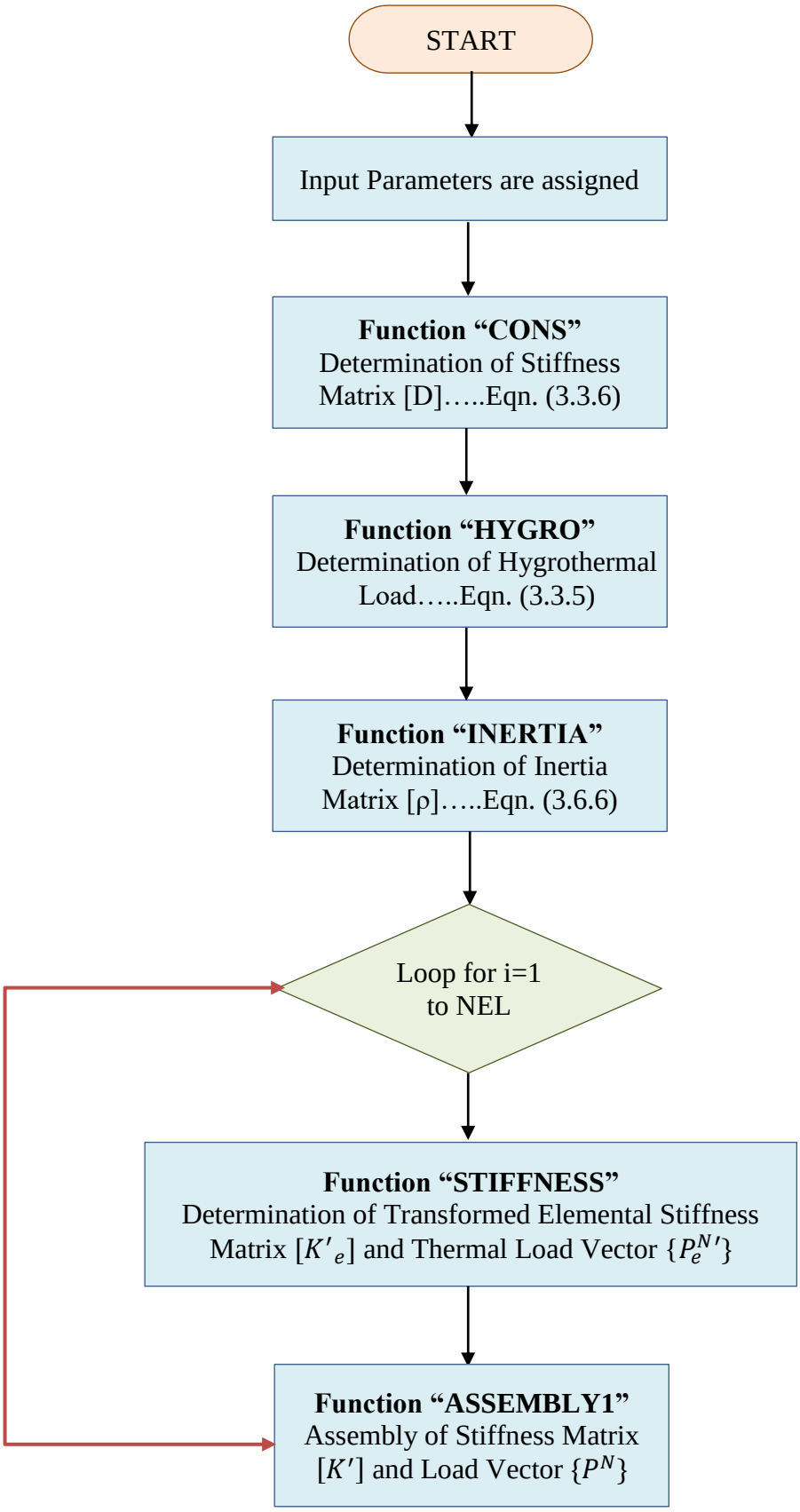

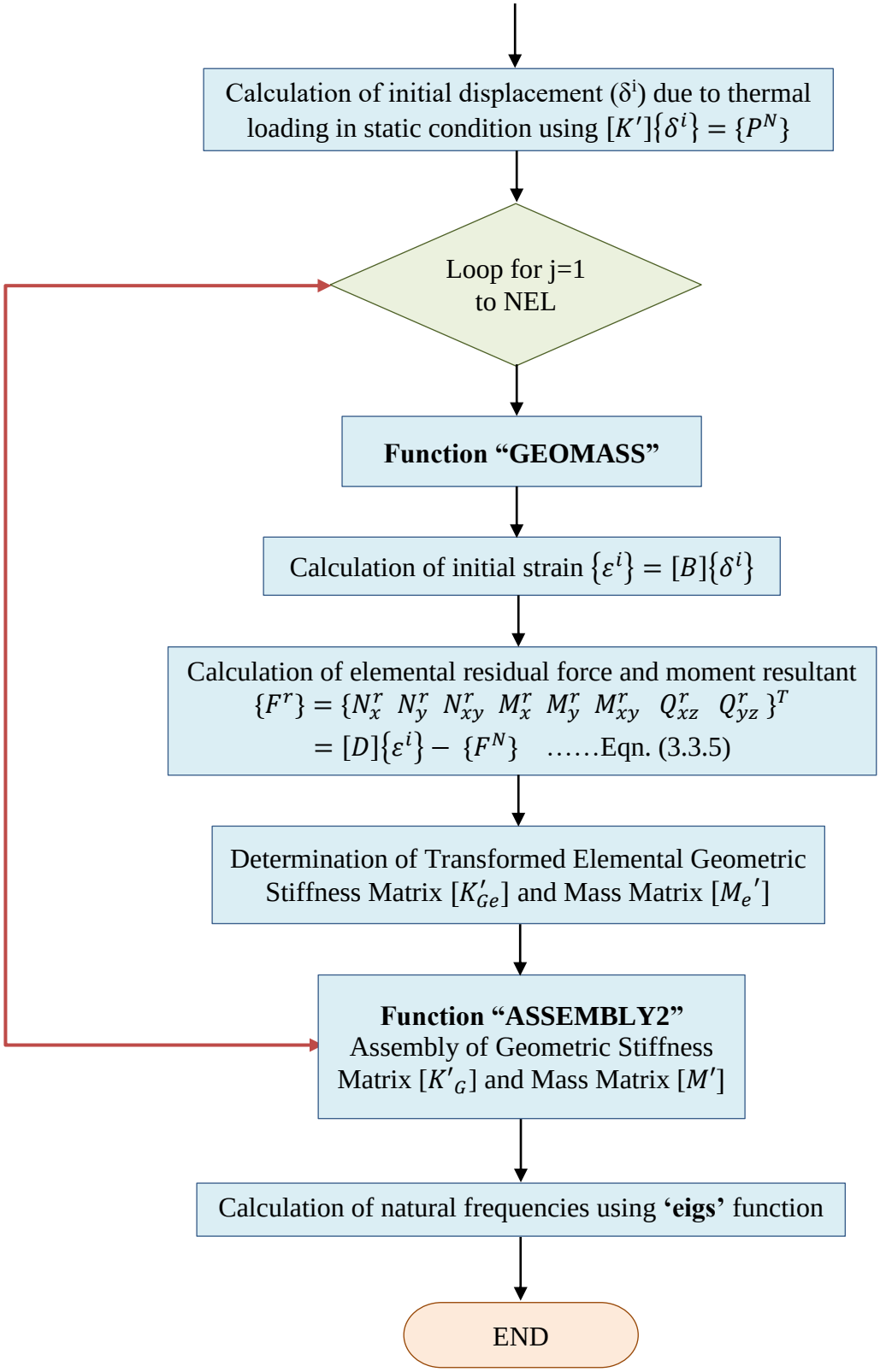
Calculation of initial displacement (δ^i) due to thermal loading in static condition using $[K']\{\delta^i\} = \{P^N\}$
Loop for j=1 to NEL
Function "GEOMASS"
Calculation of initial strain $\{\varepsilon^i\} = [B]\{\delta^i\}$
Calculation of elemental residual force and moment resultant $\{F^r\} = \{N_x^r \ N_y^r \ N_{xy}^r \ M_x^r \ M_y^r \ M_{xy}^r \ Q_{xz}^r \ Q_{yz}^r\}^T = [D]\{\varepsilon^i\} - \{F^N\}$ ……Eqn. (3.3.5)
Determination of Transformed Elemental Geometric Stiffness Matrix $[K'_{Ge}]$ and Mass Matrix $[M_e{}']$
Function "ASSEMBLY2" Assembly of Geometric Stiffness Matrix $[K'_G]$ and Mass Matrix $[M']$
Calculation of natural frequencies using **'eigs'** function
END

Chapter 4

NUMERICAL STUDY AND RESULTS

CHAPTER 4.
NUMERICAL STUDY AND RESULTS

The finite element formulation outlined in the preceding chapter has been applied to produce numerical results, examining the impact of thermal environment on FGM plates. Mesh convergence study is conducted to determine the minimum number of meshes necessary for accurate analysis. Along with this two validation studies are also undertaken to validate the results of the program against those published in established literature.

Subsequently, a series of parametric studies are executed by varying parameters such as power law index, thickness, crank angle and temperature. These systematic investigations allow for a comprehensive understanding of how these factors influence the behavior of various FGM plates under thermal environment.

4.1 Mesh Convergence and Validation Study

A mesh convergence study is conducted on a symmetric one-fold Al/ZrO_2 FGM folded plate structure, properties of which are defined in Table 3.1.2. The structure is symmetric about its ridge line and has a crank angle of 90°, as depicted in Figure 4.2.3. The folded edge comprises two equal inclined sides denoted as S, with a length denoted as L. The value of S and L are taken as 0.75 m and 1.5 m, respectively. One of the folded edges is clamped, while the remaining three edges are kept free (CFFF). We have considered two different plate thicknesses: 15 mm and 30 mm. The power law index is set to 1. The number of elements along S and L, are denoted as N_1 and N_2, respectively. The same model has been analysed using "ANSYS Student 2023 R2" software. First five natural frequencies in Hz for different values of N_1 and N_2 are shown in Table 4.1.1 and Table 4.1.2. From the results it is concluded that the arrangement with N_1=4 and N_2=8 provides acceptable mesh convergence and is thus adopted for subsequent analyses.

The validation study is divided into two segments due to the absence of a complete reference.

i) Validation of FGM folded plate formulation.

ii) Validation of thermal formulation.

4.1.1 Validation of FGM folded plate formulation

Results of one-fold Al/ZrO_2 (Table 3.1.2) FGM folded plate without any temperature increment is compared with Basu et al. [57] and ANSYS software as shown in Table 4.1.1 and Table 4.1.2. The results are found to be within the acceptable limit.

4.1.2 Validation of thermal formulation

First three non-dimensional natural frequency parameters $\left(\lambda = \frac{wb^2}{\pi^2}\sqrt{\frac{I_0}{D_0}}\right)$ of all side clamped Si_3N_4/SUS304 (Table 3.1.1) FGM square plates subjected to uniform temperature rise is compared with various published literatures in Table 4.1.3. Results are found in good agreement with those in Refs. [25, 29, 35].

Table 4.1.1: First five natural frequencies in (Hz) for different mesh numbers ($N_1 \times N_2$) of Al/ZrO_2 FGM Folded Plate (CFFF) with S/h = 50, L= 1.5 m, S =0.75 m, β=90°, Power law index(N)=1.

Source	$N_1 \times N_2$	Mode 1	Mode 2	Mode 3	Mode 4	Mode 5
Present	2x4	16.579	33.832	60.584	75.447	128.499
	3x6	16.553	33.328	60.272	71.299	125.040
	4x8	16.532	33.273	60.166	70.835	124.316
Basu et al. [57]		16.532	33.255	60.158	70.724	124.279
% Difference =		**0.00%**	**0.06%**	**0.01%**	**0.16%**	**0.03%**
ANSYS		16.510	33.139	60.063	70.887	124.880
% Difference =		**0.14%**	**0.41%**	**0.17%**	**-0.07%**	**-0.45%**

Table 4.1.2: First five natural frequencies in (Hz) for different mesh numbers ($N_1 \times N_2$) of Al/ZrO_2 FGM Folded Plate (CFFF) with S/h = 25, L= 1.5 m, S =0.75 m, β=90°, Power law index(N)=1.

Source	$N_1 \times N_2$	Mode 1	Mode 2	Mode 3	Mode 4	Mode 5
Present	2x4	32.958	65.987	120.290	143.702	240.126
	3x6	32.847	65.647	119.534	140.637	237.924
	4x8	32.766	65.592	119.244	140.249	237.352
Basu et al. [57]		32.768	65.580	119.236	140.177	237.225
% Difference =		**-0.01%**	**0.02%**	**0.01%**	**0.05%**	**0.05%**
ANSYS		32.858	65.261	119.370	139.820	239.150
% Difference =		**-0.28%**	**0.51%**	**-0.11%**	**0.31%**	**-0.75%**

Table 4.1.3: Comparison of first three non-dimensional natural frequency parameters λ for Si_3N_4/SUS304 FGM square plates (CCCC) subjected to uniform temperature rise (a=0.2 m, b/h=10, N=2, T_0=300 K).

Source	Mode sequences (ΔT = 300 K)			Mode sequences (ΔT = 500 K)		
	λ_1	λ_2	λ_3	λ_1	λ_2	λ_3
Malekzadeh and Beni [29] (FSDT)	3.6548	7.2022	7.2022	3.2163	6.5603	6.5603
% Difference =	**0.37%**	**0.41%**	**0.41%**	**0.44%**	**0.40%**	**0.40%**
Yang and Shen [25] (HSDT)	3.6636	7.2544	7.2544	3.2357	6.6281	6.6281
% Difference =	**0.61%**	**1.12%**	**1.12%**	**1.04%**	**1.42%**	**1.42%**
Thai et. al. [35] (3D Elastic Theory)	3.6936	7.2661	7.2661	3.2683	6.6457	6.6457
% Difference =	**1.42%**	**1.28%**	**1.28%**	**2.03%**	**1.68%**	**1.68%**
Present	**3.6412**	**7.1728**	**7.1728**	**3.2021**	**6.5338**	**6.5338**

In calculation of non-dimensional natural frequency parameter λ, the terms I_0 and D_0 are defined as [28]:

$$I_0 = \rho h$$

$$D_0 = \frac{Eh^3}{12(1-\nu^2)}$$

ρ, E, and ν are chosen to be the values of SUS304 at the reference temperature T_0 = 300 K.

4.2 Case Studies

Impact of various parameters such as power law index, thickness, crank angle and temperature field, on the natural frequencies of three types of functionally graded plates is presented in this section:

i) FGM Rectangular Flat Plate (see Figure 4.2.1).
ii) FGM One-Fold Plate (see Figure 4.2.3).
iii) FGM Two-Fold Plate having 90^0 crank angle (see Figure 4.2.7).

4.2.1 FGM Rectangular Flat Plate

The FGM plates are often used in situations where it is exposed to high temperature environment. Based on the procedures and analyses of foregoing sections, the influence of temperature stress in the free vibration of rectangular FGM flat plate is studied in this section. The FGM plate made up of Silicon Nitride and Stainless steel (Si_3N_4/SUS304) is taken for the study. We consider that the FGM plate has the ceramic at the heated surface (z = h/2) and the metal at the cooled surface (z = - h/2) and their compositions vary continuously in the thickness direction of the plate. The material properties are considered to be temperature dependent. For ease of understanding Figure 3.1.1 is reproduced here.

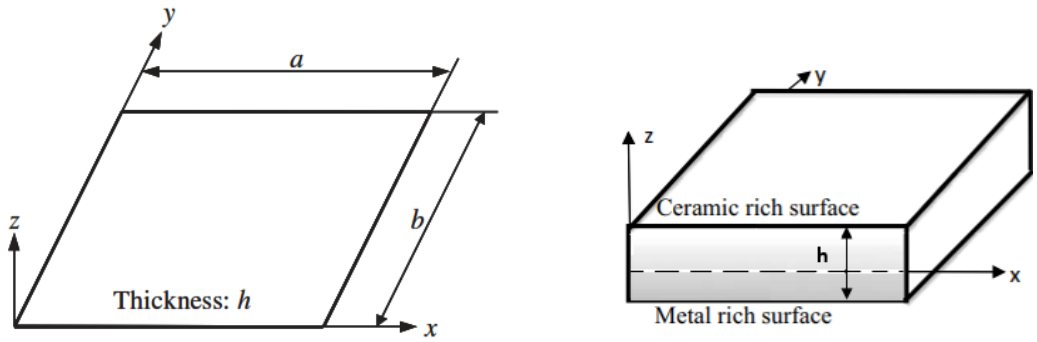

Figure 4.2.1: Geometry of FGM rectangular Flat Plate

Table 4.2.1 to Table 4.2.4 give the results of the first five natural frequency parameters (λ) of all side clamped Si_3N_4/SUS304 FGM rectangular flat plates. From the study it is observed that the thermal initial stress decreases the natural frequency of vibration. Three temperature fields: uniform temperature rise, linear temperature rise, and nonlinear temperature rise, as defined previously in Eqn. (3.2.1), Eqn. (3.2.2) and Eqn. (3.2.4), are considered. These results include

the cases of three side to thickness ratios (b/h= 20, 10, 5), two aspect ratios (a/b= 0.5, 1) and four volume fraction indices (N= 1, 2, 5, 10). It is shown that, the natural frequency parameters decrease with the increase of the volume fraction index N, as high N value denotes high metal and low ceramic content [Eqn. (3.1.1)]. This ultimately reduces the rigidity of the plate, and hence the natural frequency.

The uniform temperature change affects the vibrational frequencies more significantly than the linear and nonlinear temperature changes. It can be explained by referring to Figure 3.2.1 which shows that the temperature variation of the uniform temperature field is more intensive than those of linear and nonlinear temperature fields. For a clear demonstration, Table 4.2.5 lists the percentage reduction of frequency parameters due to the temperature rise. The temperatures of plates are raised from the initial value 300 K to the final value 600 K. It is shown that the temperature rise affects the first mode more significantly than other higher modes and the plates of volume fraction index N=10 are more sensitive to the temperature change than those of N=1. This is because, at N=10, the metal content is high and hence the effective Young Modulus value of the plate reduces.

Table 4.2.1: Natural frequency parameters (λ) for CCCC rectangular Si_3N_4/SUS304 FGM flat plates without temperature rise ΔT= 0 K.

b/h	a/b	N	λ_1	λ_2	λ_3	λ_4	λ_5
20	0.5	1	12.7734	16.3450	22.6462	30.9252	31.5317
		2	11.4748	14.6808	20.3344	27.7338	28.2991
		5	10.4280	13.3380	18.4658	25.1467	25.6805
		10	9.9451	12.7189	17.6059	23.9682	24.4795
	1	1	4.8933	9.7964	9.7964	14.2012	17.1762
		2	4.4025	8.8091	8.8091	12.7643	15.4349
		5	4.0086	8.0150	8.0150	11.6065	14.0304
		10	3.8246	7.6456	7.6456	11.0697	13.3803
10	0.5	1	10.8366	13.6422	18.3670	22.9869	24.0164
		2	9.6917	12.2022	16.4232	20.4787	21.2648
		5	8.7593	11.0280	14.8350	18.4597	18.9732
		10	8.3433	10.5032	14.1264	17.6321	17.9925
	1	1	4.5602	8.7244	8.7244	12.2435	14.4887
		2	4.0942	7.8220	7.8220	10.9687	12.9719
		5	3.7178	7.0897	7.0897	9.9314	11.7356
		10	3.5449	6.7567	6.7567	9.4619	11.1790
5	0.5	1	7.5434	9.3738	11.5887	12.2159	14.5234
		2	6.7036	8.3379	10.2887	10.8713	12.8699
		5	6.0134	7.4865	9.2468	9.7656	11.5084
		10	5.7191	7.1208	8.8252	9.2894	10.9313
	1	1	3.7388	6.5382	6.5382	8.6662	8.7909
		2	3.3408	5.8326	5.8326	7.6886	7.8368
		5	3.0158	5.2548	5.2548	6.8930	6.8930
		10	2.8718	5.0017	5.0017	6.5730	6.7112

Table 4.2.2: Natural frequency parameters (λ) for CCCC rectangular Si_3N_4/SUS304 FGM flat plates subjected to uniform temperature rise ΔT= 300 K.

b/h	a/b	N	λ_1	λ_2	λ_3	λ_4	λ_5
20	0.5	1	11.1993	14.4284	20.3587	28.4337	28.8389
		2	9.9364	12.8087	18.1055	25.3155	25.6824
		5	8.9170	11.4998	16.2820	22.7844	23.1224
		10	8.4331	10.8805	15.4255	21.6146	21.9298
	1	1	3.3625	7.9832	7.9832	12.1693	15.0307
		2	2.8714	7.0224	7.0224	10.7721	13.3365
		5	2.4687	6.2463	6.2463	9.6438	11.9679
		10	2.2586	5.8672	5.8672	9.1026	11.3165
10	0.5	1	10.1611	12.8023	17.3055	21.8971	22.9313
		2	9.0391	11.3900	15.3969	19.4508	20.1989
		5	8.1237	10.2365	13.8344	17.4952	17.8994
		10	7.7116	9.7164	13.1323	16.6838	16.9187
	1	1	4.0952	8.0550	8.0550	11.4161	13.5701
		2	3.6412	7.1728	7.1728	10.1676	12.0827
		5	3.2743	6.4560	6.4560	9.1500	10.8683
		10	3.1020	6.1256	6.1256	8.6848	10.3167
5	0.5	1	7.1792	8.9204	11.1283	11.6376	13.8579
		2	6.3519	7.8994	9.8457	10.3112	12.2252
		5	5.6699	7.0579	8.8152	9.2170	10.8748
		10	5.3778	6.6950	8.3975	8.7442	10.3010
	1	1	3.5242	6.1986	6.1986	8.3451	8.3451
		2	3.1336	5.5041	5.5041	7.3831	7.4133
		5	2.8142	4.9338	4.9338	6.5986	6.6393
		10	2.6715	4.6827	4.6827	6.2825	6.2825

Table 4.2.3: Natural frequency parameters (λ) for CCCC rectangular Si_3N_4/SUS304 FGM flat plates subjected to linear temperature rise ΔT= 300 K.

b/h	a/b	N	λ_1	λ_2	λ_3	λ_4	λ_5
20	0.5	1	12.0985	15.5216	21.6599	29.8473	30.3679
		2	10.8173	13.8796	19.3790	26.6988	27.1786
		5	9.7715	12.5384	17.5155	24.1241	24.5706
		10	9.2797	11.9089	16.6445	22.9367	23.3588
	1	1	4.2788	9.0320	9.0320	13.3336	16.2558
		2	3.7910	8.0563	8.0563	11.9150	14.5372
		5	3.3880	7.2573	7.2573	10.7554	13.1331
		10	3.1908	6.8751	6.8751	10.2059	12.4707

b/h	a/b	N	λ_1	λ_2	λ_3	λ_4	λ_5
10	0.5	1	10.5434	13.2780	17.9069	22.5147	23.5330
		2	9.4139	11.8571	15.9885	20.0520	20.8067
		5	8.4880	10.6908	14.4113	18.0763	18.5170
		10	8.0712	10.1649	13.7019	17.2655	17.5293
	1	1	4.3598	8.4347	8.4347	11.8853	14.0908
		2	3.9001	7.5445	7.5445	10.6275	12.5939
		5	3.5249	6.8160	6.8160	9.5962	11.3653
		10	3.3497	6.4807	6.4807	9.1248	10.8070
5	0.5	1	7.3840	9.1767	11.3881	11.9648	14.2496
		2	6.5550	8.1539	10.1064	10.6368	12.6134
		5	5.8710	7.3097	9.0768	9.5401	11.2565
		10	5.5779	6.9450	8.6582	9.0653	10.6778
	1	1	3.6456	6.3908	6.3908	8.5218	8.5218
		2	3.2529	5.6942	5.6942	7.5590	7.6590
		5	2.9304	5.1207	5.1207	6.7749	6.8815
		10	2.7863	4.8678	4.8678	6.4585	6.5401

Table 4.2.4: Natural frequency parameters (λ) for CCCC rectangular Si_3N_4/SUS304 FGM flat plates subjected to non-linear temperature rise ΔT= 300 K.

b/h	a/b	N	λ_1	λ_2	λ_3	λ_4	λ_5
20	0.5	1	12.1292	15.5589	21.7036	29.8936	30.4182
		2	10.8475	13.9163	19.4220	26.7443	27.2280
		5	9.7938	12.5656	17.5474	24.1582	24.6076
		10	9.2947	11.9272	16.6662	22.9600	23.3841
	1	1	4.3100	9.0686	9.0686	13.3739	16.2977
		2	3.8222	8.0925	8.0925	11.9548	14.5786
		5	3.4110	7.2839	7.2839	10.7847	13.1637
		10	3.2061	6.8928	6.8928	10.2256	12.4913
10	0.5	1	10.5556	13.2932	17.9260	22.5354	23.5542
		2	9.4259	11.8720	16.0073	20.0720	20.8277
		5	8.4971	10.7022	14.4257	18.0912	18.5332
		10	8.0775	10.1728	13.7118	17.2755	17.5405
	1	1	4.3687	8.4471	8.4471	11.9003	14.1074
		2	3.9089	7.5566	7.5566	10.6422	12.6102
		5	3.5314	6.8251	6.8251	9.6074	11.3777
		10	3.3541	6.4870	6.4870	9.1325	10.8156
5	0.5	1	7.3909	9.1852	11.3975	11.9756	14.2624
		2	6.5617	8.1622	10.1155	10.6475	12.6259
		5	5.8762	7.3161	9.0837	9.5484	11.2661
		10	5.5814	6.9494	8.6628	9.0709	10.6844
	1	1	3.6495	6.3970	6.3970	8.5284	8.6091
		2	3.2567	5.7003	5.7003	7.5654	7.6669
		5	2.9333	5.1254	5.1254	6.7796	6.8876
		10	2.7883	4.8711	4.8711	6.4616	6.5443

Table 4.2.5: Effect of temperature on frequency parameters (λ) of CCCC square Si_3N_4/SUS304 FGM flat plates (b/h=10).

N	Temp. Field	λ_1			$\lambda_2 = \lambda_3$		
		300 K	600 K	% Reduction	300 K	600 K	% Reduction
1	Uniform	4.5602	4.0952	10.20	8.7244	8.0550	7.67
	Linear	4.5602	4.3598	4.39	8.7244	8.4347	3.32
	Nonlinear	4.5602	4.3687	4.20	8.7244	8.4471	3.18
10	Uniform	3.5449	3.1020	12.49	6.7567	6.1256	9.34
	Linear	3.5449	3.3497	5.50	6.7567	6.4807	4.08
	Nonlinear	3.5449	3.3541	5.38	6.7567	6.4870	3.99

First three mode shapes for FG flat plate with aspect ratio a/b = 0.5 and 1 are shown in Figure 4.2.2 (b/h=10, N=1, Uniform temperature rise ΔT= 300 K). For a/b=1 i.e. for a square flat plate, mode 2 and 3 are similar (2,1) bending mode as the structure is symmetric. For aspect ratio 0.5, (1,1), (2,1) and (3,1) mode shapes have been observed due to rectangular shape.

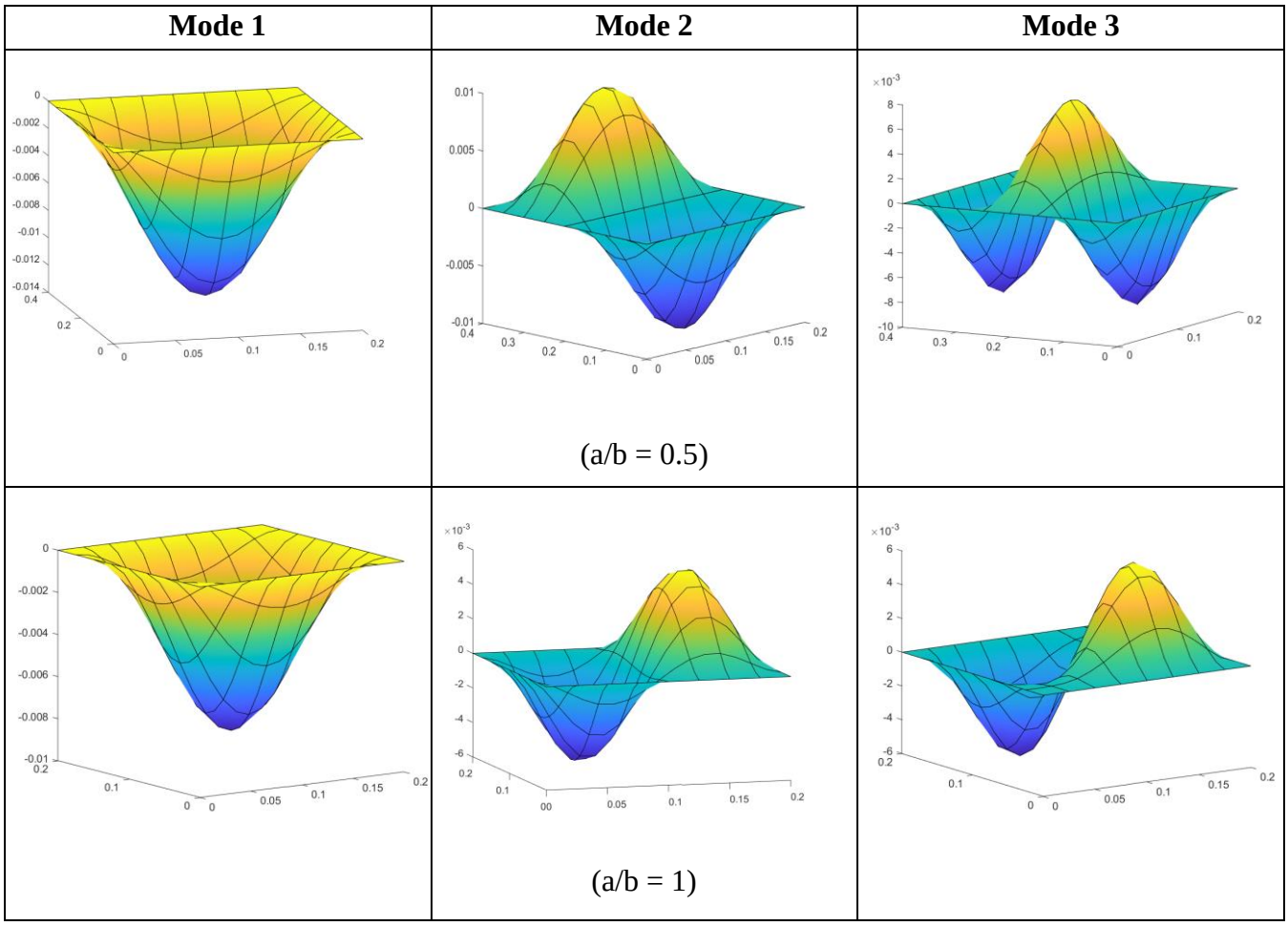

Figure 4.2.2: First three mode shapes for FG flat plate with b/h=10, N=1, Uniform temperature rise ΔT= 300 K.

4.2.2 FGM One-Fold Plate

Impact of various parameters such as power law index, thickness, crank angle, and temperature field, on the natural frequencies of functionally graded (Si_3N_4/SUS304) one-fold plates (Figure 4.2.3), clamped at all four edges, is presented in this section. The crank angles taken are 90^0, 120^0, 150^0 and 180^0 (=flat plate of dimension 1.5 m × 1.5 m). These results include the cases of two different thicknesses (h= 75 mm, 50 mm), and six volume fraction indices (N= 0, 0.5, 1, 2, 5, 10). Uniform, linear and non-linear temperature distributions are shown and the natural frequencies are tabulated from Table 4.2.6 to Table 4.2.15. From these tables, following observations can be made:

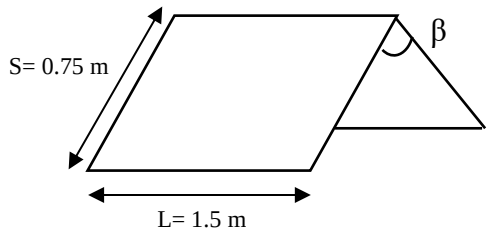

Figure 4.2.3: Geometry of FGM one-fold Plate

Variation in power law index (N): As the value of N increases, the natural frequency of the folded plates decreases exponentially as indicated from Figure 4.2.4. This is obvious as, with the increase in N value, the volume fraction of metal increases, and in turn the ceramic fraction drops, as indicated by Eqn. (3.1.1). This ultimately reduces the rigidity of the plate, and hence the natural frequency.

Variation in plate thickness: Plate having higher thickness is more rigid, for obvious reasons. Hence, the natural frequency increases as thickness of plate increases, which can be clearly observed from Table 4.2.6 to Table 4.2.15.

Variation in crank angle β: The variation in fundamental frequencies has been graphically represented for different thicknesses and crank angles in Figure 4.2.5. From Figure 4.2.5, it can be noted that stiffness of the 75mm thick FGM one-fold structure exhibit minimal sensitivity to changes in the crank angle $\beta = 90^o$ and 120^o. Rather, for $\beta = 120^o$, the stiffness is slightly higher, mass being the same for all cases. For $\beta = 150^o$, the stiffness reduces more as it approaches flat plate configuration and at $\beta=180°$ i.e., flat plate, significant decrease in the stiffness of the plate has been observed. The reduction of natural frequencies is nearly 50% compared to single-fold plates in the absence of thermal load. For one-fold plate with lesser thickness, maximum stiffness is observed at $\beta = 150^o$. The reduction in stiffness increases for uniform or linear temperature rise for lower thicknesses. For 50 mm thick flat plate ($\beta=180°$) with N more than 0.5, uniform temperature rise $\Delta T= 300$ K makes the structure too soft to get the fundamental frequency numerically.

Variation in temperature field: Three types of temperature distribution namely, uniform, linear and non-linear, as given by Eqn. (3.2.1), Eqn. (3.2.2) and Eqn. (3.2.4) is considered for the present study. Natural frequency of the plate decreases with temperature increment as the material properties constantly deteriorate with the temperature rise. Table 4.2.6 to Table 4.2.15 clearly shows that effect of uniform temperature rise is more significant than the linear and non-linear temperature rise as for these cases the thermal distribution is gradual across the thickness. This is the reason for numerical instability for flat plate under uniform temperature increase ΔT= 300 K.

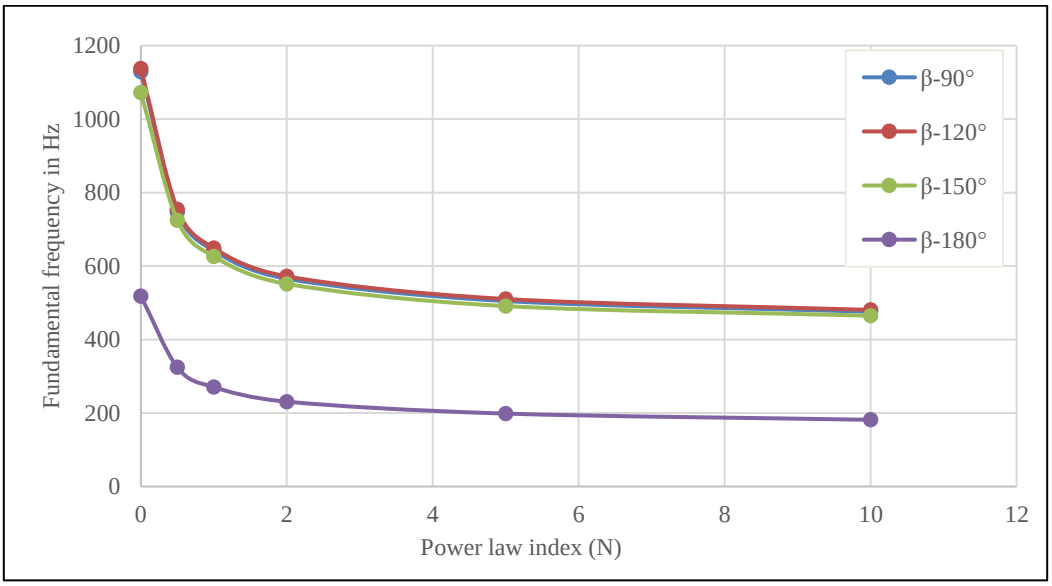

Figure 4.2.4: Variation of first natural frequency (Hz) with gradient index for uniform temperature rise (ΔT= 300 K) and 75 mm plate thickness.

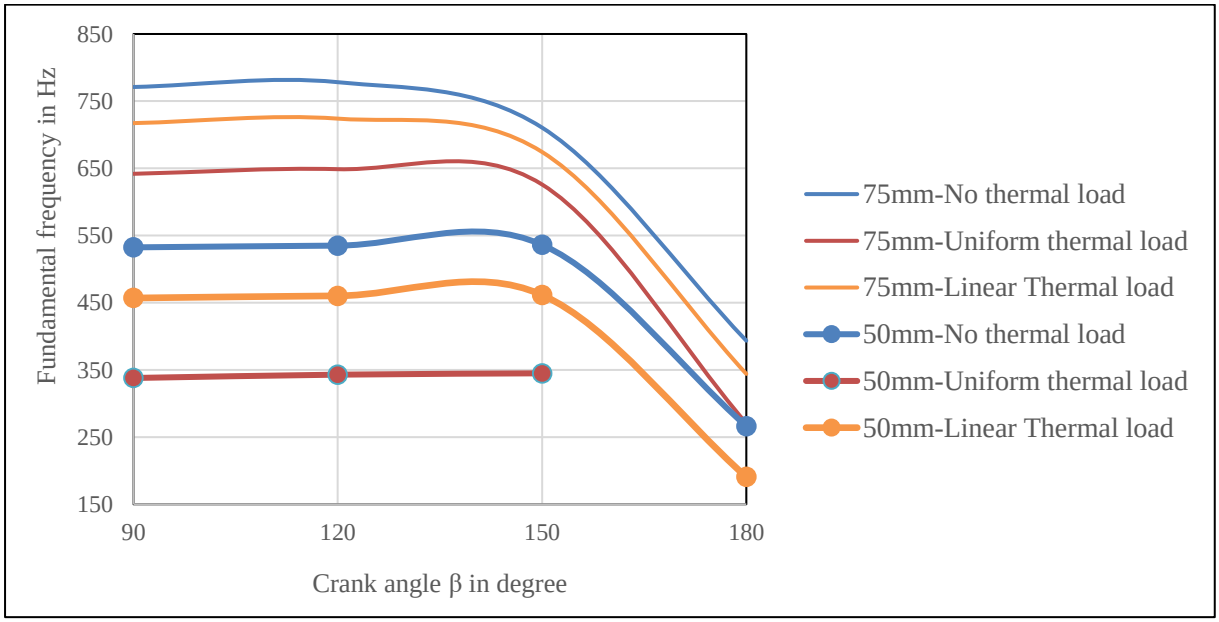

Figure 4.2.5: Variation of first natural frequency (Hz) with crank angle for uniform and linear temperature rise (ΔT= 300 K) and N=1.

First three mode shapes for FG one-fold plate with $\beta = 120^0$ and 180^0 with N=1 are shown in Figure 4.2.6. Local panel modes have been observed for FG one-fold plates. No modifications in mode shapes have been observed in folded plates for introducing thermal load. Antisymmetric bending mode has been noticed in the first and third modes whereas symmetric bending mode is seen for second mode for FG one-fold plate structures.

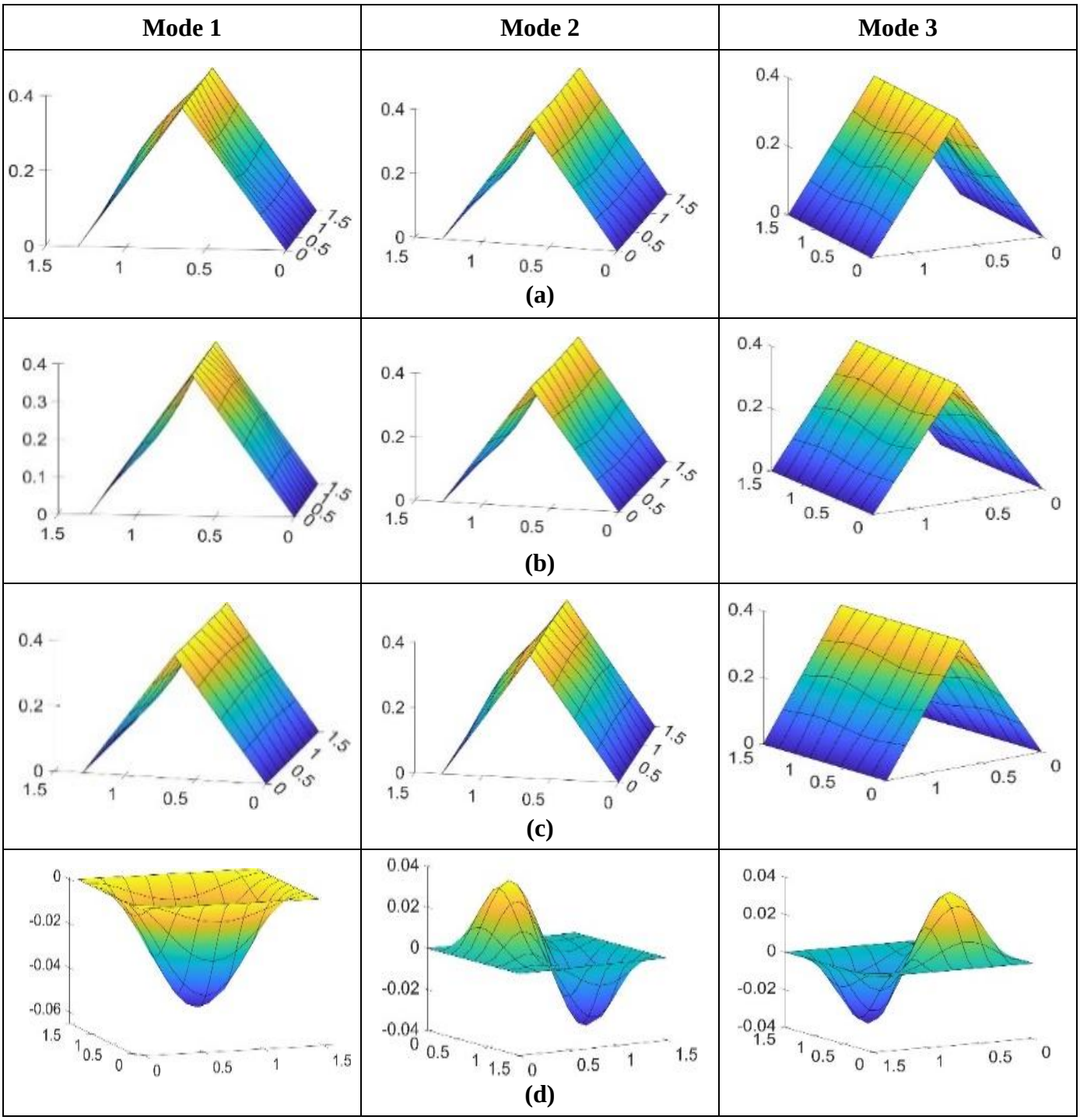

Figure 4.2.6: First three mode shapes for FG one-fold plate with N=1 (a) $\beta = 120^0$ without thermal load (b) $\beta = 120^0$ uniform temp. rise (c) $\beta = 120^0$ linear temp. rise (d) $\beta = 180^0$ linear temp. rise.

4.2.3 FGM Two-Fold Plate

In this section, a set of functionally graded (Si_3N_4/SUS304) two-fold plates, depicted in Figure 4.2.7 along with in-plane dimensions, has been analysed with crank angle, $\beta = 90^0$, clamped all round. The effect of various parameters such as power law index, thickness, and temperature increment, on the natural frequencies is presented. These results include the cases of four different thicknesses (h= 10 mm, 15 mm, 20 mm and 50 mm), and six volume fraction indices (N= 0, 0.5, 1, 2, 5, 10). Uniform, linear and non-linear temperature distributions with three different temperature increment (ΔT= 100 K, 200 K & 300 K) are shown and the natural frequencies for different cases are tabulated from Table 4.2.16 to Table 4.2.25.

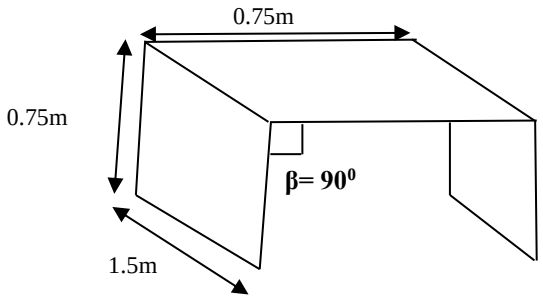

Figure 4.2.7: Geometry of FGM two-fold Plate

Comparing results with one-fold plate, it is observed that for 50 mm, two-fold folded plate produces higher fundamental frequencies than one-fold folded plates of equal thickness and material. Comparison of natural frequencies for one-fold and two-fold folded plates of 90^0 crank angle, 50 mm thickness and N=1 subjected to uniform temperature rise ΔT= 300 K is shown in Figure 4.2.8.

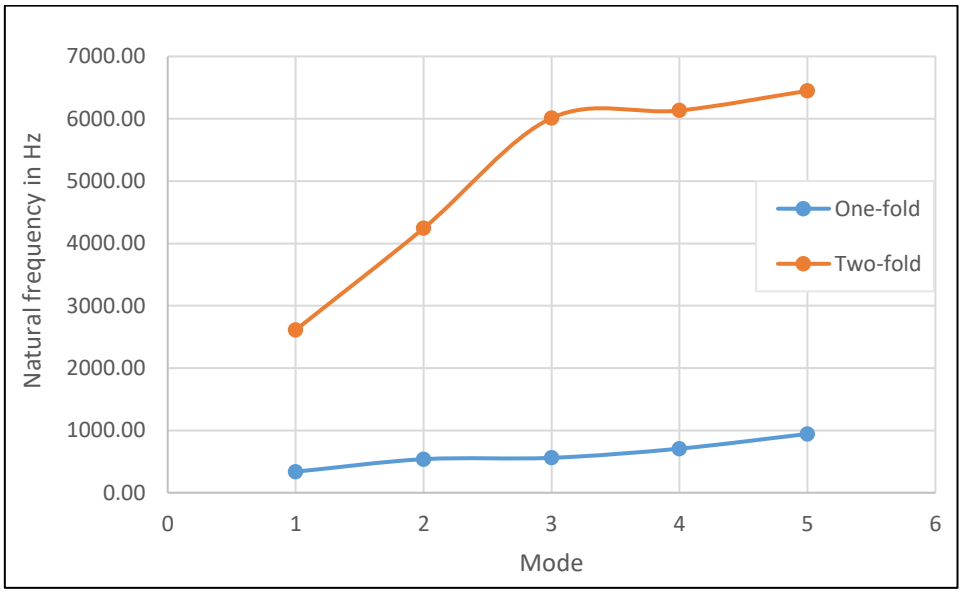

Figure 4.2.8: Comparison of natural frequencies (Hz) for one-fold and two-fold folded plates (β=90°, N=1, h=50 mm, Uniform temperature rise ΔT= 300 K).

Table 4.2.6: Natural frequencies (Hz) of CCCC one-fold Si_3N_4/SUS304 FGM Folded plates without any temperature rise ΔT= 0 K.

Thickness (mm)	N	β-90°						β-120°				
		ω1	ω2	ω3	ω4	ω5		ω1	ω2	ω3	ω4	ω5
75	0	1270.79	1635.91	1840.57	2112.71	2763.05		1280.03	1528.69	1850.86	2016.38	2774.06
	0.5	878.58	1135.29	1273.99	1464.85	1913.31		886.20	1061.79	1282.20	1397.80	1921.79
	1	771.10	996.85	1118.49	1286.01	1679.92		778.25	931.64	1126.12	1226.21	1687.72
	2	692.91	894.61	1004.85	1154.04	1508.70		699.59	834.60	1011.96	1098.89	1515.93
	5	630.99	812.00	914.18	1047.43	1371.19		636.91	756.04	920.54	996.08	1377.70
	10	602.80	774.34	872.76	998.77	1308.29		608.11	721.05	878.54	949.94	1314.25
50	0	875.60	1155.04	1280.44	1495.13	1944.70		878.54	1120.02	1283.93	1461.65	1948.71
	0.5	606.13	801.63	887.08	1037.24	1347.76		608.81	777.69	890.13	1014.04	1351.12
	1	532.39	704.46	779.29	911.36	1184.07		534.97	683.18	782.19	890.64	1187.22
	2	478.88	633.32	700.83	819.15	1064.59		481.30	613.64	703.55	799.95	1067.52
	5	436.44	576.11	638.31	744.98	968.95		438.53	557.61	640.68	726.93	971.54
	10	416.87	549.61	609.44	710.64	924.76		418.70	531.95	611.54	693.42	927.07

Thickness (mm)	N	β-150°						β-180°				
		ω1	ω2	ω3	ω4	ω5		ω1	ω2	ω3	ω4	ω5
75	0	1167.53	1283.67	1700.35	1854.94	2463.58		645.10	1292.29	1292.29	1874.39	2267.68
	0.5	811.29	889.74	1176.34	1285.99	1706.93		447.63	896.38	896.38	1299.71	1572.15
	1	710.65	781.70	1030.34	1129.77	1497.09		393.49	787.77	787.77	1141.98	1381.21
	2	634.56	702.82	921.67	1015.38	1341.60		354.02	708.38	708.38	1026.43	1241.18
	5	573.16	639.67	834.75	923.48	1216.84		322.34	644.52	644.52	933.33	1128.24
	10	547.05	610.47	796.85	881.10	1161.30		307.55	614.81	614.81	890.16	1075.96
50	0	879.70	953.43	1285.31	1308.12	1907.45		436.38	883.64	883.64	1294.62	1573.17
	0.5	610.12	662.85	891.59	906.68	1324.34		302.86	613.17	613.17	898.18	1091.37
	1	536.28	581.33	783.64	795.02	1161.08		266.30	539.08	539.08	789.53	959.34
	2	482.53	520.17	704.91	712.10	1038.97		239.70	485.10	485.10	710.26	862.98
	5	439.56	470.74	641.82	645.50	940.77		218.39	441.80	441.80	646.60	785.57
	10	419.54	449.17	612.49	615.99	897.89		208.40	421.55	421.55	616.89	749.45

Table 4.2.7: Natural frequencies (Hz) of CCCC one-fold Si_3N_4/SUS304 FGM Folded plates subjected to uniform temperature rise ΔT= 100 K.

Thickness (mm)	N	β-90°						β-120°				
		ω_1	ω_2	ω_3	ω_4	ω_5		ω_1	ω_2	ω_3	ω_4	ω_5
75	0	1227.11	1593.80	1785.63	2058.50	2694.63		1236.24	1491.38	1795.57	1965.44	2705.23
	0.5	840.96	1100.21	1227.48	1419.78	1857.02		848.43	1030.89	1235.33	1355.47	1865.08
	1	735.10	963.72	1074.22	1243.43	1626.89		742.07	902.57	1081.47	1186.28	1634.25
	2	658.11	862.99	962.23	1113.34	1458.02		664.58	807.02	968.94	1060.81	1464.80
	5	597.01	781.56	872.72	1008.18	1322.23		602.71	729.66	878.67	959.45	1328.28
	10	568.95	744.29	831.61	959.99	1259.92		574.07	695.03	836.99	913.77	1265.43
50	0	820.09	1103.36	1213.66	1430.50	1866.20		823.62	1071.55	1217.26	1399.11	1870.03
	0.5	555.25	755.44	826.75	979.70	1278.56		558.44	734.37	829.85	958.33	1281.68
	1	482.65	659.71	720.59	855.66	1117.26		485.69	641.25	723.50	836.74	1120.16
	2	430.02	589.72	643.37	764.90	999.57		432.87	572.88	646.06	747.49	1002.22
	5	388.08	533.34	581.62	691.74	905.15		390.61	517.74	583.96	675.51	907.43
	10	368.32	506.91	552.68	657.51	861.12		370.60	492.14	554.75	642.10	863.11

Thickness (mm)	N	β-150°						β-180°				
		ω_1	ω_2	ω_3	ω_4	ω_5		ω_1	ω_2	ω_3	ω_4	ω_5
75	0	1137.31	1239.40	1654.64	1799.09	2401.22		608.22	1243.60	1243.60	1817.15	2205.65
	0.5	786.00	851.46	1137.82	1238.54	1655.31		414.11	853.90	853.90	1251.08	1520.32
	1	686.74	744.98	993.79	1084.54	1448.39		360.84	746.95	746.95	1095.67	1332.14
	2	611.72	667.26	886.63	971.77	1295.06		322.07	668.82	668.82	981.85	1194.14
	5	551.19	604.91	800.91	881.05	1171.93		290.87	605.89	605.89	890.04	1082.72
	10	525.38	575.90	763.43	839.00	1116.98		276.06	576.39	576.39	847.26	1030.96
50	0	824.97	915.73	1218.38	1252.75	1838.98		385.39	821.46	821.46	1225.15	1500.07
	0.5	559.86	629.34	831.01	857.29	1264.42		254.16	555.79	555.79	835.41	1026.19
	1	487.09	549.00	724.63	747.24	1103.46		217.98	482.87	482.87	728.48	896.22
	2	434.17	488.89	647.08	665.63	983.16		191.73	429.86	429.86	650.58	801.49
	5	391.69	440.29	584.76	600.01	886.28		170.51	387.19	387.19	587.88	725.23
	10	371.52	418.81	555.38	570.59	843.71		160.07	366.78	366.78	558.19	689.24

Table 4.2.8: Natural frequencies (Hz) of CCCC one-fold Si_3N_4/SUS304 FGM Folded plates subjected to uniform temperature rise ΔT= 200 K.

Thickness (mm)	N	β-90°						β-120°				
		ω_1	ω_2	ω_3	ω_4	ω_5		ω_1	ω_2	ω_3	ω_4	ω_5
75	0	1180.14	1549.82	1727.54	2002.06	2623.85		1189.20	1452.52	1737.13	1912.43	2634.01
	0.5	797.47	1060.24	1174.32	1368.61	1793.37		804.87	995.60	1181.80	1307.36	1800.97
	1	692.37	924.72	1022.17	1193.51	1564.88		699.24	868.18	1029.04	1139.34	1571.77
	2	616.04	824.86	911.11	1064.48	1397.34		622.37	773.47	917.39	1014.90	1403.62
	5	555.32	744.10	822.20	960.10	1262.49		560.88	696.76	827.71	914.29	1268.03
	10	527.00	706.76	780.91	911.86	1200.12		531.99	662.08	785.85	868.54	1205.12
50	0	756.21	1045.95	1138.73	1359.26	1780.63		760.52	1017.49	1142.50	1330.04	1784.27
	0.5	492.88	700.69	754.84	912.13	1198.14		496.79	682.61	758.02	892.65	1201.00
	1	420.05	605.33	648.94	788.67	1037.79		423.81	589.80	651.90	771.58	1040.38
	2	367.24	535.73	571.96	698.45	920.91		370.79	521.80	574.66	682.85	923.21
	5	324.70	479.50	510.06	625.52	826.87		327.94	466.81	512.36	611.09	828.76
	10	303.79	452.51	480.21	590.69	782.23		306.83	440.65	482.24	577.04	783.82

Thickness (mm)	N	β-150°						β-180°				
		ω_1	ω_2	ω_3	ω_4	ω_5		ω_1	ω_2	ω_3	ω_4	ω_5
75	0	1105.75	1191.86	1606.82	1740.04	2336.53		566.47	1190.95	1190.95	1756.59	2140.80
	0.5	757.29	807.36	1093.98	1184.41	1596.94		373.90	804.90	804.90	1195.70	1461.60
	1	658.68	701.59	950.84	1031.49	1391.48		320.76	698.74	698.74	1041.49	1274.87
	2	584.17	624.47	844.43	919.62	1239.30		282.15	621.33	621.33	928.71	1138.10
	5	524.01	562.49	759.29	829.50	1117.02		250.91	558.87	558.87	837.65	1027.60
	10	498.19	533.26	721.80	787.29	1062.08		235.62	529.14	529.14	794.76	975.80
50	0	762.14	873.77	1143.33	1191.46	1764.88		320.88	749.40	749.40	1147.22	1419.34
	0.5	498.44	589.14	758.85	798.81	1194.42		185.83	485.10	485.10	760.83	949.84
	1	425.40	509.05	652.66	689.15	1034.31		146.34	411.84	411.84	654.33	820.67
	2	372.25	449.27	575.29	607.96	915.07		116.54	358.59	358.59	576.88	726.70
	5	329.20	400.82	512.77	542.46	818.86		90.27	315.31	315.31	514.26	650.84
	10	307.97	378.86	482.50	512.44	775.89		74.52	293.64	293.64	483.79	614.27

Table 4.2.9: Natural frequencies (Hz) of CCCC one-fold Si_3N_4/SUS304 FGM Folded plates subjected to uniform temperature rise ΔT= 300 K.

Thickness (mm)	N	β-90°						β-120°				
		ω_1	ω_2	ω_3	ω_4	ω_5		ω_1	ω_2	ω_3	ω_4	ω_5
75	0	1129.01	1503.20	1665.37	1942.49	2549.66		1138.08	1411.36	1674.61	1856.45	2559.35
	0.5	747.15	1014.66	1113.61	1310.55	1721.47		754.54	955.21	1120.72	1252.64	1728.59
	1	641.89	879.14	961.44	1135.47	1493.11		648.74	827.74	967.90	1084.61	1499.49
	2	565.65	779.55	850.62	1006.77	1326.00		571.94	733.25	856.47	960.43	1331.74
	5	504.88	699.02	761.85	902.64	1191.47		510.38	656.73	766.89	860.00	1196.44
	10	475.82	661.17	719.84	853.78	1128.41		480.77	621.55	724.30	813.64	1132.82
50	0	681.05	981.16	1053.36	1279.68	1686.24		686.43	956.13	1057.35	1252.63	1689.66
	0.5	413.85	634.99	667.77	832.09	1104.32		418.90	619.89	671.09	814.46	1106.86
	1	337.95	538.53	560.04	707.58	943.21		342.90	525.83	563.07	692.22	945.41
	2	282.24	468.22	481.60	616.73	826.00		287.06	457.02	484.30	602.76	827.85
	5	235.86	411.04	417.74	542.91	731.37		240.53	400.99	419.99	530.00	732.73
	10	210.71	382.42	385.25	506.33	685.05		215.37	373.09	387.21	494.13	686.07

Thickness (mm)	N	β-150°						β-180°				
		ω_1	ω_2	ω_3	ω_4	ω_5		ω_1	ω_2	ω_3	ω_4	ω_5
75	0	1072.34	1140.18	1556.12	1676.84	2268.54		518.41	1133.35	1133.35	1691.77	2072.18
	0.5	724.68	756.49	1044.11	1122.68	1531.01		324.66	748.25	748.25	1132.66	1395.17
	1	625.98	650.52	900.80	969.70	1325.62		270.39	641.96	641.96	978.58	1208.68
	2	551.43	573.44	794.41	858.05	1173.69		230.90	564.70	564.70	866.23	1072.45
	5	491.17	511.39	709.29	768.05	1051.59		198.52	502.29	502.29	775.50	962.39
	10	465.02	481.45	671.36	725.14	996.11		181.62	471.80	471.80	731.98	910.00
50	0	688.45	826.04	1057.85	1122.52	1683.19		230.99	663.81	663.81	1058.47	1329.06
	0.5	420.95	539.89	671.52	728.70	1107.61		37.61	394.36	394.36	670.87	859.73
	1	344.90	458.59	563.39	617.77	946.08		-	-	-	-	-
	2	288.94	397.99	484.45	535.68	828.40		-	-	-	-	-
	5	242.26	348.53	419.89	469.01	733.08		-	-	-	-	-
	10	217.10	324.99	386.96	437.19	686.28		-	-	-	-	-

Table 4.2.10: Natural frequencies (Hz) of CCCC one-fold Si_3N_4/SUS304 FGM Folded plates subjected to linear temperature rise ΔT= 100 K.

Thickness (mm)	N	β-90°						β-120°				
		ω_1	ω_2	ω_3	ω_4	ω_5		ω_1	ω_2	ω_3	ω_4	ω_5
75	0	1249.66	1615.05	1813.80	2085.85	2729.46		1258.69	1510.20	1823.78	1991.14	2740.14
	0.5	861.07	1118.47	1252.10	1443.23	1886.43		868.53	1046.94	1260.05	1377.50	1894.63
	1	754.38	981.03	1097.70	1265.66	1654.65		761.37	917.72	1105.08	1207.14	1662.19
	2	676.67	879.48	984.76	1134.56	1484.50		683.18	821.39	991.61	1080.69	1491.46
	5	614.94	797.34	894.43	1028.51	1347.64		620.69	743.36	900.54	978.48	1353.88
	10	586.72	759.84	853.06	980.04	1284.96		591.87	708.54	858.59	932.54	1290.66
50	0	848.82	1129.76	1248.03	1463.47	1906.34		851.97	1096.33	1251.50	1431.03	1910.19
	0.5	582.97	780.18	859.32	1010.44	1315.49		585.82	757.58	862.34	988.10	1318.69
	1	509.85	683.77	752.38	885.52	1153.02		512.59	663.82	755.25	865.66	1156.02
	2	456.61	613.07	674.34	793.86	1034.21		459.18	594.74	677.00	775.52	1036.98
	5	414.07	555.99	611.80	719.85	938.76		416.32	538.91	614.12	702.70	941.17
	10	394.22	529.38	582.69	685.39	894.43		396.22	513.16	584.74	669.09	896.57

Thickness (mm)	N	β-150°						β-180°				
		ω_1	ω_2	ω_3	ω_4	ω_5		ω_1	ω_2	ω_3	ω_4	ω_5
75	0	1152.59	1261.98	1677.77	1827.47	2432.96		627.13	1268.35	1268.35	1846.13	2236.99
	0.5	799.19	871.75	1158.00	1263.50	1682.32		432.20	876.43	876.43	1276.61	1547.37
	1	699.26	764.50	1013.02	1108.41	1473.94		378.53	768.66	768.66	1120.05	1357.82
	2	623.68	686.09	905.07	994.71	1319.44		339.29	689.77	689.77	1005.25	1218.70
	5	562.68	623.13	818.64	903.16	1195.33		307.62	626.12	626.12	912.55	1106.29
	10	536.71	593.92	780.91	860.85	1140.03		292.70	596.40	596.40	869.47	1054.19
50	0	853.16	935.00	1252.69	1281.03	1873.92		412.06	853.49	853.49	1260.71	1537.38
	0.5	587.14	647.27	863.62	883.73	1296.29		281.31	587.00	587.00	869.18	1061.05
	1	513.90	566.38	756.51	772.92	1134.20		245.10	513.57	513.57	761.44	930.09
	2	460.41	505.67	678.18	690.54	1012.83		218.58	459.88	459.88	682.64	834.33
	5	417.33	456.50	615.07	624.16	915.00		197.02	416.49	416.49	619.03	757.06
	10	397.07	434.91	585.52	594.58	872.14		186.68	395.96	395.96	589.11	720.79

Table 4.2.11: Natural frequencies (Hz) of CCCC one-fold Si_3N_4/SUS304 FGM Folded plates subjected to linear temperature rise ΔT= 200 K.

Thickness (mm)	N	β-90°						β-120°				
		ω_1	ω_2	ω_3	ω_4	ω_5		ω_1	ω_2	ω_3	ω_4	ω_5
75	0	1227.67	1593.80	1786.25	2058.53	2695.39		1236.52	1491.41	1795.93	1965.48	2705.74
	0.5	842.53	1100.96	1229.14	1420.77	1858.58		849.84	1031.48	1236.83	1356.40	1866.51
	1	736.50	964.33	1075.66	1244.23	1628.14		743.33	903.03	1082.78	1187.03	1635.40
	2	659.08	863.25	963.15	1113.70	1458.68		665.42	807.17	969.75	1061.15	1465.36
	5	597.22	781.18	872.73	1007.71	1321.83		602.80	729.29	878.56	959.05	1327.78
	10	568.66	743.46	831.00	958.96	1258.78		573.65	694.31	836.26	912.87	1264.19
50	0	819.92	1103.05	1213.51	1430.13	1866.16		823.33	1071.26	1216.98	1398.76	1869.86
	0.5	557.55	757.10	829.27	981.73	1281.11		560.62	735.90	832.28	960.28	1284.16
	1	484.86	661.28	722.99	857.57	1119.63		487.81	642.69	725.82	838.58	1122.46
	2	431.64	590.78	645.08	766.18	1001.17		434.41	573.85	647.71	748.72	1003.77
	5	388.60	533.46	582.07	691.85	905.34		391.06	517.82	584.33	675.62	907.56
	10	368.13	506.40	552.30	656.85	860.37		370.35	491.66	554.30	641.47	862.31

Thickness (mm)	N	β-150°						β-180°				
		ω_1	ω_2	ω_3	ω_4	ω_5		ω_1	ω_2	ω_3	ω_4	ω_5
75	0	1137.35	1239.46	1654.72	1799.22	2401.82		607.92	1243.41	1243.41	1817.08	2205.67
	0.5	786.57	852.75	1138.87	1239.94	1656.76		415.44	855.28	855.28	1252.42	1521.59
	1	687.21	746.15	994.71	1085.77	1449.57		362.13	748.22	748.22	1096.84	1333.20
	2	611.96	668.01	887.21	972.50	1295.72		322.98	669.64	669.64	982.52	1194.68
	5	551.06	604.90	800.87	880.85	1171.69		291.07	605.85	605.85	889.76	1082.27
	10	525.00	575.38	762.98	838.18	1116.13		275.80	575.78	575.78	846.34	1029.83
50	0	824.58	915.53	1217.99	1252.45	1838.97		384.75	820.87	820.87	1224.63	1499.62
	0.5	561.97	630.45	833.39	859.05	1266.44		256.50	558.21	558.21	837.84	1028.56
	1	489.14	550.04	726.91	748.90	1105.28		220.35	485.24	485.24	730.81	898.47
	2	435.66	489.58	648.69	666.78	984.36		193.52	431.58	431.58	652.21	803.02
	5	392.09	440.34	585.09	600.21	886.38		171.17	387.67	387.67	588.19	725.41
	10	371.23	418.46	554.89	570.18	843.12		160.00	366.47	366.47	557.65	688.55

Table 4.2.12: Natural frequencies (Hz) of CCCC one-fold Si_3N_4/SUS304 FGM Folded plates subjected to linear temperature rise ΔT= 300 K.

Thickness (mm)	N	β-90°						β-120°				
		ω1	ω2	ω3	ω4	ω5		ω1	ω2	ω3	ω4	ω5
75	0	1204.67	1572.00	1757.72	2030.54	2660.57		1213.37	1472.16	1767.11	1939.20	2670.60
	0.5	822.82	1082.64	1204.95	1397.30	1829.58		830.00	1015.30	1212.40	1334.34	1837.23
	1	717.31	946.66	1052.21	1221.59	1600.20		724.01	887.43	1059.08	1165.75	1607.18
	2	640.02	845.82	939.91	1091.35	1431.09		646.21	791.84	946.23	1040.17	1437.49
	5	577.72	763.43	848.97	984.92	1293.65		583.13	713.74	854.52	937.70	1299.30
	10	548.53	725.14	806.49	935.44	1229.67		553.35	678.27	811.44	890.86	1234.76
50	0	788.57	1074.64	1176.58	1394.84	1823.86		792.30	1044.55	1180.07	1364.56	1827.39
	0.5	529.48	732.15	796.62	950.85	1244.36		532.83	712.37	799.62	930.31	1247.24
	1	456.99	636.74	690.75	827.24	1083.62		460.20	619.54	693.57	809.12	1086.28
	2	403.49	566.22	612.69	735.84	965.21		406.52	550.69	615.28	719.25	967.61
	5	359.48	508.25	548.72	660.72	868.47		362.21	494.08	550.93	645.40	870.47
	10	337.96	480.38	517.85	624.74	822.34		340.47	467.12	519.79	610.29	824.05

Thickness (mm)	N	β-150°						β-180°				
		ω1	ω2	ω3	ω4	ω5		ω1	ω2	ω3	ω4	ω5
75	0	1121.71	1215.96	1631.02	1770.00	2369.95		587.28	1217.28	1217.28	1787.02	2173.50
	0.5	773.35	832.59	1118.82	1215.15	1630.08		397.16	832.80	832.80	1226.99	1494.63
	1	674.40	726.50	975.30	1061.71	1423.84		344.07	726.30	726.30	1072.21	1307.20
	2	599.30	648.46	868.01	948.64	1270.30		304.85	647.84	647.84	958.14	1169.00
	5	538.23	584.89	781.38	856.46	1145.82		272.44	583.59	583.59	864.89	1056.09
	10	511.88	554.74	742.99	813.02	1089.52		256.59	552.85	552.85	820.70	1002.82
50	0	793.63	894.82	1180.89	1222.13	1802.32		353.67	785.38	785.38	1186.05	1459.59
	0.5	534.24	612.19	800.54	832.40	1234.48		227.33	526.34	526.34	803.83	993.61
	1	461.58	532.08	694.45	722.69	1074.01		190.63	453.57	453.57	697.30	864.19
	2	407.81	471.64	616.05	640.56	953.27		162.74	399.59	399.59	618.62	768.78
	5	363.28	422.01	551.48	573.35	854.70		138.44	354.63	354.63	553.72	690.37
	10	341.42	399.54	520.17	542.49	810.59		125.45	332.30	332.30	522.11	652.45

Table 4.2.13: Natural frequencies (Hz) of CCCC one-fold Si_3N_4/SUS304 FGM Folded plates subjected to non-linear temperature rise ΔT= 100 K.

Thickness (mm)	N	β-90°						β-120°				
		ω_1	ω_2	ω_3	ω_4	ω_5		ω_1	ω_2	ω_3	ω_4	ω_5
75	0	1249.66	1615.05	1813.80	2085.85	2729.46		1258.69	1510.20	1823.78	1991.14	2740.14
	0.5	861.71	1119.05	1252.87	1443.97	1887.35		869.16	1047.45	1260.83	1378.20	1895.56
	1	755.13	981.70	1098.61	1266.53	1655.73		762.12	918.32	1106.00	1207.95	1663.27
	2	677.40	880.13	985.64	1135.39	1485.53		683.91	821.96	992.50	1081.47	1492.50
	5	615.46	797.80	895.06	1029.11	1348.38		621.21	743.76	901.17	979.03	1354.63
	10	587.05	760.14	853.47	980.43	1285.44		592.21	708.80	859.01	932.90	1291.14
50	0	848.82	1129.76	1248.03	1463.47	1906.34		851.97	1096.33	1251.50	1431.03	1910.19
	0.5	583.86	780.97	860.36	1011.42	1316.67		586.70	758.33	863.38	989.06	1319.88
	1	510.92	684.72	753.64	886.70	1154.43		513.65	664.71	756.50	866.80	1157.43
	2	457.66	613.99	675.57	795.01	1035.58		460.22	595.61	678.23	776.64	1038.36
	5	414.82	556.65	612.68	720.67	939.74		417.07	539.53	615.00	703.50	942.16
	10	394.71	529.81	583.26	685.93	895.07		396.71	513.56	585.31	669.60	897.21

Thickness (mm)	N	β-150°						β-180°				
		ω_1	ω_2	ω_3	ω_4	ω_5		ω_1	ω_2	ω_3	ω_4	ω_5
75	0	1152.59	1261.98	1677.77	1827.47	2432.96		627.13	1268.35	1268.35	1846.13	2236.99
	0.5	799.63	872.40	1158.66	1264.29	1683.18		432.78	877.15	877.15	1277.42	1548.22
	1	699.77	765.27	1013.78	1109.34	1474.94		379.23	769.52	769.52	1121.00	1358.82
	2	624.17	686.83	905.80	995.61	1320.40		339.97	690.60	690.60	1006.17	1219.66
	5	563.03	623.66	819.16	903.81	1196.01		308.11	626.71	626.71	913.20	1106.98
	10	536.93	594.27	781.25	861.27	1140.47		293.02	596.79	596.79	869.90	1054.64
50	0	853.16	935.00	1252.69	1281.03	1873.92		412.06	853.49	853.49	1260.71	1537.38
	0.5	588.02	647.85	864.67	884.59	1297.33		282.17	588.00	588.00	870.27	1062.17
	1	514.95	567.07	757.77	773.94	1135.43		246.15	514.78	514.78	762.74	931.43
	2	461.44	506.34	679.42	691.53	1014.02		219.61	461.07	461.07	683.91	835.63
	5	418.08	456.98	615.96	624.87	915.84		197.77	417.35	417.35	619.94	757.99
	10	397.56	435.22	586.10	595.03	872.69		187.17	396.52	396.52	589.70	721.40

Table 4.2.14: Natural frequencies (Hz) of CCCC one-fold Si_3N_4/SUS304 FGM Folded plates subjected to non-linear temperature rise ΔT= 200 K.

Thickness (mm)	N	β-90°						β-120°				
		ω_1	ω_2	ω_3	ω_4	ω_5		ω_1	ω_2	ω_3	ω_4	ω_5
75	0	1227.67	1593.80	1786.25	2058.53	2695.39		1236.52	1491.41	1795.93	1965.48	2705.74
	0.5	843.88	1102.18	1230.78	1422.33	1860.52		851.19	1032.57	1238.48	1357.88	1868.46
	1	738.11	965.77	1077.60	1246.08	1630.41		744.94	904.30	1084.74	1188.77	1637.69
	2	660.66	864.65	965.05	1115.50	1460.89		667.01	808.41	971.66	1062.85	1467.60
	5	598.36	782.20	874.11	1009.02	1323.45		603.95	730.18	879.96	960.28	1329.41
	10	569.41	744.14	831.91	959.82	1259.85		574.41	694.90	837.18	913.68	1265.27
50	0	819.92	1103.05	1213.51	1430.13	1866.16		823.33	1071.26	1216.98	1398.76	1869.86
	0.5	559.49	758.81	831.53	983.84	1283.63		562.54	737.51	834.53	962.34	1286.69
	1	487.22	663.34	725.72	860.12	1122.65		490.14	644.63	728.55	841.06	1125.50
	2	433.99	592.82	647.79	768.70	1004.16		436.74	575.76	650.41	751.17	1006.76
	5	390.32	534.94	584.04	693.68	907.52		392.75	519.21	586.31	677.40	909.75
	10	369.26	507.37	553.60	658.05	861.80		371.47	492.57	555.60	642.64	863.75

Thickness (mm)	N	β-150°						β-180°				
		ω_1	ω_2	ω_3	ω_4	ω_5		ω_1	ω_2	ω_3	ω_4	ω_5
75	0	1137.35	1239.46	1654.72	1799.22	2401.82		607.92	1243.41	1243.41	1817.08	2205.67
	0.5	787.49	854.12	1140.25	1241.61	1658.57		416.70	856.81	856.81	1254.13	1523.38
	1	688.29	747.78	996.34	1087.75	1451.70		363.65	750.05	750.05	1098.87	1335.32
	2	613.01	669.62	888.80	974.45	1297.79		324.49	671.43	671.43	984.51	1196.75
	5	551.81	606.07	802.02	882.27	1173.19		292.17	607.15	607.15	891.21	1083.78
	10	525.50	576.15	763.73	839.12	1117.11		276.53	576.64	576.64	847.29	1030.83
50	0	824.58	915.53	1217.99	1252.45	1838.97		384.75	820.87	820.87	1224.63	1499.62
	0.5	563.89	631.72	835.65	860.90	1268.66		258.48	560.41	560.41	840.19	1030.96
	1	491.47	551.56	729.65	751.12	1107.94		222.79	487.93	487.93	733.65	901.36
	2	437.97	491.07	651.41	668.97	986.96		195.99	434.25	434.25	655.02	805.87
	5	393.78	441.42	587.08	601.79	888.26		172.99	389.61	389.61	590.23	727.48
	10	372.34	419.17	556.19	571.22	844.35		161.21	367.74	367.74	558.99	689.91

Table 4.2.15: Natural frequencies (Hz) of CCCC one-fold Si_3N_4/SUS304 FGM Folded plates subjected to non-linear temperature rise ΔT= 300 K.

Thickness (mm)	N	β-90°						β-120°				
		ω1	ω2	ω3	ω4	ω5		ω1	ω2	ω3	ω4	ω5
75	0	1204.67	1572.00	1757.72	2030.54	2660.57		1213.37	1472.16	1767.11	1939.20	2670.60
	0.5	824.97	1084.57	1207.55	1399.76	1832.62		832.15	1017.01	1215.01	1336.67	1840.29
	1	719.90	948.95	1055.31	1224.53	1603.81		726.60	889.47	1062.21	1168.53	1610.82
	2	642.57	848.08	942.98	1094.25	1434.65		648.77	793.84	949.33	1042.91	1441.08
	5	579.60	765.11	851.23	987.06	1296.29		585.02	715.21	856.80	939.73	1301.96
	10	549.78	726.27	808.00	936.88	1231.45		554.61	679.26	812.97	892.22	1236.55
50	0	788.57	1074.64	1176.58	1394.84	1823.86		792.30	1044.55	1180.07	1364.56	1827.39
	0.5	532.68	734.91	800.28	954.26	1248.39		535.99	714.98	803.28	933.62	1251.29
	1	460.92	640.10	695.23	831.38	1088.51		464.09	622.73	698.04	813.15	1091.19
	2	407.45	569.57	617.16	739.96	970.07		410.43	553.86	619.75	723.27	972.49
	5	362.41	510.72	552.02	663.77	872.05		365.11	496.42	554.23	648.36	874.07
	10	339.91	482.02	520.05	626.76	824.73		342.40	468.68	521.99	612.26	826.44

Thickness (mm)	N	β-150°						β-180°				
		ω1	ω2	ω3	ω4	ω5		ω1	ω2	ω3	ω4	ω5
75	0	1121.71	1215.96	1631.02	1770.00	2369.95		587.28	1217.28	1217.28	1787.02	2173.50
	0.5	774.79	834.77	1120.99	1217.80	1632.93		399.21	835.24	835.24	1229.70	1497.46
	1	676.13	729.13	977.89	1064.88	1427.23		346.59	729.24	729.24	1075.45	1310.57
	2	601.01	651.06	870.57	951.77	1273.64		307.36	650.75	650.75	961.33	1172.32
	5	539.48	586.81	783.26	858.77	1148.28		274.29	585.73	585.73	867.24	1058.55
	10	512.70	556.02	744.24	814.57	1091.16		257.81	554.28	554.28	822.28	1004.47
50	0	793.63	894.82	1180.89	1222.13	1802.32		353.67	785.38	785.38	1186.05	1459.59
	0.5	537.39	614.24	804.22	835.38	1238.04		230.82	529.98	529.98	807.63	997.48
	1	465.46	534.58	698.95	726.32	1078.32		195.06	458.05	458.05	701.94	868.88
	2	411.71	474.13	620.55	644.17	957.52		167.34	404.10	404.10	623.24	773.44
	5	366.18	423.84	554.80	576.01	857.81		141.99	357.97	357.97	557.12	693.79
	10	343.34	400.76	522.38	544.26	812.65		127.89	334.51	334.51	524.37	654.72

Table 4.2.16: Natural frequencies (Hz) of CCCC two-fold (90^0 crank angle) Si_3N_4/SUS304 FGM Folded plate without temperature rise ΔT= 0 K.

Thickness	**10 mm**							**15 mm**					
N	**0**	**0.5**	**1**	**2**	**5**	**10**		**0**	**0.5**	**1**	**2**	**5**	**10**
ω_1	2949.28	2046.59	1786.14	1584.13	1417.46	1347.70		3196.87	2220.31	1937.59	1717.52	1535.52	1459.27
ω_2	3132.21	2164.92	1900.74	1709.84	1559.62	1490.69		4572.77	3154.40	2766.83	2486.64	2267.42	2168.41
ω_3	3406.42	2355.19	2067.92	1860.13	1696.46	1621.39		4958.29	3422.03	3001.86	2697.66	2459.17	2351.50
ω_4	3874.38	2679.89	2353.28	2116.78	1930.14	1844.51		5549.68	3848.41	3365.66	2996.84	2693.33	2563.25
ω_5	4375.19	3033.44	2660.53	2383.80	2160.11	2059.77		5621.15	3884.98	3408.08	3061.62	2789.51	2666.65

Thickness	**20 mm**							**50 mm**					
N	**0**	**0.5**	**1**	**2**	**5**	**10**		**0**	**0.5**	**1**	**2**	**5**	**10**
ω_1	3399.40	2362.41	2062.93	1830.43	1638.01	1556.59		4665.91	3246.91	2842.00	2530.90	2272.27	2158.67
ω_2	5879.42	4048.19	3547.24	3184.39	2901.46	2775.83		7437.81	5173.22	4520.46	4012.95	3589.16	3406.97
ω_3	6079.18	4222.88	3687.84	3273.09	2930.32	2785.87		10453.56	7195.97	6281.51	5598.32	5061.94	4842.87
ω_4	6355.59	4379.91	3838.59	3445.63	3138.39	3001.97		10754.60	7421.81	6481.56	5765.21	5174.20	4920.14
ω_5	7182.82	4955.34	4344.16	3899.17	3549.53	3393.90		11114.02	7727.14	6751.10	5991.47	5355.05	5096.51

Table 4.2.17: Natural frequencies (Hz) of CCCC two-fold (90^0 crank angle) Si_3N_4/SUS304 FGM Folded plate subjected to uniform temperature rise ΔT= 100 K.

Thickness	**10 mm**							**15 mm**					
N	**0**	**0.5**	**1**	**2**	**5**	**10**		**0**	**0.5**	**1**	**2**	**5**	**10**
ω_1	2832.88	1941.98	1685.13	1486.70	1323.05	1253.60		3100.83	2137.82	1858.66	1641.13	1460.84	1385.04
ω_2	2917.43	1962.42	1700.24	1510.72	1360.19	1288.67		4414.69	3017.17	2635.06	2358.97	2142.32	2043.33
ω_3	3179.57	2142.46	1857.74	1651.83	1488.32	1410.90		4789.24	3275.81	2861.68	2562.04	2326.60	2219.19
ω_4	3628.45	2451.09	2127.98	1894.12	1708.39	1620.77		5392.37	3709.79	3236.30	2876.39	2579.92	2451.55
ω_5	4084.33	2762.18	2395.11	2125.00	1907.00	1805.78		5434.44	3728.01	3256.29	2913.64	2645.04	2522.78

Thickness	**20 mm**							**50 mm**					
N	**0**	**0.5**	**1**	**2**	**5**	**10**		**0**	**0.5**	**1**	**2**	**5**	**10**
ω_1	3305.76	2283.09	1987.41	1757.59	1567.01	1486.13		4576.09	3175.82	2776.19	2469.02	2213.42	2101.00
ω_2	5741.51	3936.30	3442.51	3085.00	2805.99	2681.57		7322.65	5086.09	4441.48	3940.29	3521.73	3341.77
ω_3	5956.71	4123.94	3596.00	3187.18	2849.28	2706.40		10328.38	7112.04	6209.63	5535.59	5006.46	4790.35
ω_4	6206.87	4259.32	3725.78	3338.64	3035.64	2900.43		10601.54	7312.31	6383.84	5675.46	5090.56	4839.42
ω_5	7016.45	4820.89	4218.59	3780.26	3435.64	3281.63		10978.69	7631.40	6668.77	5923.44	5297.30	5042.21

Table 4.2.18: Natural frequencies (Hz) of CCCC two-fold (90^0 crank angle) Si_3N_4/SUS304 FGM Folded plate subjected to uniform temperature rise ΔT= 200 K.

Thickness	**10 mm**							**15 mm**					
N	**0**	**0.5**	**1**	**2**	**5**	**10**		**0**	**0.5**	**1**	**2**	**5**	**10**
ω_1	2629.84	1653.88	1376.56	1172.36	1002.89	913.15		2998.89	2043.60	1765.68	1548.55	1367.77	1291.20
ω_2	2695.53	1801.97	1526.64	1307.36	1126.47	1032.10		4233.89	2843.35	2461.40	2185.43	1967.59	1865.39
ω_3	2881.07	1825.68	1542.51	1342.73	1177.46	1103.04		4597.55	3092.59	2679.07	2379.96	2143.77	2033.39
ω_4	3313.09	2121.61	1786.40	1540.98	1340.18	1237.47		5219.86	3521.72	3054.16	2713.64	2426.87	2297.78
ω_5	3727.43	2398.64	2024.73	1749.81	1524.68	1412.12		5225.34	3554.55	3080.88	2724.05	2449.52	2324.49

Thickness	**20 mm**							**50 mm**					
N	**0**	**0.5**	**1**	**2**	**5**	**10**		**0**	**0.5**	**1**	**2**	**5**	**10**
ω_1	3207.54	2193.31	1899.14	1669.90	1479.02	1397.49		4486.02	3096.85	2699.76	2394.27	2139.53	2026.97
ω_2	5594.59	3802.30	3311.31	2956.24	2678.76	2553.36		7210.89	4990.23	4349.32	3850.53	3433.39	3253.60
ω_3	5831.94	4011.90	3487.20	3081.14	2745.28	2602.55		10212.17	7017.08	6120.16	5450.52	4925.16	4710.35
ω_4	6049.21	4115.97	3585.63	3201.28	2900.18	2764.27		10455.07	7191.25	6267.97	5562.03	4978.00	4726.98
ω_5	6841.32	4662.63	4064.22	3629.29	3287.18	3132.74		10852.57	7524.88	6568.68	5832.68	5211.20	4956.63

Table 4.2.19: Natural frequencies (Hz) of CCCC two-fold (90^0 crank angle) Si_3N_4/SUS304 FGM Folded plate subjected to uniform temperature rise ΔT= 300 K.

Thickness	**10 mm**							**15 mm**					
N	**0**	**0.5**	**1**	**2**	**5**	**10**		**0**	**0.5**	**1**	**2**	**5**	**10**
ω_1	2218.92	1122.71	745.86	376.82	-	-		2889.17	1935.69	1656.58	1437.61	1253.89	1175.04
ω_2	2463.56	1300.00	917.93	583.30	-	-		4020.76	2618.87	2229.28	1947.17	1721.60	1610.21
ω_3	2516.08	1564.68	1204.30	882.11	-	-		4373.81	2858.75	2437.98	2133.17	1889.86	1770.68
ω_4	2886.04	1604.14	1257.79	1003.61	-	-		4984.80	3274.52	2800.47	2456.88	2182.93	2050.01
ω_5	3272.03	1878.41	1460.15	1137.45	-	-		5024.74	3350.46	2872.83	2513.54	2219.61	2085.00

Thickness	**20 mm**							**50 mm**					
N	**0**	**0.5**	**1**	**2**	**5**	**10**		**0**	**0.5**	**1**	**2**	**5**	**10**
ω_1	3103.18	2091.72	1796.79	1566.05	1372.59	1289.06		4394.26	3009.07	2611.98	2306.10	2050.20	1936.20
ω_2	5434.02	3640.71	3147.69	2791.83	2513.17	2384.28		7100.45	4884.39	4242.97	3742.95	3323.63	3141.99
ω_3	5702.21	3884.21	3358.93	2952.70	2616.22	2471.84		10101.98	6908.99	6011.19	5341.42	4816.56	4582.06
ω_4	5877.94	3944.45	3412.28	3027.40	2725.52	2586.38		10312.25	7056.79	6132.49	5423.77	4835.67	4601.47
ω_5	6652.71	4475.27	3875.39	3440.35	3097.94	2940.48		10732.52	7405.05	6448.36	5716.72	5095.50	4838.56

Table 4.2.20: Natural frequencies (Hz) of CCCC two-fold (90^0 crank angle) Si_3N_4/SUS304 FGM Folded plate subjected to linear temperature rise ΔT= 100 K.

Thickness	10 mm							15 mm					
N	0	0.5	1	2	5	10		0	0.5	1	2	5	10
ω_1	2892.53	1998.50	1740.10	1539.68	1374.12	1304.42		3148.76	2180.70	1899.89	1681.06	1499.81	1423.76
ω_2	3032.40	2077.82	1815.58	1625.32	1474.22	1403.81		4498.13	3092.45	2707.67	2429.19	2210.58	2111.30
ω_3	3300.55	2263.09	1978.00	1771.05	1606.64	1530.16		4878.25	3355.76	2938.65	2636.36	2398.67	2290.83
ω_4	3758.89	2579.88	2255.86	2020.48	1833.34	1746.39		5472.17	3784.03	3305.48	2940.41	2640.04	2510.81
ω_5	4236.23	2912.30	2543.02	2269.04	2046.82	1945.49		5532.35	3812.39	3338.69	2994.20	2723.12	2600.25

Thickness	20 mm							50 mm					
N	0	0.5	1	2	5	10		0	0.5	1	2	5	10
ω_1	3352.14	2323.94	2026.52	1795.35	1603.80	1522.66		4619.13	3210.87	2808.84	2499.87	2242.94	2130.10
ω_2	5814.96	3996.99	3499.41	3138.93	2857.53	2732.44		7376.34	5127.48	4479.26	3975.40	3554.89	3374.27
ω_3	6017.08	4174.00	3642.70	3231.04	2890.94	2747.43		10398.61	7157.59	6248.43	5569.75	5037.48	4820.34
ω_4	6285.82	4324.51	3786.86	3396.49	3090.91	2954.94		10673.33	7364.94	6431.04	5719.15	5131.96	4880.00
ω_5	7104.26	4893.12	4286.15	3844.15	3496.53	3341.56		11050.54	7680.30	6710.42	5957.16	5326.75	5070.91

Table 4.2.21: Natural frequencies (Hz) of CCCC two-fold (90^0 crank angle) Si_3N_4/SUS304 FGM Folded plate subjected to linear temperature rise ΔT= 200 K.

Thickness	10 mm							15 mm					
N	0	0.5	1	2	5	10		0	0.5	1	2	5	10
ω_1	2831.52	1945.07	1687.98	1488.37	1322.74	1252.10		3099.25	2138.93	1859.51	1641.20	1459.62	1383.03
ω_2	2917.01	1973.03	1710.77	1518.76	1363.26	1288.44		4418.16	3024.17	2641.38	2363.61	2144.00	2043.00
ω_3	3179.21	2153.44	1868.60	1660.09	1491.43	1410.62		4792.89	3283.11	2868.25	2566.84	2328.27	2218.77
ω_4	3628.16	2462.61	2139.29	1902.66	1711.52	1620.34		5391.47	3714.08	3239.30	2877.32	2578.44	2448.66
ω_5	4081.99	2774.25	2406.93	2133.56	1909.52	1804.48		5438.28	3734.35	3262.50	2918.49	2646.60	2522.10

Thickness	20 mm							50 mm					
N	0	0.5	1	2	5	10		0	0.5	1	2	5	10
ω_1	3303.84	2283.64	1987.74	1757.21	1565.43	1483.79		4572.76	3174.07	2774.27	2466.61	2210.04	2096.91
ω_2	5748.48	3942.67	3447.79	3088.84	2807.55	2681.57		7316.70	5081.45	4436.66	3935.03	3515.60	3334.97
ω_3	5954.96	4123.51	3595.05	3185.35	2846.23	2702.58		10346.41	7119.62	6214.60	5539.03	5008.85	4792.21
ω_4	6214.05	4265.95	3731.25	3342.58	3037.18	2900.33		10595.16	7307.95	6378.85	5669.46	5083.10	4831.03
ω_5	7023.81	4827.71	4224.13	3784.14	3436.90	3281.10		10990.25	7634.09	6668.96	5919.88	5292.16	5037.07

Table 4.2.22: Natural frequencies (Hz) of CCCC two-fold (90^0 crank angle) Si_3N_4/SUS304 FGM Folded plate subjected to linear temperature rise ΔT= 300 K.

Thickness	**10 mm**							**15 mm**					
N	**0**	**0.5**	**1**	**2**	**5**	**10**		**0**	**0.5**	**1**	**2**	**5**	**10**
ω_1	2764.77	1844.44	1578.94	1381.22	1215.49	1131.40		3047.96	2094.69	1816.15	1597.66	1414.72	1336.89
ω_2	2781.42	1884.23	1627.33	1427.35	1260.02	1186.82		4331.55	2948.16	2566.45	2288.23	2065.78	1961.42
ω_3	3037.93	2020.37	1732.65	1518.72	1340.15	1250.28		4700.89	3202.72	2789.16	2487.45	2246.14	2133.27
ω_4	3478.01	2322.63	1997.04	1755.51	1554.99	1455.11		5306.51	3635.13	3164.59	2806.32	2507.41	2375.63
ω_5	3909.12	2615.12	2247.38	1971.62	1741.24	1628.73		5337.62	3651.85	3179.51	2833.03	2558.20	2430.28

Thickness	**20 mm**							**50 mm**					
N	**0**	**0.5**	**1**	**2**	**5**	**10**		**0**	**0.5**	**1**	**2**	**5**	**10**
ω_1	3254.17	2241.25	1946.35	1715.75	1522.69	1439.83		4526.39	3136.23	2738.05	2430.89	2173.39	2058.98
ω_2	5679.16	3884.53	3391.66	3033.39	2750.77	2622.52		7258.26	5034.70	4392.28	3891.51	3471.07	3288.88
ω_3	5892.24	4070.97	3544.50	3135.68	2795.93	2651.01		10296.32	7081.61	6179.64	5505.84	4975.80	4758.25
ω_4	6139.47	4203.50	3671.04	3283.17	2976.47	2837.34		10519.21	7250.23	6324.46	5615.70	5027.26	4772.96
ω_5	6940.59	4758.33	4157.39	3718.42	3369.92	3211.77		10932.47	7587.98	6626.27	5879.26	5250.98	4994.77

Table 4.2.23: Natural frequencies (Hz) of CCCC two-fold (90^0 crank angle) Si_3N_4/SUS304 FGM Folded plate subjected to non-linear temperature rise ΔT= 100 K.

Thickness	**10 mm**							**15 mm**					
N	**0**	**0.5**	**1**	**2**	**5**	**10**		**0**	**0.5**	**1**	**2**	**5**	**10**
ω_1	2892.53	2000.36	1742.30	1541.80	1375.61	1305.38		3148.76	2182.17	1901.62	1682.74	1501.00	1424.52
ω_2	3032.40	2081.33	1819.84	1629.54	1477.29	1405.82		4498.13	3094.77	2710.39	2431.84	2212.47	2112.54
ω_3	3300.55	2266.78	1982.47	1775.47	1609.85	1532.25		4878.25	3358.22	2941.55	2639.17	2400.68	2292.14
ω_4	3758.89	2583.84	2260.66	2025.20	1836.76	1748.62		5472.17	3786.41	3308.22	2942.98	2641.81	2511.94
ω_5	4236.23	2917.07	2548.74	2274.61	2050.77	1948.05		5532.35	3815.06	3341.85	2997.27	2725.31	2601.67

Thickness	**20 mm**							**50 mm**					
N	**0**	**0.5**	**1**	**2**	**5**	**10**		**0**	**0.5**	**1**	**2**	**5**	**10**
ω_1	3352.14	2325.34	2028.16	1796.94	1604.93	1523.38		4619.13	3212.06	2810.20	2501.17	2243.86	2130.69
ω_2	5814.96	3998.81	3501.50	3140.92	2858.93	2733.35		7376.34	5128.96	4480.92	3976.94	3555.96	3374.96
ω_3	6017.08	4175.72	3644.66	3232.88	2892.22	2748.25		10398.61	7158.96	6249.82	5570.93	5038.24	4820.81
ω_4	6285.82	4326.48	3789.11	3398.63	3092.42	2955.92		10673.33	7366.80	6433.07	5721.02	5133.27	4880.84
ω_5	7104.26	4895.32	4288.66	3846.53	3498.21	3342.65		11050.54	7681.90	6712.10	5958.59	5327.68	5071.49

Table 4.2.24: Natural frequencies (Hz) of CCCC two-fold (90^0 crank angle) Si_3N_4/SUS304 FGM Folded plate subjected to non-linear temperature rise ΔT= 200 K.

Thickness	**10 mm**							**15 mm**					
N	**0**	**0.5**	**1**	**2**	**5**	**10**		**0**	**0.5**	**1**	**2**	**5**	**10**
ω_1	2831.52	1949.22	1693.00	1493.30	1326.30	1254.43		3099.25	2142.04	1863.23	1644.87	1462.30	1384.78
ω_2	2917.01	1981.48	1721.27	1529.44	1371.27	1293.82		4418.16	3029.30	2647.53	2369.68	2148.44	2045.96
ω_3	3179.21	2162.23	1879.50	1671.13	1499.69	1416.14		4792.89	3288.55	2874.75	2573.24	2332.95	2221.87
ω_4	3628.16	2471.92	2150.78	1914.26	1720.16	1626.10		5391.47	3719.31	3245.39	2883.10	2582.54	2451.34
ω_5	4081.99	2785.06	2420.14	2146.68	1919.08	1810.80		5438.28	3740.08	3269.46	2925.41	2651.65	2525.44

Thickness	**20 mm**							**50 mm**					
N	**0**	**0.5**	**1**	**2**	**5**	**10**		**0**	**0.5**	**1**	**2**	**5**	**10**
ω_1	3303.84	2286.60	1991.26	1760.68	1567.96	1485.45		4572.76	3176.56	2777.17	2469.43	2212.11	2098.29
ω_2	5748.48	3946.59	3452.37	3093.26	2810.75	2683.70		7316.70	5084.51	4440.18	3938.42	3518.08	3336.62
ω_3	5954.96	4127.12	3599.26	3189.40	2849.14	2704.49		10346.41	7122.41	6217.55	5541.68	5010.68	4793.40
ω_4	6214.05	4270.16	3736.16	3347.32	3040.61	2902.60		10595.16	7311.77	6383.17	5673.63	5086.19	4833.09
ω_5	7023.81	4832.38	4229.57	3789.39	3440.69	3283.61		10990.25	7637.36	6672.51	5923.13	5294.47	5038.58

Table 4.2.25: Natural frequencies (Hz) of CCCC two-fold (90^0 crank angle) Si_3N_4/SUS304 FGM Folded plate subjected to non-linear temperature rise ΔT= 300 K.

Thickness	**10 mm**							**15 mm**					
N	**0**	**0.5**	**1**	**2**	**5**	**10**		**0**	**0.5**	**1**	**2**	**5**	**10**
ω_1	2764.77	1859.98	1598.76	1401.93	1231.60	1142.49		3047.96	2099.64	1822.15	1603.67	1419.19	1339.84
ω_2	2781.42	1891.37	1636.18	1436.26	1266.65	1191.29		4331.55	2956.73	2576.89	2298.70	2073.60	1966.70
ω_3	3037.93	2036.35	1752.96	1539.86	1356.52	1261.50		4700.89	3211.75	2800.14	2498.43	2254.32	2138.78
ω_4	3478.01	2339.29	2018.07	1777.28	1571.72	1466.53		5306.51	3644.18	3175.11	2816.11	2514.49	2380.34
ω_5	3909.12	2633.74	2270.54	1995.09	1758.82	1640.57		5337.62	3660.80	3190.72	2844.75	2566.95	2436.16

Thickness	**20 mm**							**50 mm**					
N	**0**	**0.5**	**1**	**2**	**5**	**10**		**0**	**0.5**	**1**	**2**	**5**	**10**
ω_1	3254.17	2245.93	1952.00	1721.41	1526.91	1442.63		4526.39	3140.11	2742.67	2435.48	2176.86	2061.34
ω_2	5679.16	3890.86	3399.18	3040.77	2756.23	2626.22		7258.26	5039.45	4397.89	3897.09	3475.32	3291.77
ω_3	5892.24	4076.65	3551.26	3142.34	2800.85	2654.29		10296.32	7085.91	6184.36	5510.25	4979.00	4760.41
ω_4	6139.47	4210.29	3679.08	3291.06	2982.29	2841.27		10519.21	7256.16	6331.37	5622.62	5032.61	4776.63
ω_5	6940.59	4765.82	4166.24	3727.09	3376.32	3216.08		10932.47	7593.01	6631.91	5884.73	5255.15	4997.58

Similar to one-fold folded plates, the two-fold folded plates manifest higher natural frequencies for lower values of power law index N. For better visualization of the effect of temperature increment, Figure 4.2.9 displays the first four frequencies ω_i (i= 1 to 4) versus temperature for FGM plates of 50 mm thickness. The plates of volume fraction indices N=1 subjected to uniform, linear, and nonlinear temperature rise fields are considered. For the purpose of comparison of temperature effects, the data of first natural frequency ω_1 from Figure 4.2.9 is plotted in Figure 4.2.10. Similar to flat plates and one-fold folded plates, it is observed that the uniform temperature change affects the vibrational frequencies more significantly than the linear and nonlinear temperature changes.

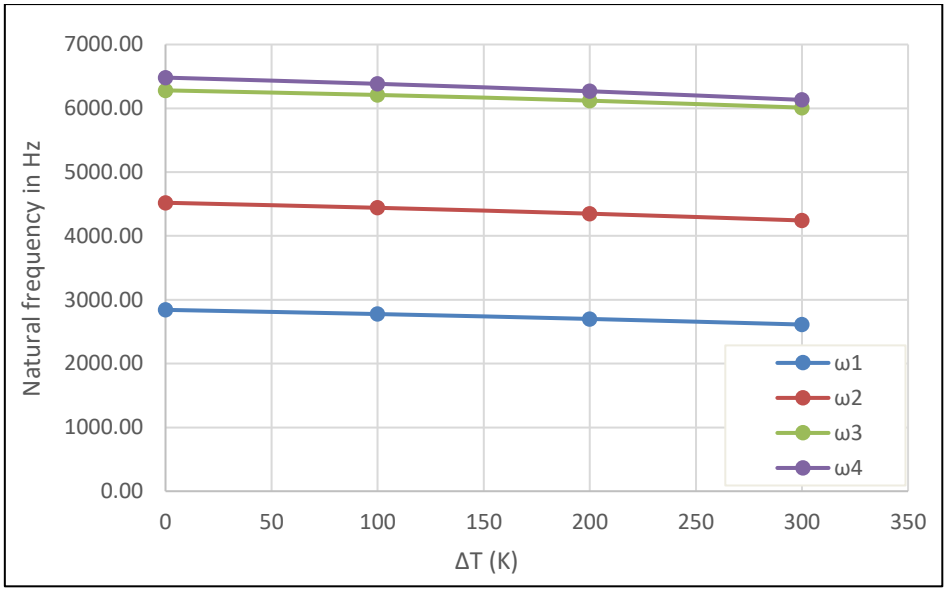

(a)

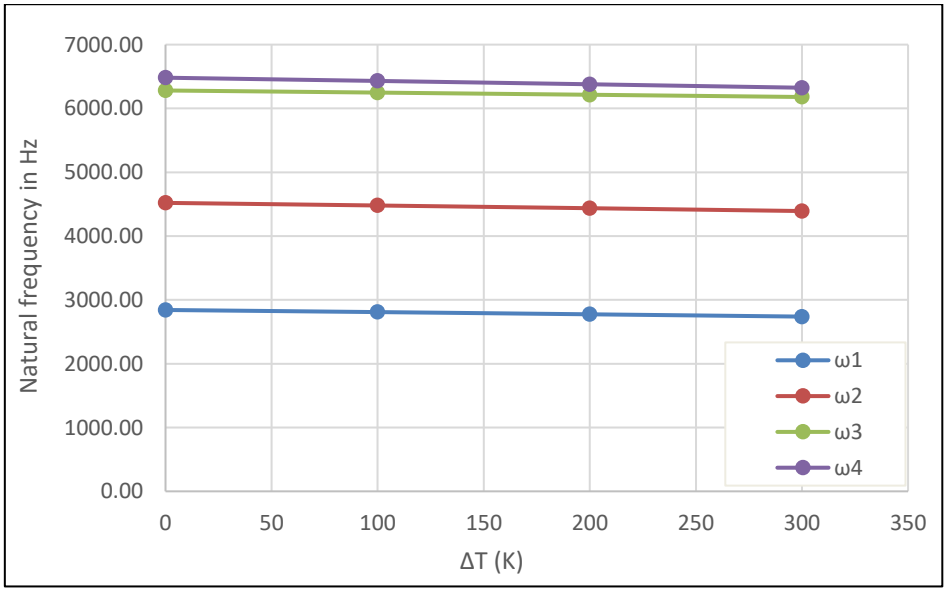

(b)

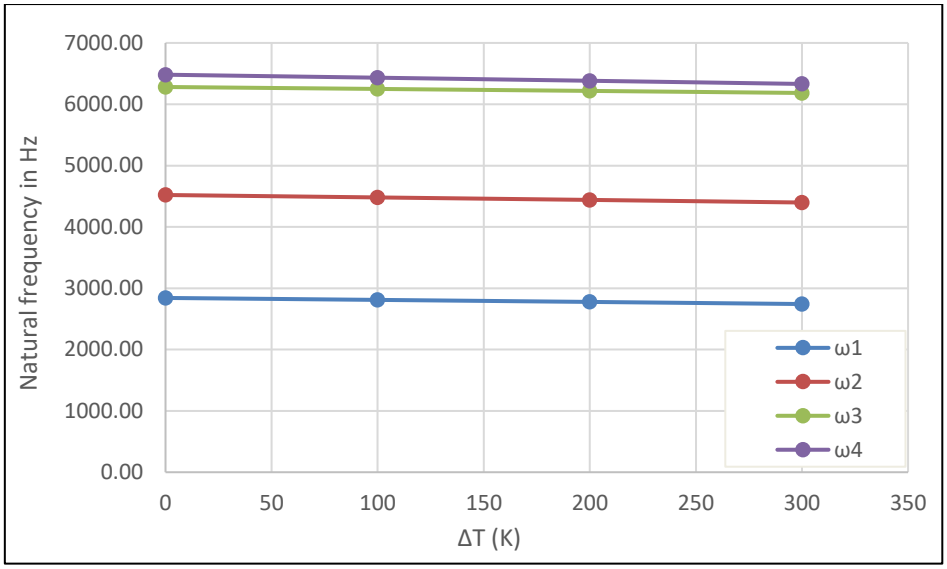

(c)

Figure 4.2.9: First four natural frequencies versus temperature for CCCC FGM two-fold plate with N=1, h=50 mm (a) Uniform temp. rise (b) Linear temp. rise (c) Non-linear temp. rise.

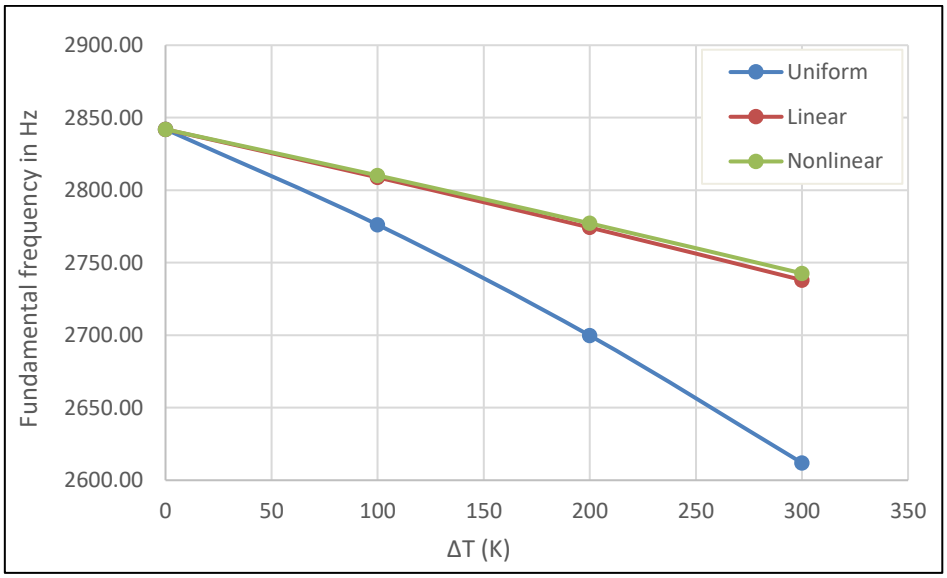

Figure 4.2.10: Variation of fundamental frequency with various temperature field for CCCC FGM two-fold plate with N=1 and h=50 mm.

First three mode shapes of Si_3N_4/SUS304 FGM two-fold folded plate, with crank angle $\beta = 90^o$ and N=1 have been plotted in Figure 4.2.11 for 10 mm and 50 mm thickness. It has been observed that the first mode shape remains unchanged for thinner plates, but when thermal load is added, the second mode bending (2,1) occurs, which is (1,1) without thermal load. Similarly, the third mode exhibits temperature-dependent bending mode (3,1) vs (2,1) when temperature increases. For thicker plate too, the first mode is similar where the structure rotates about vertical axis. When the thermal load is applied, a twisting shape is seen in the second mode. Regarding the third mode, no changes have been noted. Considerable variation in mode shapes have been observed when the plate thickness increases.

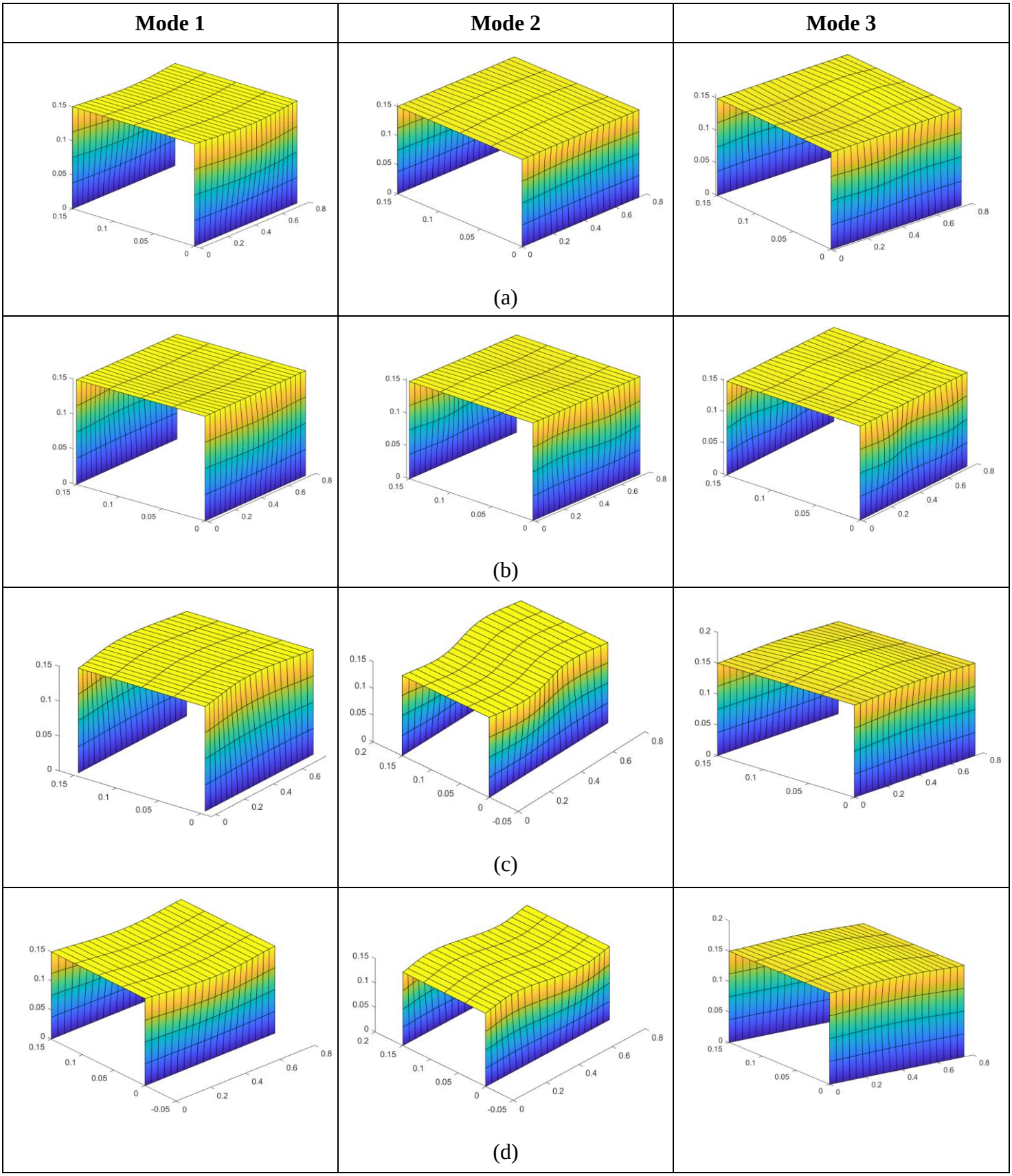

Figure 4.2.11: First three mode shapes for FG two-fold plate with N=1 (a) h = 10 mm without thermal load, (b) h = 10 mm uniform temp. rise (ΔT= 300 K), (c) h = 50 mm without thermal load (d) h = 50 mm uniform temp. rise (ΔT= 300 K).

Chapter 5

CONCLUSION

CHAPTER 5.
CONCLUSION

Functionally graded material is a high quality material that will revolutionize the manufacturing world in the 21st century. There are many roadblocks to understanding this target. Cost is a transcendent issue, with a tremendous section of the cost expended on the powder preparing and manufacturing strategy. However, the advancement of fabrication techniques, including additive manufacturing, has revolutionized the production of FGM plates. These techniques allow for precise control over material gradients and open up new possibilities for complex geometries.

In this work, dynamic response of all side clamped FGM rectangular flat and folded plates subjected to thermal environment is discussed to get the natural frequency and mode shapes using first order shear deformation theory. Material properties are assumed to be dependent on temperature and vary continuously in thickness direction according to power law distribution. In order to validate the current methodology, the results are cross-checked with the existing literature. From various parametric studies in crank angle, thicknesses, temperature field, and power law indices following conclusions can be made:

i) As temperature increases, material properties degrade, along with the development of thermal stresses, which ultimately cause a reduction in natural frequency.

ii) The impact of uniform temperature rise on vibrational frequencies is notably greater compared to that of linear and non-linear temperature rise.

iii) Folded plates provide better resistance to thermal loads in comparison to flat plates, as presence of fold increases stiffness of the plate.

iv) For flat rectangular plates the fundamental frequency of vibration decreases as the aspect ratio (a/b) increases.

v) The temperature change affects the first mode more significantly than other higher modes and the plates of power law index N=10 are more sensitive to the temperature change than those of N=1.

vi) Thicker sections, which produce higher fundamental frequencies, exhibit greater resilience against thermal loads. Thinner plates ceased to produce results in higher temperature.

vii) As ceramic constituent decreases with the increment of gradient index N, the stiffness and natural frequency of the folded plates reduces in exponential manner.

In essence, the numerical free vibration analysis of FGM folded plates not only enriches our understanding of their behavior but also provides a foundation for designing innovative structures that leverage their unique properties. As technology continues to advance, we anticipate that FGM folded plates will play an increasingly vital role in engineering solutions across diverse fields.

FUTURE SCOPE OF STUDY

The work presented in this thesis represents a limited segment of the extensive research area of functionally graded structures. There are numerous problems within this field that need to be addressed in future research. To mention a few, the current study can be extended in the following fields:

i) Consideration of the effect of environmental moisture along with temperature i.e. hygrothermal effect on FGM plates.

ii) These parametric studies can also be conducted with other materials like Ti–6Al–4V/ Zirconia etc.

iii) The present formulation is based on first order shear deformation theory. It can be modified to take higher order shear deformation theory into account.

iv) Formulation can be derived for modelling the behaviour of FGM beams and plates with integrated piezoelectric sensor and actuator.

v) Current analysis can be extended on Sandwich FGM plates, FGM Box structure, FGM cylindrical and spherical shells as well as FGM plates with change in porosity.

vi) Analysis of functionally graded material plates resting on Winkler and Pasternak elastic foundations.

vii) Buckling studies, forced vibration analysis and the effect of lateral load is a scope for further study.

REFERENCES

1. Shen, M., Bever, M.B.: Gradients in polymeric materials. Journal of Materials Science, 7, 741–746 (1972).
2. Koizumi, M., Niino, M.: Overview of FGM Research in Japan. MRS Bulletin, 20(1), 19–21 (1995).
3. Praveen, G.N., Reddy, J.N.: Nonlinear transient thermoelastic analysis of functionally graded ceramic-metal plates. International journal of solids and structures, 35(33), 4457–4476 (1998).
4. Reddy, J. N.: Analysis of functionally graded plates. International Journal for Numerical Methods in Engineering, 47(1-3), 663–684 (2000).
5. Vel, S.S., Batra, R.C.: Three-dimensional exact solution for the vibration of functionally graded rectangular plates. Journal of Sound and Vibration, 272(3-5), 703–730 (2004).
6. Hashemi, S. H., Arsanjani, M.: Exact characteristic equations for some of classical boundary conditions of vibrating moderately thick rectangular plates. International Journal of Solids and Structures, 42(3-4), 819-853 (2005).
7. Abrate, S.: Free vibration, buckling, and static deflections of functionally graded plates. Composites Science and Technology, 66(14), 2383–2394 (2006).
8. Abrate, S.: Functionally graded plates behave like homogeneous plates. Composites Part B: Engineering, 39(1), 151–158 (2008).
9. Nguyen, T. K., Sab, K., Bonnet, G.: Shear correction factors for functionally graded plates. Mechanics of Advanced Materials and Structures, 14(8), 567-575 (2007).
10. Prakash, T., Singha, M.K., Ganapathi, M.: Influence of neutral surface position on the non-linear stability behavior of functionally graded plates. Computational Mechanics, 43(3), 341–350 (2008).
11. Hosseini-Hashemi, S., Taher, H. R. D., Akhavan, H., Omidi, M.: Free vibration of functionally graded rectangular plates using first-order shear deformation plate theory. Applied Mathematical Modelling, 34(5), 1276-1291 (2010).
12. Talha, M., Singh, B.N.: Static response and free vibration analysis of FGM plates using higher order shear deformation theory. Applied Mathematical Modelling, 34(12), 3991–4011 (2010).
13. Hosseini-Hashemi, Sh., Fadaee, M., Atashipour, S.R.: Study on the free vibration of thick functionally graded rectangular plates according to a new exact closed-form procedure. Composite Structures, 93(2), 722–735 (2011).
14. Efraim, E.: Accurate formula for determination of natural frequencies of FGM plates basing on frequencies of isotropic plates. Procedia engineering, 10, 242-247 (2011).

15. Mahamood, R., Akinlabi, E., Shukla, M., Pityana, S. L. Functionally Graded Material: An overview. Proceedings of the World Congress on Engineering, Vol III (2012).
16. Jha, D.K., Kant, T., Singh, R.K.: Higher order shear and normal deformation theory for natural frequency of functionally graded rectangular plates. Nuclear Engineering and Design, 250, 8–13 (2012).
17. Kennedy, D., Cheng, R. K. H.: An equivalent isotropic model for functionally graded plates. In Proceedings of the Eleventh International Conference on Computational Structures Technology, 94, 1-13 (2012).
18. Gupta, A., Talha, M.: Recent development in modeling and analysis of functionally graded materials and structures. Progress in Aerospace Sciences, 79, 1–14 (2015).
19. Kennedy, D., Cheng, R. K. H., Wei, S., Arevalo, F. A.: Equivalent layered models for functionally graded plates. Computers & Structures, 174, 113-121 (2016).
20. Bernardo, G. M. S., Damásio, F. R., Silva, T. A. N., Loja, M. A. R.: A study on the structural behaviour of FGM plates static and free vibrations analyses. Composite Structures, 136, 124-138 (2016).
21. Chakraverty, S., Pradhan, K. K.: Vibration of functionally graded beams and plates. Academic Press (2016).
22. KP, H. K., Dharan, S.: Recent Development in Modelling and Analysis of Functionally Graded Materials (2017).
23. Burlayenko, V. N., Sadowski, T.: Free vibrations and static analysis of functionally graded sandwich plates with three-dimensional finite elements. Meccanica, 55(4), 815-832 (2020).
24. Marzavan, S., Nastasescu, V.: Free Vibration Analysis of a Functionally Graded Plate by Finite Element Method. Ain Shams Engineering Journal, 14(8), 102024–102024 (2023).
25. Yang, J., Shen, H. S.: Vibration characteristics and transient response of shear-deformable functionally graded plates in thermal environments. Journal of Sound and vibration, 255(3), 579-602 (2002).
26. Kim, Y. W.: Temperature dependent vibration analysis of functionally graded rectangular plates. Journal of sound and vibration, 284(3-5), 531-549 (2005).
27. N. Sundararajan; T. Prakash; M. Ganapathi: Nonlinear free flexural vibrations of functionally graded rectangular and skew plates under thermal environments., 42(2), 152–168. (2005).
28. Li, Q., Iu, V. P., Kou, K. P.: Three-dimensional vibration analysis of functionally graded material plates in thermal environment. Journal of Sound and Vibration, 324(3-5), 733-750 (2009).
29. Malekzadeh, P., Beni, A. A.: Free vibration of functionally graded arbitrary straight-sided quadrilateral plates in thermal environment. Composite Structures, 92(11), 2758-2767 (2010).

30. Chakraverty, S.; Pradhan, K.K.: Free vibration of exponential functionally graded rectangular plates in thermal environment with general boundary conditions. Aerospace Science and Technology, 36, 132–156. (2014).

31. Kandasamy, R., Dimitri, R., Tornabene, F.: Numerical study on the free vibration and thermal buckling behavior of moderately thick functionally graded structures in thermal environments. Composite Structures, 157, 207-221 (2016).

32. Lee, Y. H., Bae, S. I., Kim, J. H.: Thermal buckling behavior of functionally graded plates based on neutral surface. Composite Structures, 137, 208-214 (2016).

33. Swaminathan, K., Sangeetha, D. M.: Thermal analysis of FGM plates–A critical review of various modelling techniques and solution methods. Composite Structures, 160, 43-60 (2017).

34. Zghal, S., Trabelsi, S., Frikha, A., Dammak, F.: Thermal free vibration analysis of functionally graded plates and panels with an improved finite shell element. Journal of Thermal Stresses, 44(3), 315-341 (2021).

35. Thai, S., Nguyen, V. X., Lieu, Q. X.: Bending and free vibration analyses of multi-directional functionally graded plates in thermal environment: A three-dimensional Isogeometric Analysis approach. Composite Structures, 295, 115797 (2022).

36. Goldberg, J. E., Leve, H. L.: Theory of prismatic folded plate structures (1957).

37. Cheung, Y. K.: Folded plate structures by finite strip method. Journal of the Structural Division, 95(12), 2963-2982 (1969).

38. Pulmano, V.A., Bosler, J.C., Hall, A.S.: Finite element solution for folded plates with variable thickness, IASS World Congress on Pace Enclosures, 511–520 (1976).

39. Irie, T., Yamada, G., Kobayashi, Y.: Free vibration of a cantilever folded plate. The Journal of the Acoustical Society of America, 76(6), 1743-1748 (1984).

40. Bar-Yoseph, P., Hersckovitz, I.: Analysis of folded plate structures. Thin-walled structures, 7(2), 139-158 (1989).

41. Golley, B. W., Grice, W. A.: Prismatic folded plate analysis using finite strip-elements. Computer Methods in Applied Mechanics and Engineering, 76(2), 101-118 (1989).

42. Eterovic, A. L., Godoy, L. A.: An exact strip method for folded plate structures. Computers & structures, 32(2), 263-276 (1989).

43. Liu, W. H., Huang, C. C.: Vibration analysis of folded plates. Journal of Sound and Vibration, 157(1), 123-137 (1992).

44. Danial, A. N., Doyle, J. F., Rizzi, S. A.: Dynamic analysis of folded plate structures. ASME J. Vib. Acoust., 118(4), 591–598 (1996).

45. Bathe, K.J.: Finite Element Procedures. Prentice Hall of India Pvt. Ltd., New Delhi (1996).

46. Zienkiewicz, O.C., Cheung, Y.K.: The Finite Element Method in Structural and Continuum Mechanics. McGraw Hill Co., London, (1967).

47. Guha Niyogi, A., Laha, M. K., Sinha, P. K.: Finite element vibration analysis of laminated composite folded plate structures. Shock and Vibration, 6(5-6), 273-283 (1999).

48. Pal, S., Guha Niyogi, A.: Application of folded plate formulation in analyzing stiffened laminated composite and sandwich folded plate vibration. Journal of Reinforced Plastics and composites, 27(7), 693-710 (2008).

49. Lee, S. Y., Wooh, S. C., Yhim, S. S.: Dynamic behavior of folded composite plates analyzed by the third order plate theory. International Journal of Solids and Structures, 41(7), 1879-1892 (2004).

50. Haldar, S., Sheikh, A.H.: Free vibration analysis of isotropic and composite folded plates using a shear flexible element. Finite elements in Analysis and Design, 42(3), 208–226 (2005).

51. Peng, L.X., Liew, K.M., Kitipornchai, S.: Bending analysis of folded laminated plates by the FSDT meshfree method, The Twelfth East Asia-Pacific Conference on Structural Engineering and Construction, Hong Kong, 14, 2714-2721 (2011).

52. Thinh, T. I., Van Binh, B., Tu, T. M.: Bending and vibration analysis of multi-folding laminate composite plate using finite element method. Vietnam Journal of Mechanics, 34(3), 185-202 (2012).

53. Nguyen-Minh, N., Nguyen-Thoi, T., Bui-Xuan, T., Vo-Duy, T.: Static and free vibration analyses of stiffened folded plates using a cell-based smoothed discrete shear gap method (CS-FEM-DSG3). Applied Mathematics and Computation, 266, 212-234 (2015).

54. Guo, X., Zhang, Y., Zhang, W., Sun, L.: Theoretical and experimental investigation on the nonlinear vibration behavior of Z-shaped folded plates with inner resonance. Engineering Structures, 182, 123-140 (2019).

55. Das, S., Niyogi, A. G.: Free-vibration analysis of epoxy-based cross-ply laminated composite folded plates subjected to hygrothermal loading. Journal of The Institution of Engineers (India): Series C, 101, 541-557 (2020).

56. Mohammadi, H., Setoodeh, A. R.: FSDT-based isogeometric analysis for free vibration behavior of functionally graded skew folded plates. Iranian Journal of Science and Technology, Transactions of Mechanical Engineering, 44, 841-863 (2020).

57. Basu, D., Pramanik, S., Das, S., Niyogi, A. G.: Finite Element Free Vibration Analysis of Functionally Graded Folded Plates. Iranian Journal of Science and Technology, Transactions of Mechanical Engineering, 47(2), 697-716 (2023).

58. Zhang, J., Li, L.: Free vibration of functionally graded graphene platelets rein-forced composite porous L-shaped folded plate. Engineering Structures, 297, 116977 (2023).

59. Pham, Q. H., Tran, T. T., Nguyen, P. C.: Free and forced vibration analyses of unsymmetrical functionally graded porous folded sandwich plates using MITC3 elements. Ain Shams Engineering Journal, 102640 (2024).

60. Mohammadi, M., Rajabi, M., Ghadiri, M.: Functionally graded materials (FGMs): A review of classifications, fabrication methods and their applications. Processing and Application of Ceramics, 15(4), 319-343 (2021).

61. Sam, M., Jojith, R., Radhika, N.: Progression in manufacturing of functionally graded materials and impact of thermal treatment—A critical review. Journal of Manufacturing Processes, 68, 1339-1377 (2021).

62. Elishakoff, I. E., Pentaras, D., Gentilini, C.: Mechanics of functionally graded material structures. World Scientific (2015).

63. Aydogdu, M., Taskin, V.: Free vibration analysis of functionally graded beams with simply supported edges. Materials & design, 28(5), 1651-1656 (2007).

64. Reddy, K. S. K., Kant, T.: Three-dimensional elasticity solution for free vibrations of exponentially graded plates. Journal of Engineering Mechanics, 140(7), 04014047 (2014).

65. Chung, Y. L., Chi, S. H.: The residual stress of functionally graded materials. Journal of the Chinese Institute of Civil and Hydraulic Engineering, 13, 1–9 (2001).

66. Bhandari, M., Purohit, K.: Response of functionally graded material plate under thermomechanical load subjected to various boundary conditions. International Journal of Metals (2015).

67. Daikh, A. A.: Temperature dependent vibration analysis of functionally graded sandwich plates resting on Winkler/Pasternak/Kerr foundation. Materials Research Express, 6(6), 065702 (2019).

68. Touloukian, Y.S.: Thermophysical Properties of High Temperature Solid Materials, MacMillan, New York (1967).